The Synthesis and *In Vitro* Evaluation of Short Interfering RNAs that Contain Internal Modified Alkyl Spacers

By

Christopher J. McKim

A dissertation submitted for partial fulfillment of the qualifications required for the degree of

Masters of Science

University of Ontario Institute of Technology

Faculty of Science

Applied Biosciences

August 2014

Abstract

The ability to silence genes effectively at the pre-translational level through the use of short interfering ribonucleic acid (siRNA) has become a widely studied area since the discovery of the RNA interference pathway in 1998. The ability to silence genes at this point in the central dogma of cell biology offers the chance for excellent gene knockdown specificity as the gene silencing tool is tailored for an exact messenger RNA sequence. There are some inherent problems associated with this type of technology which arise from the chemical structure of RNA including poor cell permeability due to the polyanionic backbone or due to the fact that RNA is a natural substrate for nucleases. In an attempt to mitigate these problems there has been considerable focus on chemical modification of siRNAs such as alteration of the ribose ring or backbone. Backbone alterations such as abasic alkyl linkers have been shown to retain, if not improve, gene-silencing capability while providing a means of centrally destabilizing the siRNA duplex, even when occupying the site of the catalytic protein, Argonaute2, whose action was thought to be an essential part of the RNA interference pathway. This study herein reports the synthesis of novel abasic alkyl linkers and an evaluation of their dose-dependent ability to silence genes *in vitro* while occupying central regions within the sense stand.

Acknowledgements

The first person that I wish to acknowledge is my supervisor Dr. Jean-Paul Desaulniers. The only reason I am here today I because he was kind enough to accept me in to his research group and he has been a constant source of inspiration throughout this entire process.

I would also like to extend many thanks to the members of my masters committee: Dr. Yuri Bolshan and Dr. Liliana Trevani. I really appreciate the time and effort put in by these individuals to help me throughout the entire project.

I would like to thank Dr. Sean Forrester and Dr. Anatoli Chkrebtii for taking the time to be involved in the defense process.

Many thanks go out to members past and present of the Desaulniers research group for their help directly or indirectly with my work and they are: Dr. Tim Efthymiou, Brandon Peel, Gordon Hagen, Kalai Krishnamurthy, Blake Roberts and Jessica Pauze.

A special mention goes out to Genevieve Barnes and Michael Allison for helping me with random problems over the past two years, your expertise has helped more than you know.

To my parents; thank you for all the support over the entirety of my university career that has finished off with this paper. There is no way I could have made it this far without the support.

And finally to my girlfriend Alex, your encouragement and support has made such a profound difference whilst undertaking this project. Thank you for always being there and keeping this grad student's sanity intact.

Statement of Contributions

All of the studies reported in this dissertation were performed by myself under the supervision of Dr. Jean-Paul Desaulniers. For the luciferase assay, Kalai Krishnamurthy and Jessica Pauze helped with cell passaging, plating, transfections and the luciferase readings as part of their honours thesis project in biology and work study tasks respectively. The synthesis of the smaller propargyl modified linker was done with the help of Blake Roberts as a part of his honours thesis project in chemistry. For the real time PCR work I would like to acknowledge Gordon Hagen for aiding me substantially with this biological work. The introduction, experimental and discussion of this dissertation were written by the author under the supervision of Dr. Jean-Paul Desaulniers.

Statement of Originality

To the best of this author's knowledge the study herein is considered to be a novel contribution to the scientific community.

List of Figures

List of Tables

List of Schemes

List of Abbreviations

A: Adenosine

Ago: Argonaute

BCL2: B-cell lymphoma protein 2

bp: base pair

C: Cytosine

CD: Circular dichroism

CPG: Controlled pore glass

EDTA: Ethylenediaminetetraacetic acid

DCM: dichloromethane (CH_2Cl_2)

DIPEA: *N,N*-diisopropylethylamine

DMAP: 4-(dimethylamino)pyridine

DMEM: Dulbecco's modified Eagle medium

DMF: *N,N*-dimethylformamide

DMSO: dimethylsulfoxide

DMT: 4,4'-dimethoxytrityl

DNA: 2'-deoxyribonucleic acid

ds: double-stranded

dd: doublet of doublets

dt: doublet of triplets

dT: 2'-deoxythymidine

EMAN: methylamine 40% wt. in H_2O and methylamine 33% wt. in ethanol (1:1)

ESI-MS: Electrospray ionization mass spectrometry

EtOAc: Ethyl acetate

EtOH: Ethanol

FBS: Fetal bovine serum

G: Guanosine

J: Coupling constant (Hz)

MALDI-TOF: Matrix assisted laser desorption ionization – time of flight

MeCN: Acetonitrile

MeOH: Methanol

miRNA: micro RNA

mRNA: Messenger RNA

nt: nucleotide

NMR: Nuclear magnetic resonance

ONs: Oligonucleotides

PAGE: Polyacrylamide gel electrophoresis

PCR: Polymerase chain reaction

PS: Phosphorothioate

P/S: Penicillin-Streptomycin

qRT-PCR: Quantitative real-time PCR

RISC: RNA-induced silencing complex

RNA: Ribonucleic acid

RNAi: RNA interference

rt.: Room temperature

siRNA: Small interfering RNA

t: Triplet

T: Thymidine

TBE: Tris-boric acid EDTA

TBS: *tert*-butyldimethylsilyl

TCA: Trichloroacetic acid

TEA: Triethylamine

THF: Tetrahydrofuran

TLC: Thin-layer chromatography

T_m: Melting temperature

U: Uridine

UV: Ultraviolet

wt: Wild-type

Table of Contents

1.0 - Introduction and Literature Review

1.1 – DNA vs. RNA: The Biomolecules of Life

The instructions to all life are written in a language where only four letters are used; these letters each represent a specific chemical structure. These compounds form long biopolymers which are known as deoxyribonucleic acid (DNA) which form the human genome; the ability of genes to be expressed is accomplished through another biopolymer known as ribonucleic acid (RNA) [1]. These nucleic acids are repeating units of heterocyclic bases appended off of a ribose sugar-phosphate backbone (**Figure 1-1**). This biopolymer is polyanionic due to the phosphate being deprotonated at neutral pH [2]. There are two important differences between DNA and RNA. Firstly, in DNA the four nitrogenous bases are adenine (A), cytosine (C), guanine (G) and thymine (T); RNA is the same except for thymine being replaced by uracil (U). Another difference is that RNA has a hydroxyl group at the 2' position of the ribose ring whereas DNA has only a methylene group at the 2' position [3]. The addition of the 2' hydroxyl is a very crucial difference between the nucleic acids because it imparts different structural conformations. The 2' hydroxyl forces the pentofuranose ring to adopt a C3'-*endo* conformation, which is the preferred structural conformation of RNA and is a result of the gauche effect between the 4'O and 2'OH [4]. Whereas DNA primarily exists in a long double stranded form used to contain genetic information, RNA tends to exists in shorter single strands that exhibit many biologically active forms such as mRNA, miRNA and tRNA [5]. Single stranded RNAs have complementary regions that form small double helices which can pack together to form structures similar to proteins that are capable of carrying out chemical catalysis [6].

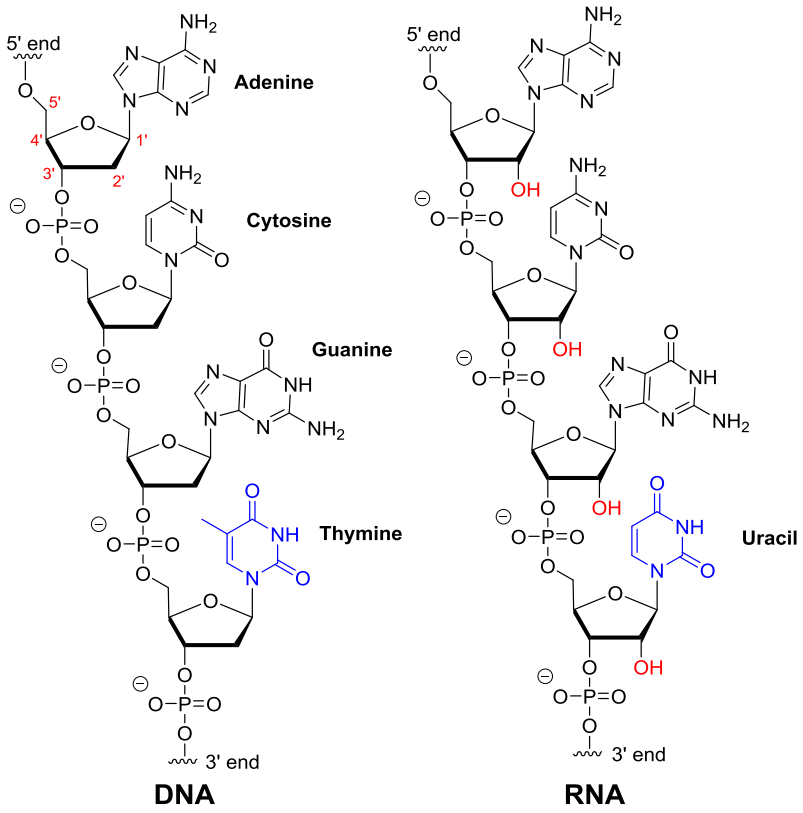

Figure 1-1: Structural comparison of RNA and DNA. The sugar numbering is depicted on the adenine base on the DNA strand.

Both DNA and RNA have the capability of existing in a double stranded form, pairing up with another strand to form a duplex. The duplex is held together through the hydrogen bonding occurring between to the complementary base pairs; this is known as Watson and Crick or canonical base pairing where A bonds with U or T and G bonds with C [7]. The two strands are antiparallel (5' and 3' ends are reversed) to each other and the resulting duplex exists as a double helix [8].

Arguably the most important pathway in molecular biology, involving both DNA and RNA, is the conversion of genetic information into functioning molecules such as proteins; this pathway is known as the central dogma of molecular biology (**Figure 1-2**). The pathway begins when the double stranded genomic DNA is unwound; at this point one of

two things can happen: 1) DNA replication in preparation for cell division or 2) RNA production via transcription [9]. Transcription takes the genetic information and changes it into messenger RNA (mRNA) which then leaves the cell's nucleus and associates with organelles in the cytoplasm known as ribosomes. The ribosome then creates specific proteins by, in essence, 'reading' the mRNA sequence [10]. It is possible in some instances for RNA to be reverse transcribed back in to single stranded DNA; such is the case with HIV which possesses a reverse transcriptase enzyme [11]. Since the 1970's there has been much interest in manipulating gene expression in living cells by targeting this pathway

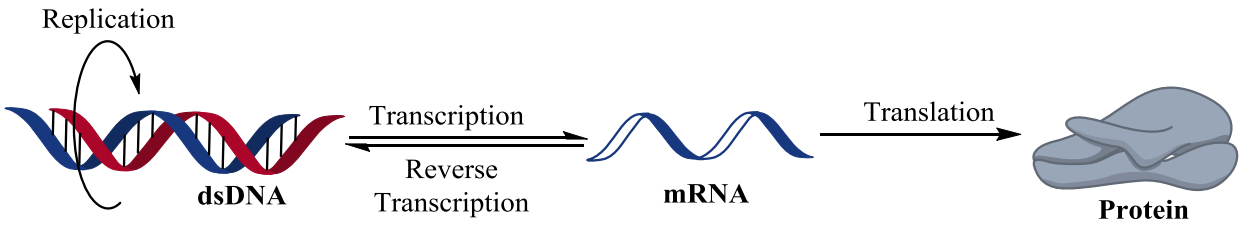

Figure 1-2: The central dogma in molecular biology.

for possible gene analysis and therapeutic agents [12]. Traditional therapeutics tend to target post-translational molecules such as proteins, whereas oligonucleotides can be made with a certain sequence to compliment that of a specific mRNA to target this pathway at the pre-translational level, affording a new specific means of gene suppression [13]. There is great interest in utilizing this idea as a means to treat diseases which are the result of aberrant gene expression such as cancer [14].

1.2 – The RNA Interference Pathway

The RNA interference (RNAi) pathway is highly conserved, ancient in origin and exists in a wide variety of organism for the purpose of gene expression regulation [15] and

protection from foreign DNA and RNA [16]. This pathway was discovered in 1998 by two scientists, Fire and Mello, while they were investigating the effects of using antisense RNAs to knock-down the abundant unc-22 mRNA in the model organism *C. elegans*. Fire and Mello unexpectedly stumbled upon the RNAi pathway when obtaining unexpected high knock-down with double-stranded RNA (dsRNA)[17]. This opened up a brand new avenue in the gene silencing capability of RNA; dsRNA that exhibited gene silencing capability became known as short interfering RNA (siRNA) and has rapidly become a widely used tool for molecular biology gene knock-down experiments and is being investigated for its therapeutic applicability [18].

1.2.1 - The mechanism of siRNA and RNAi in humans

Short interfering RNAs are dsRNA molecules that are typically 19 to 21 base pairs in length and possess a definitive two-base pair overhang on the 3' end of each strand (**Figure 1-3**) [19]. This siRNA is first bound by an Argonaute2 protein that is specific for dsRNA that is in the A-form helical conformation [20]. Binding of this Argonaute2 protein facilitates the assembly of several other proteins, which include a double stranded *trans*-activated binding domain protein (TRBP), Dicer and others; together all of which form the RNA induced silencing complex (RISC) [21]. The RISC then chooses a single strand, known as the antisense strand, by having TRBP and Dicer assess which strand has the least thermodynamically stable 5' end and the complementary strand becomes degraded [22]. When RISC has this single strand it is now in its activated form at which time it seeks out mRNA within the cytoplasm that is complementary [23]. When a complementary mRNA sequence is located a duplex is then formed between the antisense strand and the mRNA

resulting in the mRNA strand in the duplex being cleaved at the phosphodiester bond between the base pairs across from the 9th and 10th base pairs counting from the 5' end of the antisense strand [24]. The resulting cleaved mRNA dissociates from RISC and can no longer be translated in to the proper protein.

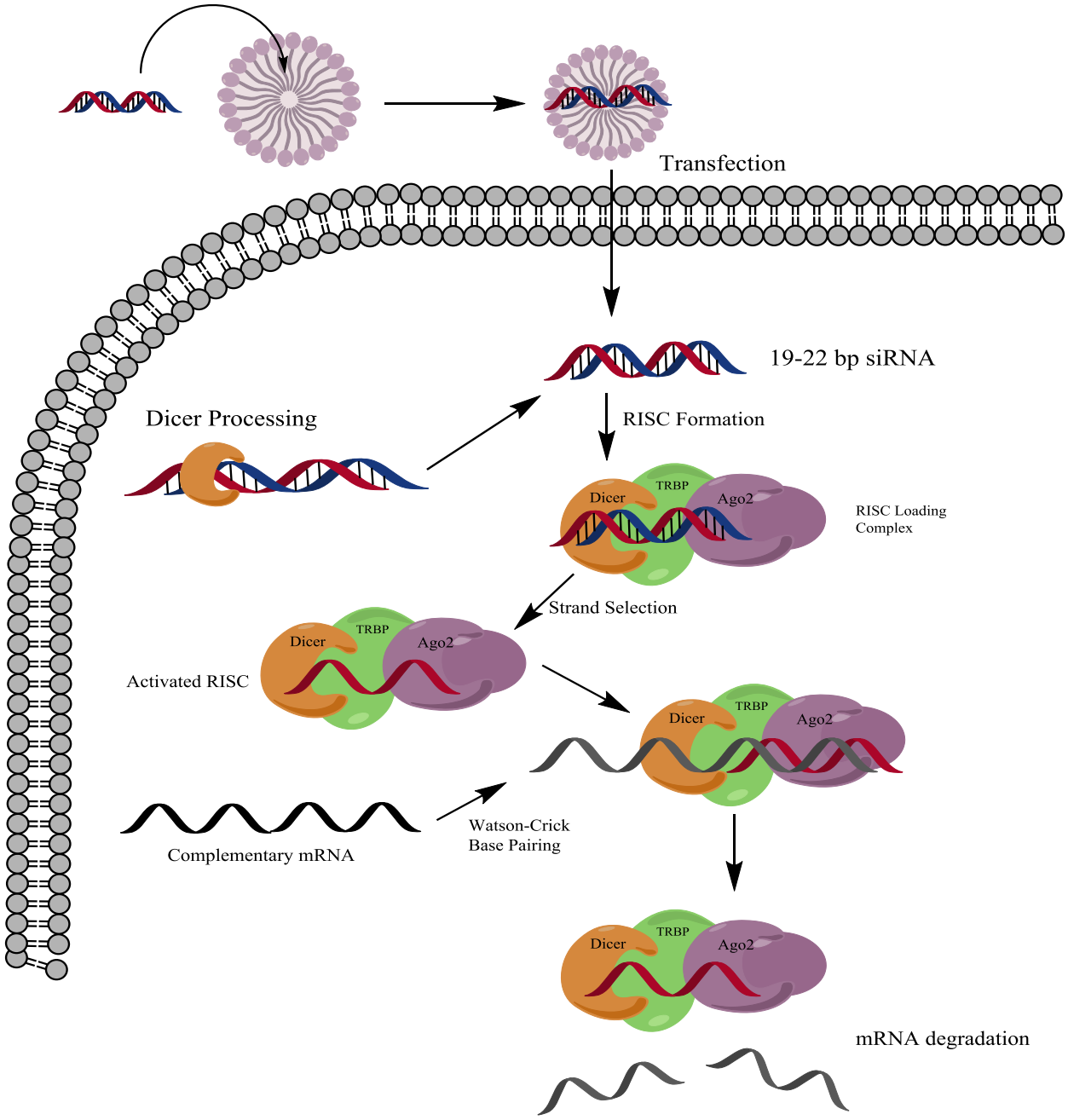

Figure 1-3: The RNA interference pathway within humans.

This pathway is initiated one of two ways: 1) synthetic siRNAs can be directly transfected in to cells using transfecting agents such as cationic polymers, this is the route taken for siRNAs used as molecular biology tools and therapeutic applications or 2) native long endogenous dsRNA is processed by the enzyme Dicer in to siRNA [25]. An example of native dsRNA is pre-microRNAs which are expressed from RNA coding genes in the genome; the primary transcript becomes processed into the trademark stem-loop and enters the cytoplasm converging with the synthetic siRNA pathway at RISC [26]. The enzyme Dicer has two distinct RNase III motifs, a dsRNA binding domain and a RNA helicase domain [27] which it uses to catalyze the cleavage of long dsRNA. When Dicer was knocked down in human HeLa cells it was shown that dsRNA built up in the cytoplasm [28].

Another essential enzyme to the RNAi pathway is the Argonaute2 endonuclease which carries out a significant portion of the pathway's catalytic activity including the eventual mRNA cleavage [29]. Ago2 also plays a key role in removing the inactive sense strand from the duplex [30]. It is not fully understood as to whether Ago2 is complexed with DICER and TRBP while the active guide strand is being directed towards its target or whether Ago2 is performing RNAi independently [31]. This endonuclease is comprised of three main domains; a PAZ on the carboxyl terminus, a PIWI domain on the amino terminus and a central Mid section [32] as is shown in (**Figure 1-4**). The section responsible for the catalytic activity of the enzyme is the PIWI domain which resembles the RNase H endonuclease [33]. The Mid domain of Ago2 has been identified as the region which associates with the phosphorylated 5' end of the antisense strand while the PIWI domain binds to the 5' region of the antisense strand [34]. The PAZ domain interacts with the 3' overhang of the antisense strand and there is no known interaction with the 3'

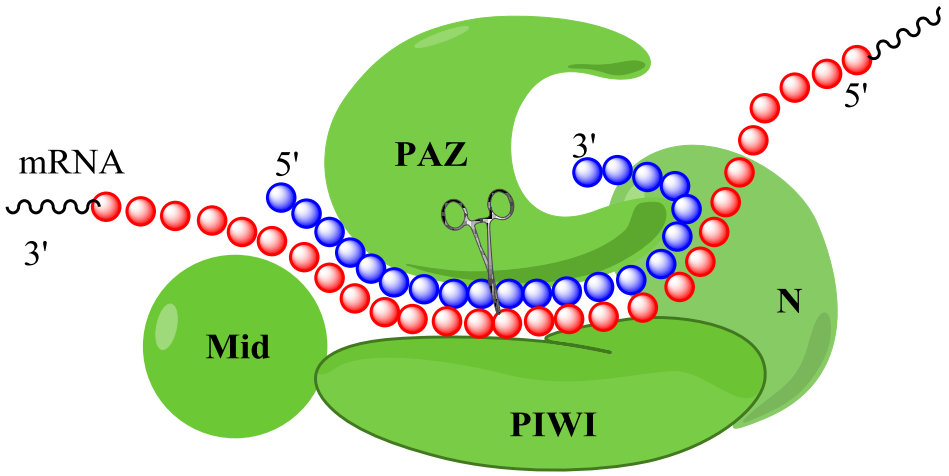

Figure 1-4: Argonaute2 catalytic region with an antisense RNA and its complementary mRNA.

region of the strand [35]. It is important to keep these interacting regions in mind when attempting to impart chemical modifications on siRNAs as these interactions need to be maintained in order to retain function whether as a molecular biology tool or as a possible therapeutic agent [36].

1.2.2 – Problems with siRNA Therapeutics

The use of RNA as a therapeutic agent has been around for a while; it began in the late 1970's when it was demonstrated that simple antisense RNA oligonucleotides could directly interfere with mRNA translation within a cell by binding to a complementary mRNA strand and preventing the ribosomal assembly necessary for translation [37]. A specifically tailored antisense oligonucleotide can inhibit the translation of mRNA of an overexpressed gene, as is the case in many cancers, thus mitigating the effects [38]. Decades later there are only two antisense oligonucleotide therapeutics that have been FDA approved: most recently Mipomersen (marketed as Kynamro in 2013) and before that Formivirsen (marketed as Vitravene in 1998) [39]. With decades of research in the field it

seems worrisome that only two drugs have made it to market. With siRNAs the situation is even bleaker having been around for sixteen years there are no FDA approved drugs. It is important to note however that there are others currently in clinical trials [40]. A major factor in the delay in the emergence of other therapeutics arises from the structure of RNA itself which possesses several noticeable pitfalls when assessing its use as a therapeutic. The main issues that need to be taken into consideration are: 1) enzymatic degradation, 2) polyanionic nature of RNA at physiological pH and; 3) off-target effects [41].

There are mechanisms that exist within every organism that target all nucleic acids for degradation, particularly RNA, which results in a shortened duration of activity. This occurs due to the presence of exo- and endo-nucleases that exist in the blood serum, of which RNA is a natural substrate due to the phosphodiester linkages [42]. Fortunately for siRNAs, RNA duplexes are more resistant to nucleases; however unmodified RNA duplexes are still readily degraded within serum [43]. In the case of siRNAs it is currently believed that an enzyme closely related to *ERI-1* is the main catalytic portion of the degradation pathway [44]. An interesting trait of this degradation pathway is that it has been shown that cleavage of siRNAs typically happens after pyrimidines [43] which could be useful when selecting an mRNA sequence to target. Another important note about the phosphodiester bond is its susceptibility to hydrolysis at physiological pH since phosphorous is oxophilic and the attack of water at its electron deficient center is a favourable reaction [45]. Keeping this in mind, it is also possible for the hydroxyl group on the ribose sugar 2' position to perform a nucleophilic attack on the closest phosphorous atom in a form of self-hydrolysis [46].

With a pK_a close to zero, the hydroxyl group on the phosphodiester linkage is deprotonated at physiological pH which means that RNA strands have a polyanionic backbone [46]. This severely hinders RNA's ability to be cell membrane permeable which in the end directly affects delivery to cells due to the presence of many negatively charged moieties on the surface of the cellular membrane [47]. This large charge density also hinders RNA's ability to associate with serum proteins, such as albumin, resulting in the strands becoming heavily hydrated making them easier targets for hydrolysis [48].

Since the siRNA antisense strand relies on Watson-Crick base pairing to identify the target mRNA it is possible that other mRNA sequences that possess a high degree of similarity to the target could accidently be degraded [49]. Duplexes with a mismatch can still form RISC tolerable substrates which can result in off-target silencing [49]. This can be particularly troublesome if the unintended target belongs to a vital pathway. Sometimes when an siRNA is associating with RISC there is an error in strand selection and the active RISC is formed with the guide strand resulting in only off target effects [50].

In order to further pursue RNAs as therapeutics these issues need to be addressed. There are currently two main avenues being studied: 1) new delivery systems such as nanoparticle delivery and 2) chemical modifications to oligonucleotides, which will be the main focus of this dissertation herein.

1.2.3 – Chemical Modifications of siRNAs

Organic chemists have been synthesizing chemically modified oligonucleotides for decades now with the hopes of finding a biocompatible modification that mitigates the pitfalls of RNA whilst retaining potent gene silencing ability. While current modifications

do show certain positive features there is currently no universally accepted chemical modification that satisfies these criteria so the search for new modifications continues.

Looking at the structure of a 21 bp oligonucleotide the thought of performing a chemical modification at a specific position seems daunting; however in reality it is quite simple using well established nucleic acid synthetic methods which synthesize oligos one bp at a time on a controlled-pore glass (CPG) support [51]. One of the most commonly utilized method is the dimethoxytrityl (DMT)-phosphoramidite solid phase synthesis [52] (**Figure 1-5**) which uses a 5' triphenyl alcohol protecting group and a 2' phosphite group to methodically build specific sequences and allowing modifications to be specifically incorporated into the oligonucleotide by making modification phosphoramidites.

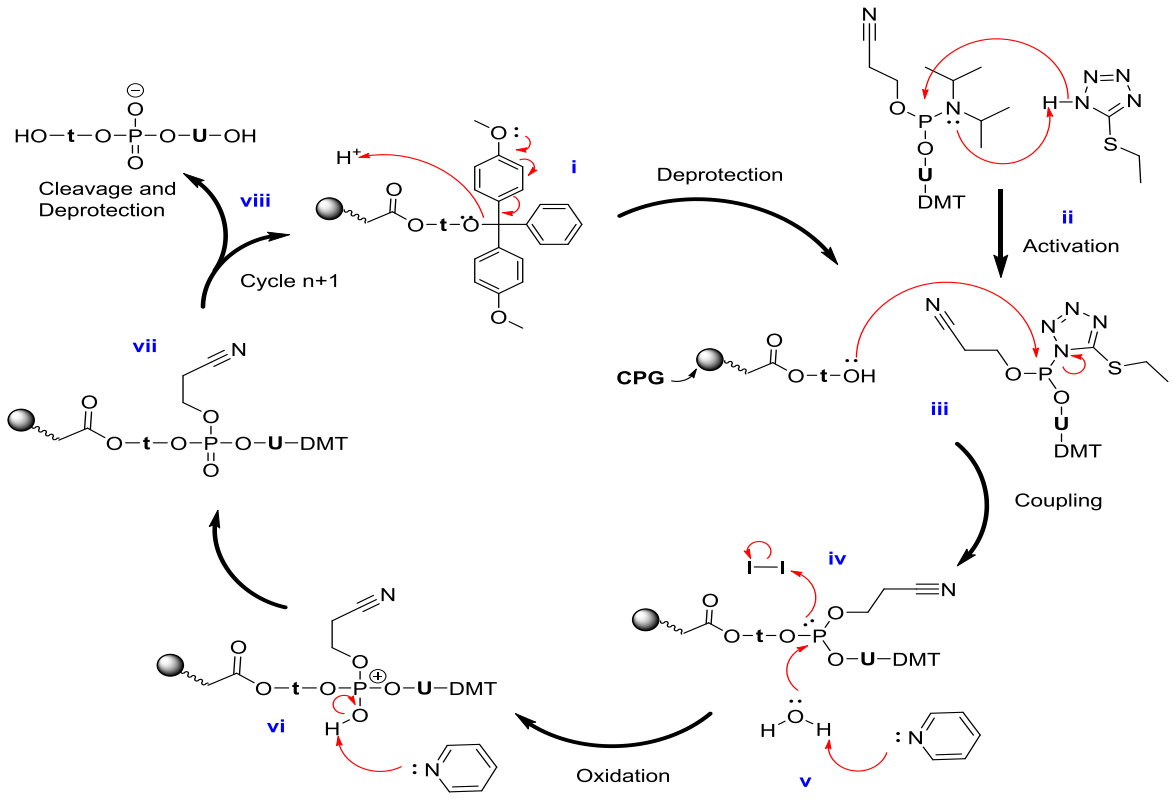

Figure 1-5: DMT-Phosphoramidite oligonucleotide synthetic loop for solid-phase RNA synthesis.

The solid support (CPG) usually comes with a DMT protected dT base already attached to the solid support so the synthesis proceeds in the 3' → 5' direction and is fully automated. The initial step is the acid mediated deprotection of the 5' DMT group (i) using trichloroacetic acid which produces a primary alcohol that will couple with the next nucleobases [53]. As the arrows show, the trityl cation that will be formed is resonance stabilized by the methoxy groups, making it easily cleaved off [53]. Before the subsequent base couples it must be activated with ethylthiotetrazole (ii), which is an excellent leaving group, which displaces the diisopropylamine group. Phosphorous is oxophilic so the free primary alcohol readily attacks the phosphite center of the activated base coupling the two nucleobases (iii), the rate of which is greatly increased due to the activation step [54]. RNA has a phosphate linkage as opposed to a phosphite so the newly formed phosphite linkage needs to be oxidized which is initiated by the nucleophilic attack of phosphorous on iodine (iv) [54]. Deprotonation of water by pyridine (v) results in the formation of a nucleophilic hydroxide anion which attacks the phosphorous center resulting in a positively charged intermediate which is readily deprotonated by another molecule of pyridine (vi) which produces the stable phosphate (vii) [53]. At this point the cycle has completed and the oligonucleotide can either keep cycling by coupling successive bases or the loop can be terminated if the desired sequence has been achieved; cleavage and deprotection results in the formation of an oligonucleotide in its native form, not considering incorporated modifications (viii).

There are a large variety of chemical modifications for oligos with more constantly emerging. The types of modifications fall in to one of three categories: 1) backbone modifications; 2) ribose sugar modifications and 3) nucleobase modifications [55].

Modifying the backbone has been extensively studied due to the fact that it can allow for mitigation of some of the polyanionic nature of an oligo as well as allowing for creation of linkages that are resistant to exo- and endo-nucleases [56]. One such example is the phosphorothioate (PS) where a sulfur atom is substituted for one of the non-bridging oxygen atoms [57] which makes the oligo much more resistant to degradation by nucleases. This cost-effective modification is compatible with many oligo synthesis protocols and is found in the FDA approved antisense drug Vitravene [58]. The PS linkage imparts chirality on to the linkage and one of the stereoisomers is a poor substrate for nucleases [59]; diastereoselective syntheses have been described [60] but typically a diastereomeric mixture results. Several PS linkages can be incorporated which further enhances stability while retaining silencing ability [61]. Silencing ability is lost however when this modification is placed within the AGO2 cleavage site as stereochemistry introduced by the PS linkage is not tolerated by the catalytic region [62].

Sugar modifications are useful for controlling the ribose ring puckering which is a crucial physical property of oligonucleotides for binding with complementary sequences, duplex conformation and enzyme substrate toleration [63]. The ribose conformation is controlled by alteration of the gauche and anomeric effects. For dsRNA, the preferred conformation is the C3'-*endo*/C2'-*exo* or sometimes referred to as the 'North' conformation [63]. Many sugar modifications are well tolerated in RNAi with one of the most popular ones being the 2'-fluoro modification [64], an RNA mimic. This modification retains the desired 'North' conformation which can be attributed to the strong gauche effect that arises from the 2'-fluorine [65]. The 2'-Fluoro is a modification that is well tolerated in siRNAs in both the sense and antisense strands.

The final type of modification is the modification of the nucleobases which has been shown to affect the thermal stability of duplexes, mitigate immunostimulation and affect off-target effects [66]. A more recent trend in nucleobases modification has seen the attachment of fluorescent modifications for the application of studying oligonucleotide therapeutics [67]. The fluorescent groups allow for monitoring of the oligos and has allowed for the development of enzymatic assays, such as the one developed for RNase H-mediated cleavage [68]. An example of a nucleobases modification is the 2,4-difluorotoluene (dFT) which can substitute thymine in DNA and Uracil in RNA [69]. It has been shown that this modification when placed in the 5' region of the guide strand increased specificity, increased RNA stacking and an increased binding affinity for RISC [70]. Unfortunately, this modification is not well tolerated elsewhere as the duplex becomes destabilized as the dFT is unable to hydrogen bond to the complementary base [70].

Since modifications introduce new chemical functionalities into siRNAs there is going to be some changes to the biophysical characteristics of the duplex; two of the important ones being the helical conformation and the thermal stability (melting temperature, T_m)[71]. The helical conformation must be A-form in order to have activity otherwise the siRNA duplex would not be a properly tolerated substrate for RISC [72]. The thermal stability is important because if the T_m of the duplex is too low the strands will dissociate with greater ease; if siRNA dissociated before RISC association RNAi is unable to occur [73]. A decrease in T_m is imparted on to duplexes for most chemical modifications as the modifications distort optimal hydrogen bonding or in some cases remove it completely

[74]. There are examples of modifications, such as those to the minor groove of the helix, that are actually capable of increasing the thermal stability of a duplex [75].

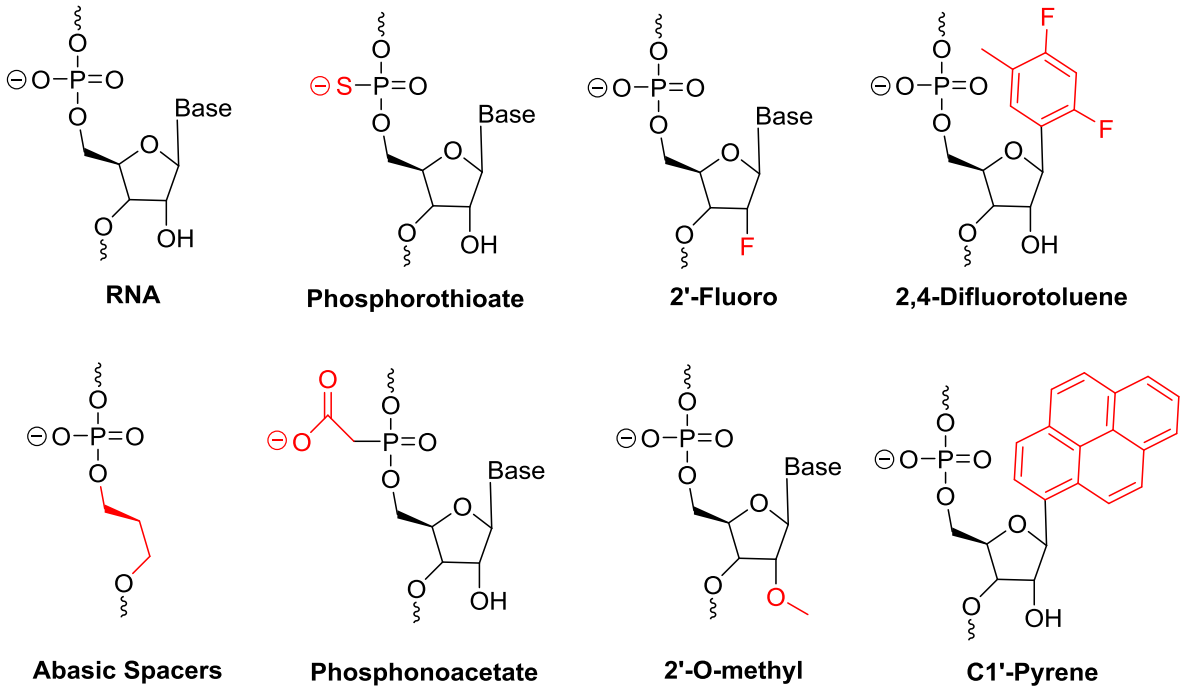

Figure 1-6: Some common chemical modifications to RNA.

1.3 – Alkyl Linker Modified Nucleic Acids

Since there is no universally accepted chemical modification that satisfies the criteria for drug design chances are if an siRNA therapeutic obtains FDA approval it will have some new type of modification never seen before. In Figure 1-6 examples of backbone modifications are shown by the phosphorothioate and the phosphonoacetate modifications. Another type of backbone modification is also present, the abasic alkyl spacers. These spacers are a relatively new and are very intriguing because of the way these spacers are surprisingly tolerated within the central region of siRNAs unlike many other modifications [76]. Even when spanning the AGO2 catalytic region of the sense

strand, effective silencing is still observed even though the alkyl linkages are most likely not cleaved whilst retaining potency close to wild-type [77]. Even more intriguing is that the incorporation of these modifications within the central region of the sense strand reduces off-target effects without reducing silencing activity [78]. The linker has no rigidity to it which allows RNA duplexes to maintain their active A-helix conformation [79]. An appealing feature about these linkers if they were to ever make it in to *pharma* is that the synthesis of the phosphoramidites is simple and very cost-effective. Since this type of backbone modification is relatively new there has not been much variety in the types of abasic linkers that have been tested; the two major types are: 1) simple alkyl chains and 2) polyethylene glycol chains [79]. This is where the knowledge gap begins; there is currently no peer-reviewed literature on simple abasic alkylamino chain spacers that have been modified and incorporated in to RNA for gene silencing purposes.

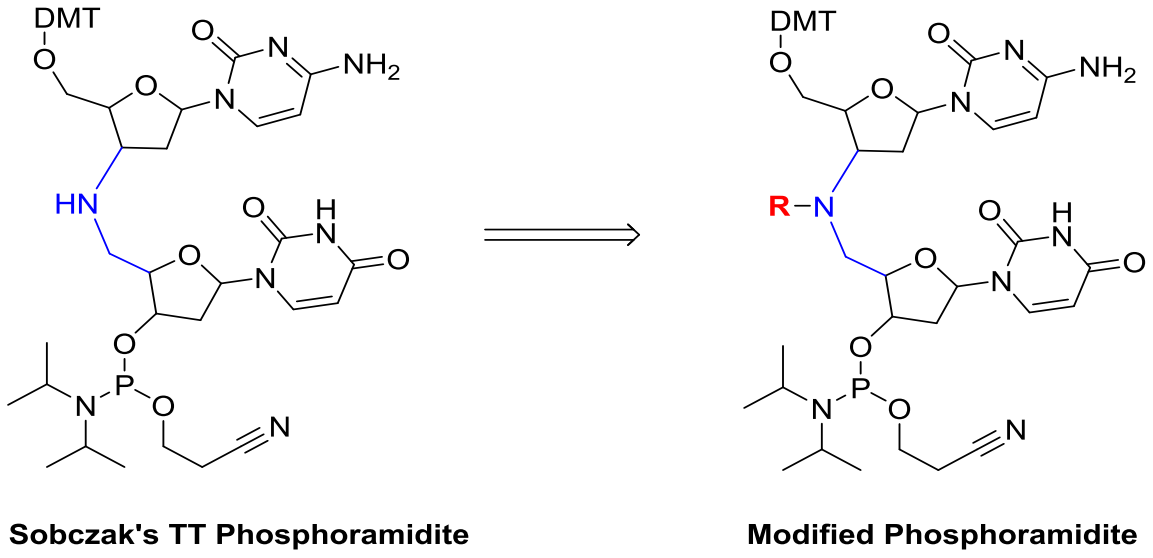

Figure 1-7: The structure of Sobczak's amine linker phosphoramidite and the easy single step modification that is possible.

A study in 2011 by Sobczak et al., showed that siRNAs with simple alkyl-amino linkages between bases retained excellent gene silencing ability. The linker simply replaced the phosphodiester bond between bases, which offers an easy modification site on the secondary amine (**Figure 1-7**). Although this is an excellent novel type of modifiable linkage its progress in biological studies has been hindered due to the complex synthesis. Using this type of modification approach on a secondary amine, an abasic linker with evenly dispersed secondary amines (**Figure 1-8**) could be a potential pathway to begin investigating how modified abasic spacers behave in RNAi.

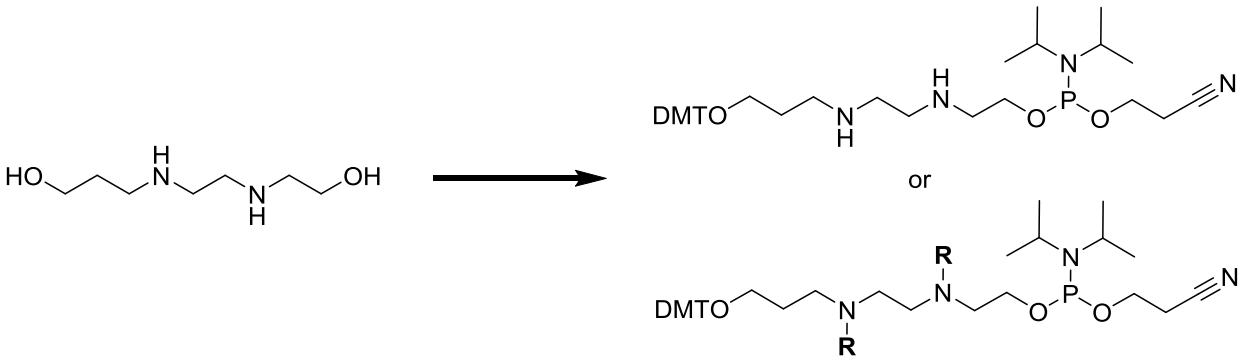

Figure 1-8: New amine dispersed abasic linkers.

1.3.1 – Modification Purpose and Benefits

The readily available starting material can be turned in to a phosphoramidite for RNA synthesis in a few easy steps. This linker affords the ability to test many easy and readily usable modifications in a timely and cost effective manner as the synthesis is cheap, straightforward and comparatively high yielding compared to introducing modifications on Sobczak's linker, as an example. The addition of this modification would replace two base

pairs (**Figure 1-9**) and with the introduction of this linker new favourable characteristics are imparted up an RNA strand.

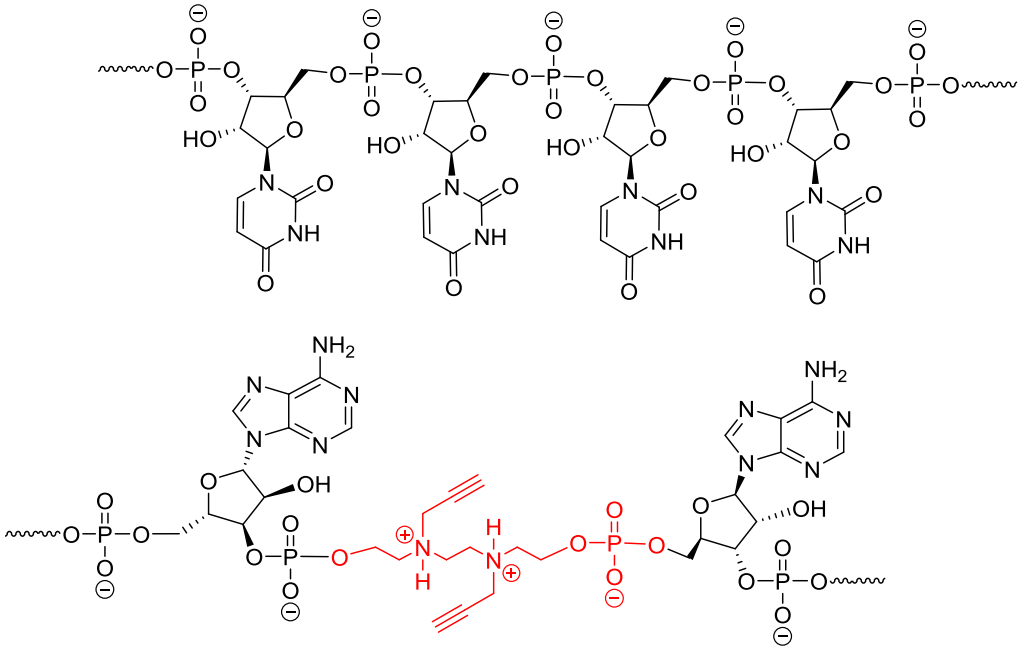

Figure 1-9: Structural representation of the new propargyl modified linker in an RNA duplex at physiological pH.

The first noticeable trait of this linker is that both tertiary amines are protonated at physiological pH. This is an excellent feature for addressing cell delivery; as mentioned earlier there is electrostatic repulsion between oligonucleotides and the surface of cell membranes. Not only does this linker introduce two positive charges, it also removes a negatively charged phosphodiester which further decreases the polyanionic nature. The fine tuning of adding multiple linkers could afford a very simple means of significantly reducing the polyanionic nature of nucleic acid strands while retaining activity.

As the two previous figures depict, attaching simple modifications to this new linker scaffold is very simple; this provides a new platform from which more intricate chemistry

can be done. Figure 1-9 shows the modified linker with a terminal propargyl group. This alkyne could be easily reacted to attach biological moieties using the well-established azide-alkyne click reaction which has been proven as a biocompatible way of attaching biological moieties [80]. Biomolecules such as cholesterol are commonly seen affixed to siRNAs; however these are usually 3' modifications. Another attractive feature of affixing biological moieties is that with an abasic linker such as this one, the molecular weight doesn't increase much (if at all) compared to wild type, which is beneficial as smaller molecules have easier times traversing cellular membranes simply due to their size [81].

The introduction of this linker into an siRNA duplex would undoubtedly decrease the thermal stability of the duplex as two of the base pairs are removed therefore removing the stabilizing hydrogen bonding at the site of the modification. An interesting study in 2010 by Maier et al., showed that destabilization using base pair mismatches in the central region of the sense strand in siRNAs (bp 9 – 12) could significantly improve their potency [82]. By replacing central region mismatched with this linker, it is plausible that the introduction of destabilization occurring would be beneficial in this case as well. What is now really interesting about placing this modification near the central region is that if activity is retained it will open up a new avenue in exploring modifications in and around the Argonaute2 cleavage site.

With the literature showing a lot of promise for alkyl spacers in siRNAs, there are more than enough reasons to pursue developing new modifications based around these abasic alkylamino spacers.

1.4 – Project Definition

With the excellent ability to silence genes at the pre-translational level having many uses there is promise for siRNAs in the near future, such as being used as therapeutic agents to treat genetic diseases. These siRNA therapeutics will most likely have some sort of synthetic chemical modification(s). As the library of chemical modifications keeps growing new siRNAs will be synthesized that have enhanced cellular permeability, lower degradation by nucleases and reduced off-target effects.

This project will involve the incorporation of an abasic alkyl spacer with secondary nitrogen atoms into RNA oligonucleotides. A more simplified version of this type of spacer was previously studied by Dr. Tim Efthymiou and this is an extension of his work. The modification will be synthesized using organic chemistry and synthetically incorporated into RNA oligonucleotides. The synthesized RNA strands will be annealed with their compliment sequence strands to form siRNA duplexes. The siRNA strands will undergo hybridization testing to assess how the modifications affect the thermal stability of the RNA duplex as well as to whether the introduction of this modification alters the helical conformation of the native alpha helical structure of wt RNA duplexes. The siRNAs will also have their ability to silence gene expression assessed firstly using the dual luciferase reporter system which is an exogenous target. This bioassay is a screening method that will be used to identify certain siRNA duplexes that show promise with this chemical modification is certain positions. The top performing strands in the luciferase assay will be identified and used as a screen to select which anti-BCL2 strands should be tested. The effectiveness of these strand's ability to effectively knock down the BCL2 gene will be

studied using qRT-PCR which provides a more clinically relevant assessment of the actual silencing capability of siRNAs with these modifications.

2.0 - Experimental

2.1 – General Synthetic Method

All chemicals and solvents were purchased from commercial sources without further purification unless indicated otherwise. Amine bases, such as TEA, were distilled under N_2 gas using a simple glass still head before their usage. All flash chromatography purifications were done using Silicycle Siliaflash 60 (230-400 mesh). ^{1}H, ^{13}C and ^{31}P NMRs were recorded in $CDCl_3$ using an Oxford AS400 (400 MHz) NMR spectrometer. High resolution mass spectrometry was performed using a Micromass AutoSpec Ultra Magnetic sector mass spectrometer.

2.2 – Synthesis and Characterization of Organic Compounds

2.2.1 – Synthesis of *N,N'*-bis(2-((tert-butyldimethylsilyl)oxy)ethyl)ethane-1,2-diamine – Compound (1)

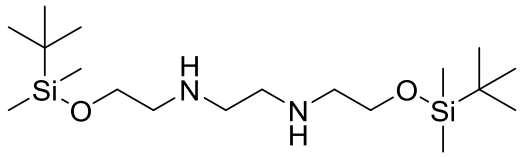

(1)

A solution of *N,N'*-bis(2-hydroxyethyl)ethandiamine (4.95 g, 33.4 mmol) in 175 ml of CH_2Cl_2 was prepared and allowed to stir for 10 minutes to dissolve the starting material. To this was added diisopropylethylamine (14.5 ml, 83.5 mmol) followed by the drop-wise addition of a solution of *tert*-butyldimethylsilylchloride (10.57 g, 70.1 mmol) in 50ml of CH_2Cl_2 over several minutes. The reaction was left stirring at room temperature for 12

hours. A saturated sodium bicarbonate solution extraction was performed and the organic layer was dried with Na_2SO_4. The organic layer was concentrated *in vacuo* to afford an oil which was purified by silica gel chromatography eluting with a gradient of MeOH/CH_2Cl_2 (100% CH_2Cl_2 to 5% MeOH in CH_2Cl_2) to afford the title compound as a clear yellow oil (8.39 g, 68%); ^{1}H NMR (400 MHz, $CDCl_3$) δ 0.04 (s, 12H), 0.87 (s, 18H), 2.40 (br. s, 2H), 2.72 (t, 4H, *J* = 5.86 Hz), 2.76 (s, 4H), 3.70 (t, 4H, *J* = 5.5 Hz); ^{13}C NMR (125 MHz, $CDCl_3$) δ – 5.36, 18.26, 25.90, 53.13, 57.54, 62.82, 77.85; ESI-HRMS (ES^+) m/z calculated for $C_{18}H_{44}N_2O_2Si_2$: 377.3014, found 377.3023 $[M+H]^+$

2.2.2 – Synthesis of *N,N'*-diallyl-*N,N'*-bis(2-((tert-butyldimethylsilyl)oxy)ethyl)ethane-1,2-diamine – Compound (2)

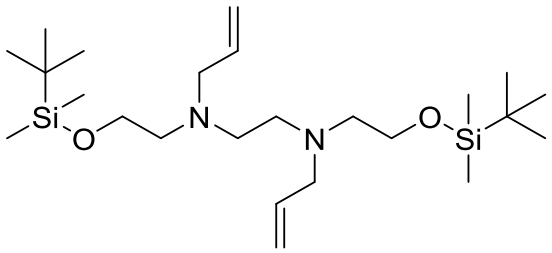

(2)

A solution of **1** (2.03 g, 5.395 mmol) in 50 ml of CH_2Cl_2 was prepared and allowed to cool in an ice bath while a mineral oil-sodium hydride dispersion (60% NaH) (0.68 g, 16.2 mmol) was washed three times with hexanes to remove as much mineral oil as possible. The sodium hydride was then slowly added to the solution of **1**. Once the reaction mixture was no longer bubbling; allyl bromide (1.16 ml, 13.5 mmol) was added over the course of 3 minutes. The reaction was gradually warmed to room temperature then left to stir for 6 hours and was then extracted with saturated sodium bicarbonate. The organic layer was

collected and dried with Na_2SO_4 then concentrated *in vacuo* to afford an oil which was purified using silica gel chromatography eluting with a gradient of Hexanes/EtOAc (100% Hexanes to 30% EtOAc in Hexanes) to afford the title compound as a yellow oil (2.46 g, 74%); ^{1}H NMR (400 MHz, $CDCl_3$) δ 0.05 (s, 12H), 0.89 (s, 18H), 2.59 (s, 4H), 2.61 (t, 4H, J = 7.03 Hz), 3.15 (d, 4H, J = 6.3 Hz), 3.67 (t, 4H, J = 6.6 Hz), 5.13 (dd, 4H, J = 9.8 Hz), 5.84 (m, 2H) : ^{13}C NMR (125 MHz, CDCl3) δ -5.29, 18.32, 25.95, 52.73, 56.38, 58.58, 61.90, 117.13, 135.97; ESI-HRMS (ES^+) m/z calculated for $C_{24}H_{52}N_2O_2Si_2$ 468.3567, found 468.3498 $[M+H]^+$

2.2.3 – Synthesis of 2,2'-(ethane-1,2-diylbis(allylazanediyl))bis(ethan-1-ol) – Compound (3)

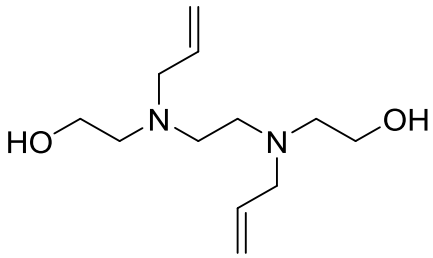

(3)

To a solution of **2** (0.59 g, 1.42 mmol) in 10ml of THF was added 1.0M tetrabutylammonium fluoride (4.96 ml, 4.96 mmol) over 3 minutes. The reaction mixture was left stirring at room temperature for 4.5 hours at which point TLC revealed consumption of the starting material **2** (R_f = 0.92 in 15% MeOH in CH_2Cl_2) . The reaction mixture was concentrated *in vacuo* which produced a thick yellow oil which was further purified using silica gel chromatography eluting with a gradient of MeOH/CH_2Cl_2 (2% MeOH in CH_2Cl_2 to 5% MeOH in CH_2Cl_2) to afford the title compound as a thick yellow oil

(0.30 g, 92%); ^{1}H NMR (400 MHz, $CDCl_3$) δ 2.70 (m, 8H), 3.27 (d, 4H, J = 6.6 Hz), 3.66 (t, 4H, J = 5.1 Hz), 5.23 (dm, 4H, J = 11.7 Hz), 5.91 (m, 2H): ^{13}C NMR (125 MHz, $CDCl_3$) δ 51.62, 55.61, 58.18, 59.86, 118.44, 134.58; ESI-HRMS (ES^+) m/z calculated for $C_{12}H_{24}N_2O_2$: 229.1911, found 229.1920 $[M+H]^+$

2.2.4 – Synthesis of 2-(allyl(2-(allyl(2-(bis(4 -methoxyphenyl)(phenyl)methoxy)ethyl)amino)ethyl)amino)ethan-1-ol – Compound (4)

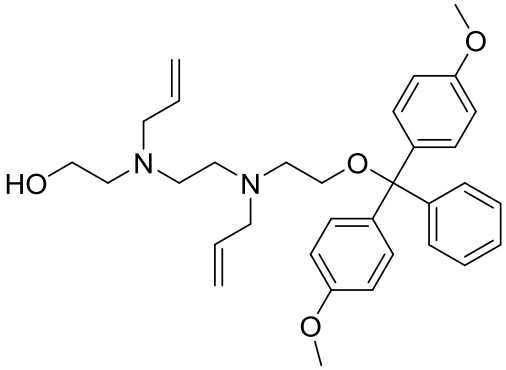

(4)

To a solution of **3** (0.61 g, 2.61 mmol)in 30 ml of CH_2Cl_2 was added diisopropylethylamine (0.37 ml, 2.09 mmol) followed by the drop-wise addition of 4,4'-dimethoxytrityl chloride (0.71 g, 2.10 mmol) in 5 ml of CH_2Cl_2 over 10 minutes. The reaction was left to stir overnight at which time the reaction became bright yellow. The reaction was extracted with saturated sodium bicarbonate and the organic layer was collected and dried with Na_2SO_4. The organic layer was concentrated *in vacuo* to produce an orange- yellow oil which was further purified using silica gel chromatography eluting with a gradient of Hexanes/EtOAc (50% hexanes in EtOAc to 10% hexanes in EtOAc) to afford the title compound as an oil (0.63 g, 46 %); ^{1}H NMR (400 MHz, CDCl3) δ 1.23 (s, 1H), 2.67 (m, 4H),

2.76 (t, 2H, J = 5.5 Hz), 2.87 (t, 2H, J = 5.7 Hz), 3.20 (m, 4H), 3.26 (t, 2H, J = 5.6 Hz), 3.55 (t, 2H, J = 4.7 Hz), 3.75 (s, 6H), 5.14 (dd, 4H, J = 10.2 Hz), 5.83 (m, 2H), 6.8 (dt, 4H, J = 9.4 Hz) , 7.17-7.27 (m, 7H), 7.39 (m, 2H) ; ^{13}C NMR (125 MHz, $CDCl_3$) δ 29.64, 50.45, 51.44, 52.78, 55.18, 55.58, 57.25, 57.84, 59.03, 60.39, 86.55, 113.11, 126.78, 127.76, 127.82, 129.92, 133.62, 135.89, 144.68, 158.46; ESI-HRMS (ES^+) m/z calculated for $C_{33}H_{42}N_2O_4$: 530.3113, found 530.3183 $[M+H]^+$

2.2.5 – Synthesis of 2-(allyl(2-(allyl(2-(bis(4-methoxyphenyl)(phenyl)methoxy)ethyl)amino)ethyl)amino)ethyl (2-cyanoethyl) diisopropylphosphoramidite – Compound (5)

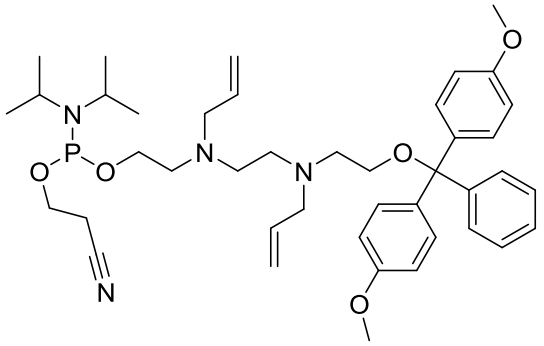

(5)

A solution of **4** (0.33 g, 0.63 mmol) in 10 ml of dry CH_2Cl_2 was prepared in a flame dried round bottom flask under a $N_{2(g)}$ atmosphere. Freshly distilled diisopropylethylamine (0.55 ml, 3.16 mmol) was added via an inert transfer. 2-cyanoethyl-*N,N*-diisopropylchlorophosphoramidite (0.42 ml, 1.89 mmol) was added to the reaction over 15 seconds. The reaction proceeded for 3 hours at which point TLC analysis indicated consumption of the starting material **4** (R_f = 0.18 in EtOAc)**.** The reaction mixture was concentrated *in vacuo* producing a yellow oil which was further purified using silica gel chromatography eluting with a gradient of Hexanes/EtOAc (20% EtOAc in hexanes to 50%

EtOAc in hexanes, with each mobile phase having 2% triethylamine) to afford the title compound as a clear oil (0.45 g, 71%); ^{1}H NMR (400 MHz, $CDCl_3$) δ 1.18 (m, 12H), 2.57 (m, 6H), 2.70 (m, 5H), 3.14 (m, 6H), 3.61 (m, 3H), 3.80 (s, 6H), 5.16 (m, 4H), 5.83 (m, 2H), 6.82 (d, 4H, J = 9 Hz), 7.20 – 7.35 (m, 7H), 7.45 (m, 2H); ^{13}C NMR (125 MHz, $CDCl_3$) δ 20.27, 24.62, 42.93, 52.66, 54.14, 55.18, 58.27, 61.65, 62.23, 85.98, 112.99, 117.25, 126.58, 127.69, 128.19, 130.00, 135.79, 136.51, 145.21, 158.33; ^{31}P NMR (125 MHz, $CDCl_3$)δ 147.64; ESI-HRMS (ES^+) m/z calculated for $C_{43}H_{62}N_3O_5P$: 730.4124, found 647.3183 $[M+H]^+$ (Hydrolyzed product).

2.2.6 – Synthesis of *N,N'*-bis(2-((tert-butyldimethylsilyl)oxy)ethyl)-*N,N'*-di(prop-2-yn-1-yl)ethane-1,2-diamine – Compound (6)

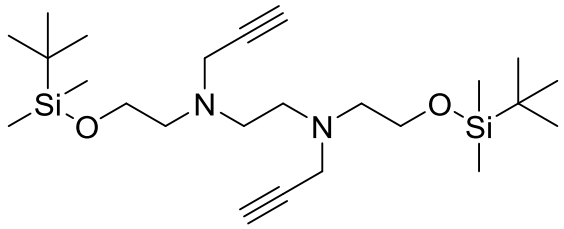

(6)

A solution of **1** (5.07 g, 13.47 mmol) in 50 ml of dry CH_2Cl_2 was prepared in flame dried glassware sealed with a septum under a $N_{2(g)}$ atmosphere. To this was added diisopropylethylamine (7.1 ml, 40.4 mmol) that had been freshly distilled under $N_{2(g)}$ using a syringe and needle. An anhydrous transfer of propargyl bromide (80% wt/ml solution in toluene) (3.1 ml, 33.7 mmol) to the reaction was accomplished and this reaction was stirred for 12 hours at room temperature while remaining under an $N_{2(g)}$ atmosphere. The reaction solution was extracted with saturated sodium bicarbonate. The organic layer was collected and dried with Na_2SO_4 and was subsequently dried *in vacuo* to afford an oil which

was further purified using silica gel chromatography eluting with a gradient of hexanes/EtOAc (100% hexanes to 20% EtOAc in Hexanes) to afford the title compound as a dark yellow oil (5.36 g, 88%); ^{1}H NMR (400 MHz, $CDCl_3$) δ 0.00 (s, 12H), 0.84 (s, 18H), 2.11 (s, 2H), 2.61 (m, 8H), 3.44 (t, 4H, J = 1.6 Hz), 3.61 (t, 4H, J = 6.3 Hz); ^{13}C NMR (125 MHz, $CDCl_3$) δ -5.29, 18.32, 25.95, 52.73, 56.38, 58.58, 61.92, 117.13, 135.97; ESI-HRMS (ES^+) m/z calculated for $C_{24}H_{48}N_2O_2Si_2$: 453.3327 found 453.3325 $[M+H]^+$

2.2.7 – Synthesis of 2,2'-(ethane-1,2-diylbis(prop-2-yn-1-ylazanediyl))bis(ethan-1-ol) – Compound (7)

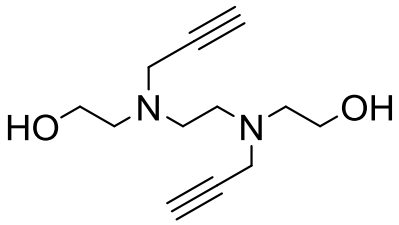

(7)

A solution of **5** (1.79 g, 3.95 mmol) in 10 ml THF had 1.0M tetrabuytlammonium fluoride (13.8 ml, 13.8 mmol) added drop-wise over the course of 3 minutes. The reaction mixture was left stirring at room temperature for 5 hours, at which point TLC revealed consumption of the starting material **5** (R_f = 0.72 in EtOAc). The reaction mixture was concentrated *in vacuo* which produced a dark yellow oil which was further purified using silica gel chromatography eluting with a gradient of MeOH/CH_2Cl_2 (2% MeOH in CH_2Cl_2 to 10% MeOH in CH_2Cl_2) to afford the title compound as a thick yellow oil (0.82 g, 93%); ^{1}H NMR (400 MHz, $CDCl_3$) δ 2.23 (s, 2H), 2.74 (m, 8H), 3.49 (s, 4H), 3.62 (t, 4H, J = 5.1 Hz) ; ^{13}C NMR (125 MHz, CDCl3) δ 42.38, 49.75, 54.60, 58.80, 72.96, 77.78; ESI-HRMS (ES^+) m/z calculated for $C_{12}H_{20}N_2O_2$: 225.1598, found 225.1598 $[M+H]^+$

2.2.8 – Synthesis of 2-((2-((2-(bis(4-methoxyphenyl)(phenyl)methoxy)ethyl)(prop-2-yn-1-yl)amino)ethyl)(prop-2-yn-1-yl)amino)ethan-1-ol – Compound (8)

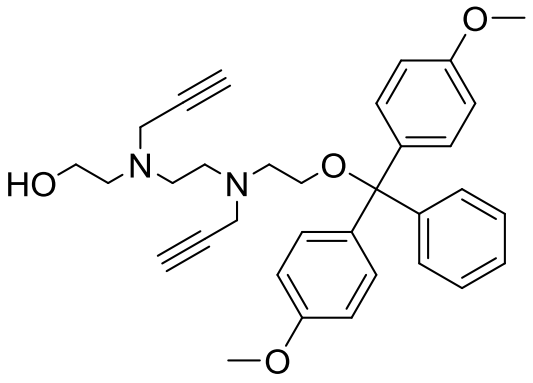

(8)

A solution of **7** (0.54 g, 2.41 mmol) in 30 ml of CH_2Cl_2 was added diisopropylethylamine (0.34 ml, 1.93 mmol) which was left to stir. Another solution of 4,4'-dimethoxytrityl chloride in 5 ml of CH_2Cl_2 was prepared and was subsequently added to the solution being stirred drop-wise over 10 minutes. The reaction was left to stir overnight at which point it was extracted with saturated sodium bicarbonate. The organic layer was collected and dried with Na_2SO_4 and concentrated *in vacuo* to produce a dark oil which was further purified using silica gel chromatography eluting with a gradient of Hexanes/EtOAc (20% EtOAc in Hexanes to 100% EtOAc) to afford the title compound as a dark oil (0.56 g, 46%); ^{1}H NMR (400 MHz, CDCl3) δ 1.27 (s, 1H), 2.19 (dt, 2H, J = 14.85 Hz), 2.67 (m, 6H), 2.79 (t, 2H, J = 5.9 Hz), 3.24 (t, 2H, J = 5.7 Hz), 3.41 (m, 2H), 3.47 (m, 2H), 3.52 (t, 2H, J = 5.3 Hz), 3.80 (s, 6H), 6.84 (dt, 4H, J = 8.6 Hz), 7.20-7.35 (m, 7H), 7.44-7.48 (m, 2H); ^{13}C NMR (125 MHz, CDCl3) δ 42.24, 42.70, 50.26, 51.49, 53.20, 54.38, 55.01, 58.80, 61.67, 72.42, 76.13, 85.89, 112.73, 126.33, 127.42, 127.87, 129.70, 136.03, 144.75, 158.06; ESI-HRMS (ES^+) m/z calculated for $C_{33}H_{38}N_2O_4$: 527.2904, found 527.2899 $[M + H]^+$

2.2.9 – Synthesis of 2-((2-((2-(bis(4-methoxyphenyl)(phenyl)methoxy)ethyl)(prop-2-yn-1-yl)amino)ethyl)(prop-2-yn-1-yl)amino)ethyl (2-cyanoethyl) diisopropylphosphoramidite – Compound (9)

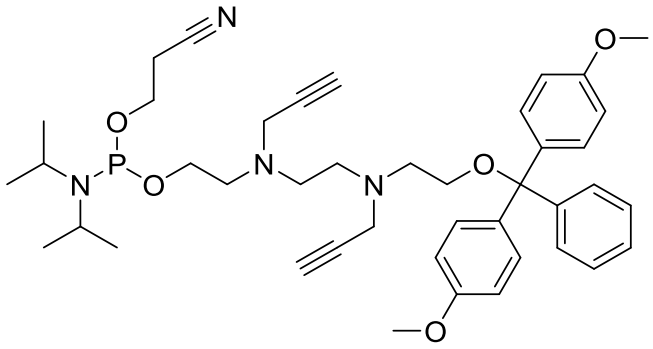

(9)

A solution of **8** (0.36 g, 0.68 mmol) in 10 ml of dry CH_2Cl_2 was prepared using flame dried glassware under a $N_{2(g)}$ atmosphere. To this solution was added freshly distilled diisopropylethylamine (0.59 ml, 3.40 mmol). 2-cyanoethyl-*N,N*-diisopropylchlorophosphoramidite (0.45 ml, 2.04 mmol) was added over 15 seconds and then the reaction was stirred for 2.5 hours at which point TLC analysis showed consumption of the starting material, **8** (R_f = 0.88 in EtOAc). The reaction was concentrated *in vacuo* affording a yellow oil which was further purified using silica gel chromatography eluting with a gradient of Hexanes/EtOAc (20% EtOAc in Hexanes to 50% EtOAc in Hexanes keeping 2% TEA with each mobile phase) affording the title compound as a clear oil (0.35 g, 70.5%); ^{1}H NMR (400 MHz, $CDCl_3$) δ 1.29 (m, 12H), 2.19 (dt, 2H, J = 10.94 Hz), 2.64 (m, 8H), 2.78 (m, 6H), 3.16 (t, 2H, J = 5.9 Hz), 3.46 (m, 5H), 3.79 (s, 6H), 6.82 (dt, 4H, J = 8.6 Hz), 7.20-7.35 (m, 7H), 7.44-7.48 (m, 2H); ^{13}C NMR (125 MHz, $CDCl_3$) δ 20.32, 21.20, 22.96, 24.52, 25.89, 43.07, 45.24, 47.65, 52.04, 53.87, 55.16, 58.51, 62.36, 72.93, 79.03, 86.01, 113.00, 117.62, 126.57, 128.15, 129.98, 136.40, 145.13, 158.32; ^{31}P NMR (125 MHz,

$CDCl_3$) δ 147.91; ESI-HRMS (ES^+) m/z calculated for $C_{42}H_{55}N_4O_5P$ 726.3911, found 644.2881 $[M+H]^+$ (Hydrolyzed product).

2.2.10 – Synthesis of *N,N′*-(ethane-1,2-diyl)bis(*N*-(2-((tert butyldimethylsilyl) oxy)ethyl)acetamide) – Compound (10)

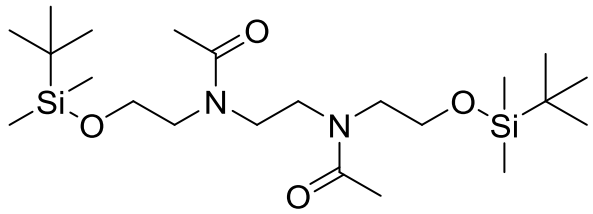

(10)

To a solution of **1** (0.48 g, 1.28 mmol) in 15 ml of CH_2Cl_2 was added 4,4-dimethylaminopyridine (DMAP) (0.08 g, 0.67mmol) and this mixture was stirred until both reagents fully dissolved. To this solution was added acetic anhydride (0.38 ml, 3.99 mmol) and the resulting mixture was left to stir for 20 hours at which point the reaction was extracted with saturated sodium bicarbonate. The organic layer was collected and dried with Na_2SO_4 which was concentrated *in vacuo* to afford a yellow oil which was further purified using silica gel chromatography eluting with a gradient of MeOH/CH_2Cl_2 (2% MeOH in CH_2Cl_2 to 5% MeOH in CH_2Cl_2) to afford the title compound as a white-yellow powder. (0.56 g, 93%); ^1H NMR (400 MHz, $CDCl_3$) δ 0.03 (s, 12H), 0.87 (s, 18H), 2.12 (s, 6H), 3.46 (m, 8H), 3.73 (t, 4H, J = 5.5 Hz); ^{13}C NMR (125 MHz, $CDCl_3$) δ -5.55, 18.16, 21.72, 25.80, 43.22, 51.23, 60.77, 171.72: ESI-HRMS (ES^+) m/z calculated for $C_{22}H_{48}N_2O_4Si_2$: 461.3225 found 461.3242 $[M+H]^+$

2.2.11 – Synthesis of *N,N′*-(ethane-1,2-diyl)bis(N-(2-hydroxyethyl)acetamide) – Compound (11)

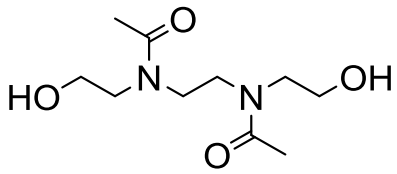

(11)

To a solution of **10** (1.02 g, 2.21 mmol) in 10 ml of THF was added triethylamine trihydrofluoride (0.51 ml, 3.10 mmol) drop-wise over 5 minutes. The resulting reaction mixture was allowed to stir at room temperature for 3 hours at which point TLC analysis indicated the consumption of the starting material, **10** (R_f = 0.79 in 15% MeOH in CH_2Cl_2). The reaction was concentrated *in vacuo* to afford an pale yellow oil which was further purified using silica gel chromatography eluting with a gradient of MeOH/CH_2Cl_2 (5% MeOH in CH_2Cl_2 to 20% MeOH in CH_2Cl_2) to afford the title compound as a pale golden coloured oil (0.47 g, 92%); ^{1}H NMR (400 MHz, $CDCl_3$) δ 2.11 (s, 6H), 3.50 (m, 8H), 3.79 (t, 4H, J = 5.5 Hz); ^{13}C NMR (125 MHz, $CDCl_3$) δ 21.87, 46.19, 53.40, 60.27; ESI-HRMS (ES^+) m/z calculated for $C_{10}H_{20}N_2O_4$: 233.1496 found 233.1500 $[M+H]^+$

2.2.12 – Synthesis of *N*-(2-(bis(4-methoxyphenyl)(phenyl)methoxy)ethyl)-*N*-(2-(N-(2-hydroxyethyl)acetamido)ethyl)acetamide – Compound (12)

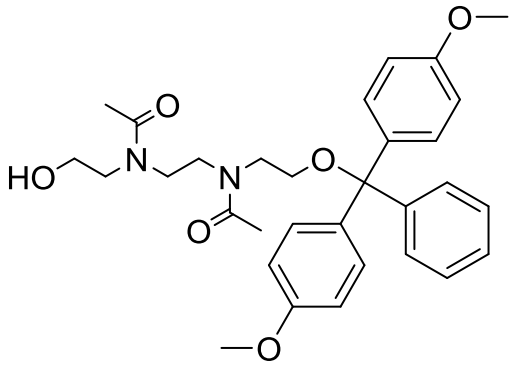

(12)

A solution of **11** (1.12 g, 4.82 mmol) in 30 ml of CH_2Cl_2 had triethylamine (0.34 ml, 3.35 mmol) added to it and the resulting mixture was allowed to stir for 10 minutes to dissolve the starting material. Meanwhile, another solution of 4,4'-dimethoxytrityl (0.98 g, 2.89 mmol) in 5 ml of CH_2Cl_2 was prepared and added drop-wise to the first solution over a period of 10 minutes. The reaction was then left to stir at room temperature overnight at which point the reaction was extracted with saturated sodium bicarbonate. The organic layer was collected and dried with Na_2SO_4 and concentrated *in vacuo* to afford a yellow oil. This oil was further purified using silica gel chromatography eluting with a gradient of MeOH/CH_2Cl_2 (2% MeOH in CH_2Cl_2 to 10% MeOH in CH_2Cl_2) to afford the title compound as a bright yellow oil (1.13 g, 44%); ^{1}H NMR (400 MHz, $CDCl_3$) δ 2.13 (m, 6H), 3.27 (m, 2 H), 3.37-3.64 (m, 8H), 3.70-3.84 (m, 8H), 6.84 (m, 4H), 7.17-7.33 (m, 7H), 7.36-7.41 (m, 2H); ^{13}C NMR (125 MHz, $CDCl_3$) δ 21.96, 46.90, 53.95, 55.23, 60.44, 81.37, 86.68, 113.12, 127.02, 127.76, 129.12, 129.95, 135.73, 139.51, 147.37, 158.52, 172.92; ESI-HRMS (ES^+) m/z calculated for $C_{31}H_{38}N_2O_6$: 557.2622, found 557.2611 $[M+H]^+$

2.2.13 – Synthesis of 2-(*N*-(2-(*N*-(2-(bis(4-methoxyphenyl)(phenyl)methoxy)ethyl)acetamido)ethyl)acetamido)ethyl (2-cyanoethyl) diisopropylphosphoramidite – Compound (13)

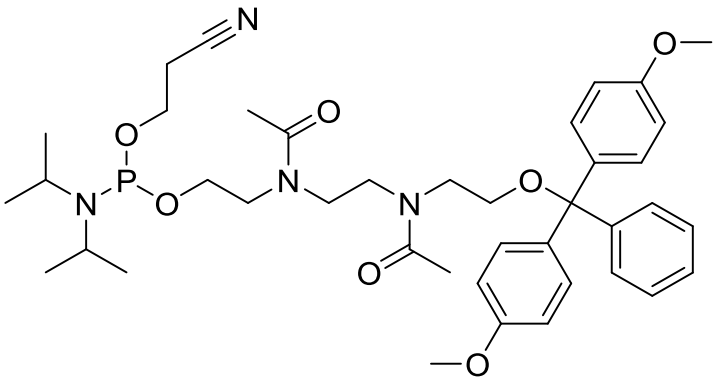

(13)

A solution of **12** (0.12 g, 0.21 mmol) in 8 ml of dry CH_2Cl_2 was prepared in flame dried glassware. To this was added freshly distilled triethylamine (0.15 ml, 1.03 mmol) and the reaction was placed under a $N_{2(g)}$ atmosphere. 2-cyanoethyl-*N,N*-diisopropylchlorophosphoramidite (0.14 ml, 0.56 mmol) was added over 15 seconds and then the reaction was stirred at room temperature for 3.5 hours at which point TLC analysis indicated consumption of the starting material, **12** (R_f = 0.28 in EtOAc wth 2% TEA). The reaction was then concentrated *in vacuo* which produced a yellow oil. This oil was then further purified using silica gel chromatography eluting with a gradient of Hexanes/EtOAc (50% Hexanes in EtOAc to 100% EtOAc keeping 2% TEA for each mobile phase) to afford the title compound as a clear oil (0.11 g, 71%); ^{1}H NMR (400 MHz, $CDCl_3$) δ 1.26 (m, 12H), 2.13 (m, 6H), 3.27 (m, 2H), 3.36-3.66 (m, 8H), 3.72 (m, 1H), 3.81 (s, 6H), 6.79-6.86 (m, 4H), 7.17-7.33 (m, 7H), 7.37 (m, 2H); ^{13}C NMR (125 MHz, $CDCl_3$) δ 17.01, 20.18, 21.97, 22.54, 23.61, 24.91, 25.52, 42.77, 42.93, 46.30, 47.06, 49.74, 51.13, 53.54,

54.18, 55.70, 58.78, 58.94, 62.01, 62.86, 72.44, 78. 31, 86.08, 113,59, 118.29, 126.97, 127.95, 128.04, 129.67, 136.72, 145.83, 158.49, 172.41; ESI-HRMS (ES^+) m/z calculated for $C_{40}H_{55}N_4O_7P$: 734.3881, found 651.2703 $[M+H]^+$ (Hydrolyzed Product)

2.2.14 – Synthesis of (3S,8S,9S,10R,13R,14S,17R)-10,13-dimethyl-17-((R)-6-methylheptan-2-yl)-2,3,4,7,8,9,10,11,12,13,14,15,16,17-tetradecahydro-1H-cyclopenta[a]phenanthren-3-yl methanesulfonate – Compound (14)

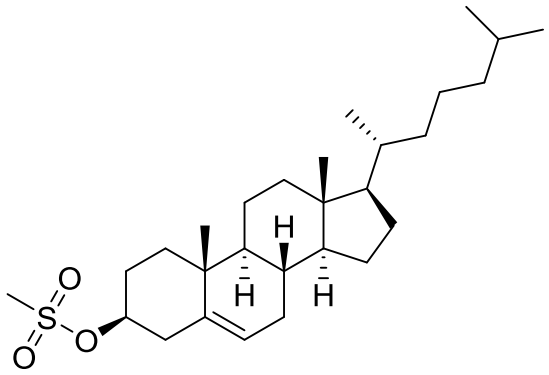

(14)

To a solution of cholesterol (2.14 g, 5.81 mmol) in 15 ml of CH_2Cl_2 was added triethylamine(0.88 ml, 8.71 mmol) followed by mesylchloride (0.80 g , 6.97 mmol). The reaction was left stirring for 16 hours at which point the reaction was concentrated *in vacuo* to produce a white solid which was purified further using silica gel chromatography eluting with a gradient of EtOAc/Hexanes (100% Hexanes to 25% EtOAc in Hexanes) to afford the title compound as a white crystalline powder (2.59 g, 96%, R_f = 0.77 in 25% EtoAc in hexanes). NMR shifts as reported by (Krishna and Verma, 2011), ^{1}H NMR (400 MHz, $CDCl_3$) δ 0.64 (s, 6H), 0.82 (d, 3H), 0.87 (d, 3H), 0.98 (s, 6H), 1.03-1.15 (m, 5H), 1.22 (d, 2H), 1.30-1.34 (m, 3H), 1.41-1.53 (m, 9H), 1.75-1.81 (m, 1H), 1.85-1.88 (dd, 1H), 1.93-2.04 (m, 2H), 2.43-2.51, (m, 2H), 2.97 (s, 3H), 4.48 (s, 1H), 5.37 (s, 1H); ^{13}C NMR (125 MHz,

$CDCl_3$) δ 19.4, 20.7, 22.7, 23.2, 24.6, 27.3, 27.7, 28.1, 29.9, 30.0, 31.9, 35.8, 36.1, 36.76, 37.2, 37.7, 38.6, 39.9, 44.0, 50.8, 55.9, 56.49, 82.0, 123.69, 138.53.

2.2.15 – Synthesis of (3R,8S,9S,10R,13R,14S,17R)-3-azido-10,13-dimethyl-17-((R)-6-methylheptan-2-yl)-2,3,4,7,8,9,10,11,12,13,14,15,16,17-tetradecahydro-1H-cyclopenta[a]phenanthrene – Compound (15)

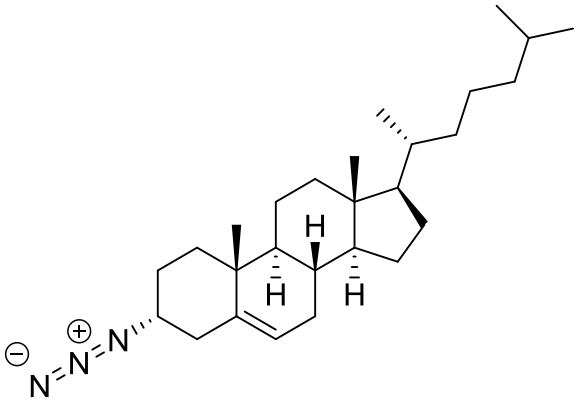

(15)

To a solution of **14** (1.04 g, 2.18 mmol) in 50ml DMF was added sodium azide (0.71 g, 10.9 mmol). The round bottom flask was then equipped with a condenser column and the reaction was warmed to 75 ˚C where it proceeded for 24 hours. The reaction was cooled to room temperature and subsequently concentrated *in vacuo* which produced a white powder which was further purified using silica gel chromatography eluting with hexanes to afford the title compound as a white-yellow crystalline powder (0.56 g, 62%, R_f = 0.91 in 25% EtOAc in hexanes) NMR shifts as reported by (Krishna and Verma, 2011), ^{1}H NMR (400 MHz, $CDCl_3$) δ 0.60 (s, 6H), 0.79 (d, 3H), 0.84 (d, 3H), 0.93 (s, 6H), 0.97-1.04 (m, 5H), 1.18 (d, 2H), 1.25-1.27 (m, 3H), 1.36-1.46 (m, 9H), 1.5 (s, 1H), 1.76-1.78 (dd, 2H), 1.92-1.95 (m, 2H), 2.16-2.21 (m, 2H), 5.27 (s, 1H); ^{13}C NMR (125 MHz, $CDCl_3$) δ 19.4, 20.7, 22.7, 23.2,

24.6, 27.3, 27.7, 28.1, 29.9, 30.0, 31.9, 35.8, 36.1, 36.76, 37.2, 37.7, 39.9, 44.0, 50.8, 55.9, 56.49, 56.77, 121.76, 140.70.

2.2.16 – Synthesis of 2,2'-(prop-2-yn-1-ylazanediyl)bis(ethan-1-ol) – Compound (16)

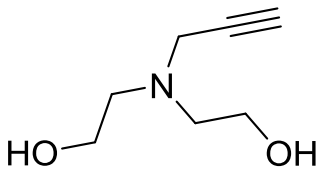

(16)

To a solution of diethanolamine (9.44 g, 89.8 mmol)in 150 ml of CH_2Cl_2 on ice was added anhydrous potassium carbonate (62.1 g, 449 mmol) with vigorous stirring. Once the solution was cooled the dropwise addition of propargyl bromide (80% wt/wt, 10.0 ml, 89.8 mmol) was carried out over 5 minutes. The reaction was then left to stir for 60 hours, allowing the ice bath to melt gradually bringing the reaction up to room temperature. The reaction mixture was then filtered using a sintered glass funnel to remove the potassium carbonate. The filtrate was concentrated *in vacuo* to produce a dark amber oil which was further purified using silica gel chromatography eluting with CH_2Cl_2 to 10% MeOH in CH_2Cl_2 to produce a clear amber oil (4.15 g, 32.2%), ^{1}H NMR (400 MHz, $CDCl_3$) δ 2.20 (t, 1H, J = 2.4 Hz), 2.72 (t, 4H, J = 5.2 Hz), 3.47 (s, 2H), 3.62 (t, 4H, J = 5.2 Hz); ^{13}C NMR (125 MHz, $CDCl_3$) δ 42.16, 55.16, 58.11, 73.09, 78.36.

2.2.17 – Synthesis of 2-((2-(bis(4-methoxyphenyl)(phenyl)methoxy)ethyl)(prop-2-yn-1-yl)amino)ethan-1-ol – Compound (17)

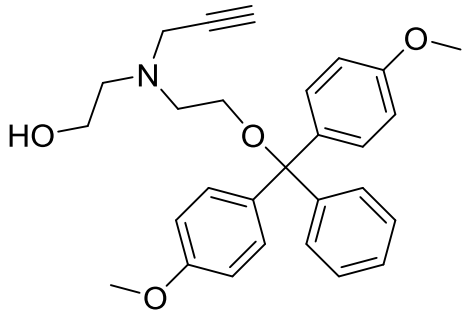

(17)

To a solution of **14** (1.98 g, 13.8 mmol) in 25 ml of CH_2Cl_2 was added triethylamine (1.73 ml, 1.24 mmol) followed by the dropwise addition of 4,4' – dimethoxytriphenylmethyl chloride (3.74 g, 11.0 mmol) in 5 ml of CH_2Cl_2. The reaction mixture was left to stir overnight at room temperature after which it was extracted with a saturated $NaHCO_3$ solution. The organic layer was collected and dried with Na_2SO_4 followed by the concentration *in vacuo* to produce a green-yellow oil which was further purified by silica gel chromatography eluting with a gradient of CH_2Cl_2 to 10%MeOH in CH_2Cl_2 to produce a clear yellow oil (2.83 g, 45.9%), ^{1}H NMR (400 MHz, $CDCl_3$) δ 2.19 (t, 1H, J = 6 Hz), 2.73 (t, 2H, J = 5.6 Hz), 2.80 (t, 2H, J = 5.6 Hz), 3.19 (t, 2H, J = 6 Hz), 3.44 (d, 2H, J = 2.4 Hz), 3.59 (t, 2H, J = 5.2 Hz), 3.80 (s, 6H), 6.84 (dt, 4H, J = 8.8 Hz), 7.21 (m, 1H, J = 7.6 Hz), 7.30 (td, 2H, J = 7.6 Hz), 7.34 (dt, 4H, J = 8.8 Hz), 7.45 (d, 2H, J = 8 Hz); ^{13}C NMR (125 MHz, $CDCl_3$) δ 42.77, 52.57, 55.20, 55.65, 56.57, 61.95, 72.82, 78.83, 86.21, 113.07, 126.71, 127.78, 128.14, 129.96, 136.29, 144.98, 156.41.

2.2.18 – Synthesis of 2-((2-(bis(4-methoxyphenyl)(phenyl)methoxy)ethyl)(prop-2-yn-1-yl)amino)ethyl (2-cyanoethyl) diisopropylphosphoramidite – Compound (18)

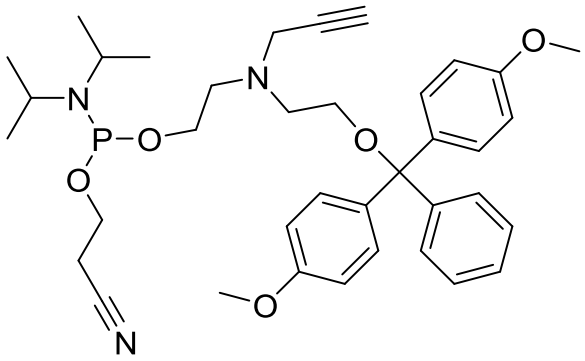

(18)

To a solution of **17** (204 mg, 0.458 mmol) in 5 ml of anhydrous CH_2Cl_2 under an $N_{2(g)}$ atmosphere was added freshly distilled triethylamine (0.32 ml, 2.29 mmol). After warming to room temperature in a desiccator, 2-cyanoethyl-*N,N*-diisopropylchlorophosphoramidite (0.31 ml, 1.38 mmol) was added to the reaction mixture which stirred for 2 hours. The reaction mixture was then concentrated *in vacuo* to produce a cloudy oil which was further purified using silica gel chromatography eluting with a gradient of 20% EtOAc in hexanes to 80% EtOAc in hexanes while maintaining a 2% triethylamine for each concentration. The product was isolated as a clear oil (0.12 g, 41.2%) , ^{1}H NMR (400 MHz, $CDCl_3$) δ 1.17 (dd, 12H, J = 9.6 Hz), 2.19 (t, 1H, J = 2.4 Hz), 2.56 (m, 2H), 2.81 (dt, 4H, J = 14.2 Hz), 3.16 (t, 2H, J = 6.4 Hz), 3.46 (d, 2H, J = 1.2 Hz), 3.58 (m, 2H), 3.69 (m, 2H), 3.78 (m, 2H), 3.79 (s, 6H), 6.82 (dt, 4H, J = 9.2 Hz), 7.20 (tt, 1H, J = 7.2 Hz), 7.28 (t, 2H, J = 8 Hz), 7.34 (dt, 4H, J = 8.8 Hz), 7.46 (d, 2H, J = 7.2 Hz); ^{13}C NMR (125 MHz, $CDCl_3$) δ 20.29, 24.51, 24.56, 42.94, 43.06, 43.60, 53.96, 56.15, 58.53, 61.81, 62.42, 72.89, 78.24, 86.01, 112.99, 117.83, 126.59, 127.89, 129.96, 136.38, 145.12, 158.32.

2.2.19 – Synthesis of 2-((2-(bis(4-methoxyphenyl)(phenyl)methoxy)ethyl)((1-(((3R,8S,9S,10R,13R,14S,17R)-10,13-dimethyl-17-((R)-6-methylheptan-2-yl)-2,3,4,7,8,9,10,11,12,13,14,15,16,17-tetradecahydro-1H-cyclopenta[a]phenanthren-3-yl)methyl)-1H-1,2,3-triazol-4-yl)methyl)amino)ethan-1-ol – Compound (19)

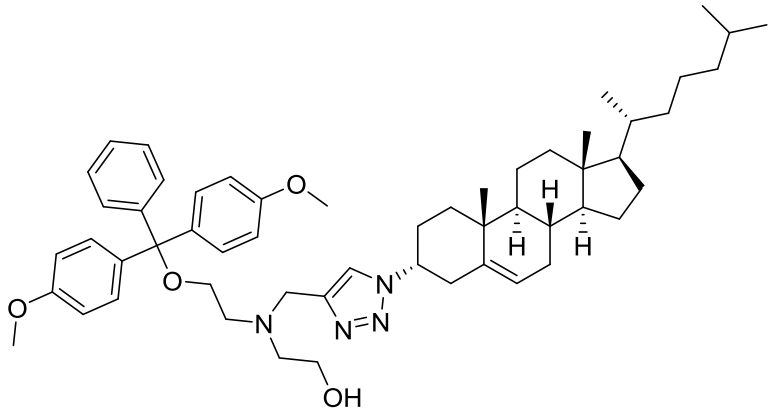

(19)

To a solution of 2-((2-(bis(4-methoxyphenyl)(phenyl)methoxy)ethyl)(prop-2-yn-1-yl)amino)ethan-1-ol (0.62 g, 1.39 mmol) in a 1:1:1 mixture of THF, water and *tert*-butanol was added **15** (1.14 g, 2.77 mmol), copper sulfate pentahydrate (0.17 g, 0.69 mmol) and (+)-sodium ascorbate (0.55 g, 2.77 mmol) in that order. The reaction was stirred for 18 hours at room temperature at which the reaction was the concentrated *in vacuo* and was subsequently extracted using water and CH_2Cl_2. The organic layer was collected and dried with Na_2SO_4 which produced a green oil. Silica gel chromatography was then used to further purify the product using gradient eluting with hexanes/EtOAc (50% hexanes in EtOAc to 100% EtOAc)to afford the title compound as a thick clear oil (0.92 g, 77%); ^{1}H NMR (400 MHz, $CDCl_3$) δ 0.67 (s, 2H), 0.88 (m, 10H), 0.99-1.19 (m, 11H), 1.24-1.56 (m, 11H), 1.66 (d, 1H, J = 8.7 Hz), 1.82 (s, 1H), 1.99 (m, 2H), 2.05-2.25 (m, 3H), 2.50 (d, 1H, J = 8.9 Hz), 2.73 (d, 4H, J = 5.6 Hz), 2.96 (m, 3H), 3.24 (s, 2H), 3.58 (s, 2H), 3.79 (s, 6H), 3.89 (s, 2H), 4.87 (s, 1H), 5.41 (s, 1H), 6.79-6.86 (m, 4H), 7.17-7.33 (m, 7H), 7.37 (m, 2H), 7.68 (s,

1H); ^{13}C NMR (125 MHz, $CDCl_3$) δ 11.51, 17.21, 18.37, 18.95, 20.29, 22.22, 22.48, 23.51, 23.84, 26.09, 27.67, 27.85, 31.31, 31.56, 32.48, 35.44, 35. 67, 35.86, 36.72, 39.08, 39.18, 41.90, 49.62, 55.74, 56.14, 112.74, 124.09, 126.40, 127.45, 127.82, 129.66, 135.97, 137.59, 144.67, 158.06; ESI-HRMS (ES^+) m/z calculated for $C_{55}H_{76}N_4O_4$: 856.5772 found 879.5783 $[M + Na]^+$

2.2.17 – Synthesis of 2-((2-(bis(4-methoxyphenyl)(phenyl)methoxy)ethyl)((1-(((3R,8S,9S,10R,13R,14S,17R)-10,13-dimethyl-17-((R)-6-methylheptan-2-yl)-2,3,4,7,8,9,10,11,12,13,14,15,16,17-tetradecahydro-1H-cyclopenta[a]phenanthren-3-yl)methyl)-1H-1,2,3-triazol-4-yl)methyl)amino)ethyl (2-cyanoethyl) diisopropylphosphoramidite – Compound (20)

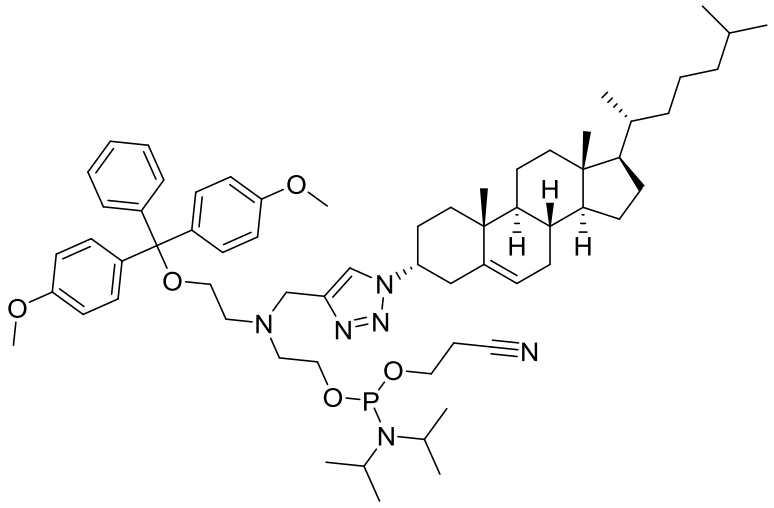

(20)

To a solution of **16** (0.33 g, 0.38 mmol) in 10 ml of dry CH_2Cl_2 was prepared in flame dried glassware and put under a $N_{2(g)}$ atmosphere. Freshly distilled triethylamine (0.16 ml, 1.14mmol) and 2-cyanoethyl-*N,N*-diisopropylchlorophosphoramidite (0.26 ml, 1.15 mmol) were then added to the solution via an anhydrous transfer. The reaction was allowed to stir at room temperature for 1.5 hours at which point TLC analysis revealed the consumption of

the starting material, **16,** (R_f = 0.23 in EtOAc). The reaction mixture was the concentrated *in vacuo* which produced a yellow oil which was further purified using silica gel chromatography using gradient elution of Hexanes/EtOAc (50% Hexanes in EtOAc to 100% EtOAc) affording the title compound as a clear oil (0.27 g, 68%); ^{1}H NMR (400 MHz, $CDCl_3$) δ 0.67 (s, 2H), 0.86-1.56 (m, 44H), 1.66 (m, 2H), 1.79-2.12 (m, 6H), 2.22 (d, 1H, J = 8.9 Hz), 2.47 – 2.60 (m, 3H), 2.78 (m, 4H), 2.94 (d, 1H, J = 5.6 Hz), 3.18 (s, 2H), 3.62 (m, 4H), 3.70-3.81 (m, 9H), 3.88 (s, 2H), 4.14 (m, 1H), 5.39 (m, 1H), 6.77-6.87 (m, 4H), 7.16-7.35 (m, 7H), 7.37 (m, 2H), 7.71 (s, 1H) , ; ^{13}C NMR (125 MHz, $CDCl_3$) δ 11.81, 14.18, 18.68, 19.26, 20.32, 20.54, 22.54, 22.80, 23.83, 23.89, 23.96, 26.67, 27.99, 31.64, 31.98, 35.75, 36.16, 37.03, 39.49, 41.80, 42.92, 43.05, 49.94, 54.24, 55.16, 56.38, 56.42, 58.33, 58.51, 60.35, 62.48, 85.99, 112.99, 117.62, 121.91, 124.20, 126.61, 127.69, 129.98, 136.45, 136.44, 137.93, 144.27, 145.19, 158.32; ^{31}P NMR (125 MHz, $CDCl_3$) δ 147.61 ; ESI-HRMS (ES^+) m/z calculated for $C_{64}H_{93}N_6O_5P$ 1056.6002, found 1056.6063 [M+H] (Hydrolyzed product).

2.3 – Chemical Synthesis and Purification of Oligonucleotide Strands

All reagents used in the synthesis of the oligonucleotides strands were purchased from Glen Research (Virginia, USA). All of the oligonucleotide strands were synthesized using an Applied Biosystems 394 DNA/RNA synthesizer on a 0.2 μM cycle with a 999 second coupling time. All reagent solutions are attached to the synthesizer directly and DNA/RNA phosphoramidites were diluted to 0.1 M using anhydrous acetonitrile immediately before use. Synthesis was carried out on a CPG solid support to which dT at 0.2 μM is attached. Antisense strands were chemically phosphorylated at the 5' end using 2-[2-(4,4'-dimethoxytrityloxy)ethylsulfonyl]ethyl-(2-cyanoethyl)-(*N,N*-diisopropyl)-phosphoramidite

(Glen Research). Oligonucleotide cleavage from the solid supports was done by flushing the CPG column with 1.5 ml of EMAM (methylamine 33% wt. in ethanol and methylamine 40% wt. in H_2O, 1:1) (Sigma-Aldrich) for 1 hour at to remove the strands from the column followed by an additional incubation period of 24 hours to deprotect the bases. The samples were then dried and resuspended in 125 µL of 3HF-Et_3N (Sigma-Aldrich) and 100 µL of DMSO and then this solution was incubated at 65 ˚C for 2 hours to remove the 2'-*O*-TBS protecting groups.

The purification of the oligonucleotides begins with an EtOH precipitation followed by the desalting using a Millipore Amicon Ultra 3000 MW cellulose centrifugal filters. PAGE purification using a 40% denatured gel was done as for allyl and acetyl modified strands. Strands were physically excised from the gel and desalted using the centrifugal filters. Wild-type luciferase strands were purchased from Integrated DNA Technologies (IDT). Sense and antisense strands were annealed by combining equimolar amounts and heating at 90 ^oC for 2 minutes in binding buffer (75 mM KCl, 50 mM Tris-HCl, 3 mM $MgCl_2$, pH 8.3) followed by the gradual cooling to room temperature over 3 hours to afford the siRNAs.

2.4 – Biophysical Characterization

The siRNA samples for the biophysical characterization testing were prepared by adding equimolar amounts (350 pM) of modified sense strand and w.t. antisense strand (IDT Technologies) in an eppendorf tube. The strands were suspended in 380 µL of sodium phosphate buffer (90 mM NaCl, 10mM Na_2HPO_4, 1 mM EDTA, pH = 7) and heated to 90 ˚C for 2 minutes after which the solution was gradually allowed to cool down to room temperature. The siRNA samples are the transferred to a 1 mm quartz cuvette (QS) and all

measurements were done using a J-815 CD Spectrometer and data was recorded using Jasco's Spectra Manager 2.0 software.

2.4.1 - Helical Conformation Analysis Using Circular Dichroism

Circular dichroism studies were carried out at 25 ˚C over a wavelength range of 200 to 300 nm scanning at a rate of 20 nm per minute. Each sample was measured four times and the average spectra is obtained using Jasco's Spectra Manager 2.0 software

2.4.2 - UV-Monitored Thermal Denaturation of siRNA Duplexs

Melting temperature studies were done at 260 nm and all samples were run with a baseline of sodium phosphate buffer. The temperature was increased from 10 ˚C to 90 ˚C at a rate of 0.5 ˚C per minute. T_m data was analyzed using Meltwin 3.5 software. The average of triplicate measurements is taken at the T_m of the duplex.

2.5 Cell Culture Maintenance

The cell line used for the biological analysis of these siRNAs is human epithelial cervix carcinoma cells, commonly referred to as HeLa cells. Cells were kept in cell culture flasks with 25 ml of DMEM modified by adding 10% fetal bovine serum (Perbio) and 1% Penicillin-Streptomycin (Sigma) and stored in an incubator set at 37.5 ^{o}C with a 5% CO_2 atmosphere that is humidified.

Cells were passaged twice a week, once cells became confluent, according to the following protocol. The cell culture flask was washed twice with 1X phosphate buffered saline (PBS) with a pH of 7.4 (Invitrogen) and then incubated with 2 ml of 0.25% Trypsin (SAFC Bioscience) for 2 minutes at 37.5 ˚C. This 2 ml of cell solution was transferred to a

Falcon tube and diluted with 5 ml of DMEM with 10% FBS and pelleted at 1,500 rpm for 5 minutes. The supernate was discarded and the pellet was resuspended in 10 ml of DMEM with 10% FBS. A haemocytometer was used obtain a cell count followed by a dilution to make a cell concentration of 1,000,000 cell per ml. From this 1 ml was added to a new cell culture flask that already contains 24 ml of DMEM with 10% FBS and 1% P/S. at 37.5 ˚C. The remaining cell solution was utilized for plating when needed.

2.6 – Cell Based Assays

2.6.1 – Plating and Transfection

For the luciferase assay, 100 µl of the 1,000,000 cells per ml solution were added to the wells of a 12 well plate already containing 400 µL of DMEM with 10% FBS per well. For qRT PCR, 50 µL of the 1,000,000 cells per ml solution was added to the wells of a 24 well plate that already has 350 µL of DMEM with 10% FBS per well. After plates are prepared they were incubated at 37.5 ˚C with 5% CO_2 for 24 hours.

A mixture of 1µL siRNA, and 1 µL of Lipofectamine 2000 (and 100 ng of pGL and SV plasmid for luciferase assay) was prepared in Gibco's Opti-Mem Reduced Serum Medium to a total volume of 100 µl (200 µL for Luciferase assay). A different solution is made for each siRNA and for every concentration. These solutions were then transferred to the well plates and incubated for another 24 hours.

2.6.2 – Dual Luciferase Reporter Assay

After the post transfection incubation period each well was washed with twice with 1X PBS and then 250 µL 1X Passive Lysis Buffer was added to lyse the cells over a period of

20 minutes on a shaker. Then 10 µL cell lysate was transferred to a Costar 96 well plate (making triplicates of each lysate) immediately and a Synergy HT (Bio-Tek) plate luminometer was used to measure fluorescence. Fluorescence studies were done using the Dual-Luciferase Reporter Assay kit (Promega). According to the kit's protocol, 50 µL of LAR II substrate was first added to induce firefly luciferase luminescence followed by the addition of 50 µL of Stop&Glow to quench firefly luciferase and induce *Renilla* luciferase luminescence. The firefly luciferase signal was normalized with the *Renilla* luciferase signal and the signal for the cells transfected with no siRNA were taken as 100% expression to which the other strands are compared.

2.6.3 – qRT PCR Targeting the BCL2 Oncogene

On a 24 well plate, 50,000 cells were added to each well of a 24-well plate with 350 µL of DMEM with 10% FBS in a 5% CO_2 environment at 37 ^{o}C. After 24 hours cells were treated with 1 nM and 20 nM concentrations of siRNAs targeting the BCL2 oncogene using Lipofectamine 2000 in 1X OptiMem; each siRNA (1 µL) was added to a tube on ice along with 50 µL of OptiMem and combined with a second tube with 1 µL of Lipofectamine and 50 µL of OptiMem after a period of 20 minutes. At this point there were roughly 250,000 cells in each well and after transfection the final volume in the well in 500 µL. After 24 hours from transfection the cells were lysed for reverse transcription which was accomplished using a Cells-to-cDNA II Kit (Ambion) following the manufacturer's protocol. The amplification of *BCL2*, GAPDH, and 18S were done on a CFX96 Real-Time reactor (Bio-Rad), using SsoFast EvaGreen Supermix (Bio-Rad) as the source of EvaGreen dye and *Taq* polymerase. Forward and reverse primers for GAPDH were added giving a final

concentration of 800 nM, 18S's primers were 100 nM and the BCL2 primers were 500 nM bringing each reaction volume to a total of 20 µL. The GAPDH forward and reverse primers were 5' – ACG GCT GCT TTT AAC TCT GG – 3' and 5' – TTG ATT TTG GAG GGA TCT CG – 3' respectively which produced a 200 bp amplicon. The 18S forward and reverse primers were 5' – CGC CTA CCA CAT CCA AGC AAG – 3' and 5' – CGC TCC CAA GAT CCA ACT AC – 3' respectively which produced a 247 bp amplicon. The BCL2 forward and reverse primers were 5' – CTG GTG GGA GCT TGC ATC AC – 3' and 5' – ACA GCC TGC AGC TTT GTT TC – 3' respectively which produced a 150 bp amplicon. There were non-reverse transcriptase controls performed accompanied with a no template control. The reactor protocol was carried out as follows: pre-heat the chamber to 95 ˚C for 2 min, followed by 40 cycles of 95 ˚C for 5 sec, 52 ˚C for 15 sec and 72 ˚C for 5 sec. The last step was the gradual raising of the temperature from 65 ˚C to 95 ˚C for the melting temperature analysis of the PCR products at 260 nm. The expression of BCL2 was normalized to GAPDH and 18S using the comparative C*t* method while error was expressed as the overall coefficient of variance.

3.0 - Results and Discussion

3.1 – Organic Synthesis of Phosphoramidites

In this paper the scope of chemical modification in siRNA is expanded with the synthesis of modified alkyl spacer phosphoramidites and there subsequent incorporation in to RNA oligonucleotides. The double base linker utilizes a protection-deprotection strategy for modification followed by attachment of the two groups needed for DMT-Phosphoramidite chemistry; the synthesis of the all five linkers is described herein. The synthesis begins with the *tert*-butyldimethylsilyl (TBS) protection the alcohol groups of *N,N'*- bis(2-hydroxyethyl)ethandiamine to produce **1** in a 68% yield (**Scheme 3-1**). The TBS groups are commonly used alcohol protecting groups [83] that are needed in this case to prevent the alcohols from becoming alkylated under basic conditions in the subsequent reaction. It is important to use just over two equivalents of TBS-Cl in order to only protect the alcohols groups and to not react the nitrogen atoms. Once the secondary nitrogens are the only nucleophiles left, a strong base, sodium hydride in this case, is used in combination with allyl bromide to alkylate the nitrogen atoms to produce **2** in a 74% yield via an S_N2 mechanism and/or through a nucleophilic attack on the alkene. Once the modification is on the linker the TBS groups need to come off, this was accomplished with TBAF which is an organic fluoride salt. The fluoride anion undergoes a nucleophilic attack on the silicon atom producing a pentavalent centre, which can exist due to hybridization with silicon's vacant d-orbitals which will collapse breaking the Si-O bond due to the newly formed and highly stable Si-F bond [84] producing **3** in a 92% yield. The dimethoxytrityl protecting group is one of two chemical groups needed for DMT-Phosphoramidite chemistry. This group is

used to protect alcohols for oligonucleotide synthesis because it is quite easy to knock off with acid and the cation formed is highly coloured and stable, making the coupling of bases easy to monitor [85]. The attachment of the DMT group proved to be the least efficient step in the synthesis simply due to the symmetry of the molecule being protected; even though a single DMT group might be attached it is still very possible for the other alcohol group to undergo the same reaction and it was observed. This is the reason less than one equivalent of DMT-Cl is used in basic conditions to afford **4** in just a 46% yield. The final step is the attachment of the phosphite group; which is the most synthetically challenging step because of the sensitivity of the phosphite group towards moisture [86]. The phosphite group was attached to the linker using base and produced **5** in a 71% yield producing the phosphoramidite with an overall 15% yield. The phosphite group will become oxidized to a phosphate during oligonucleotide synthesis.

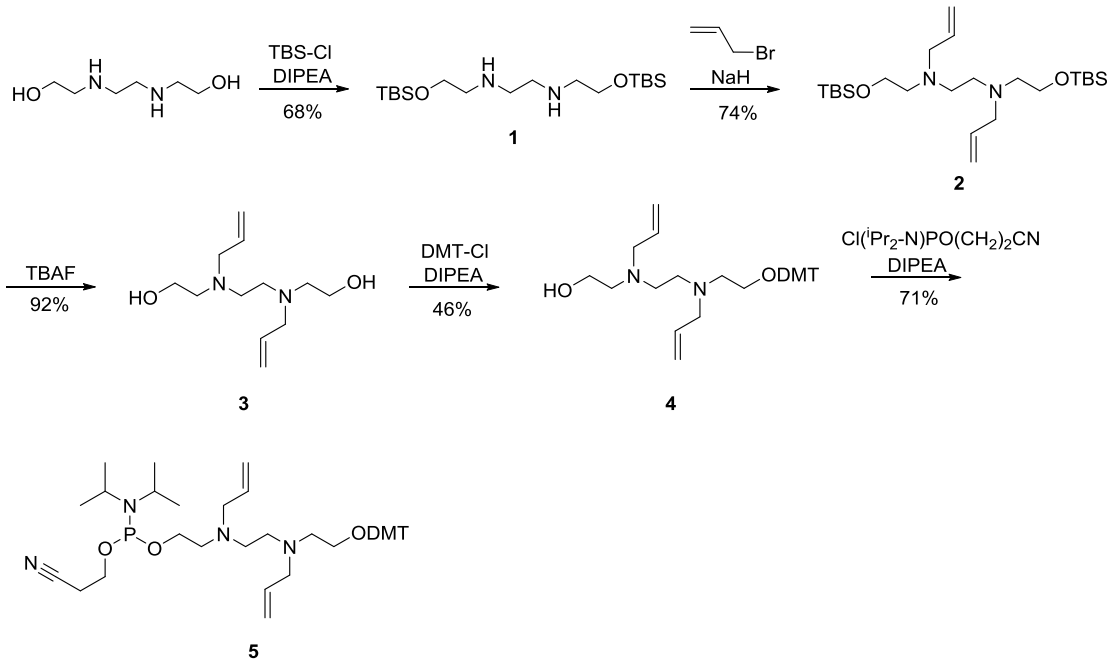

Scheme 3-1: Synthesis of allyl modified phosphoramidite.

The propargyl synthetic scheme (**Scheme 3-2**) is almost identical to that of the allyl linker. The only difference comes during the attachment of the propargyl substituents on the nitrogen atoms. The conditions utilized for the allyl scheme used NaH as the base; this base is too strong for this scheme as it is capable of deprotonating the alkyne proton (pKa ~ 25) compared to an alkene (pKa ~ 44) [87]. Substituting the base with a weaker base, such as DIPEA in this case, allows for alkylation to proceed with the only downfall being a longer reaction time due to the equilibrium established by the base [88].

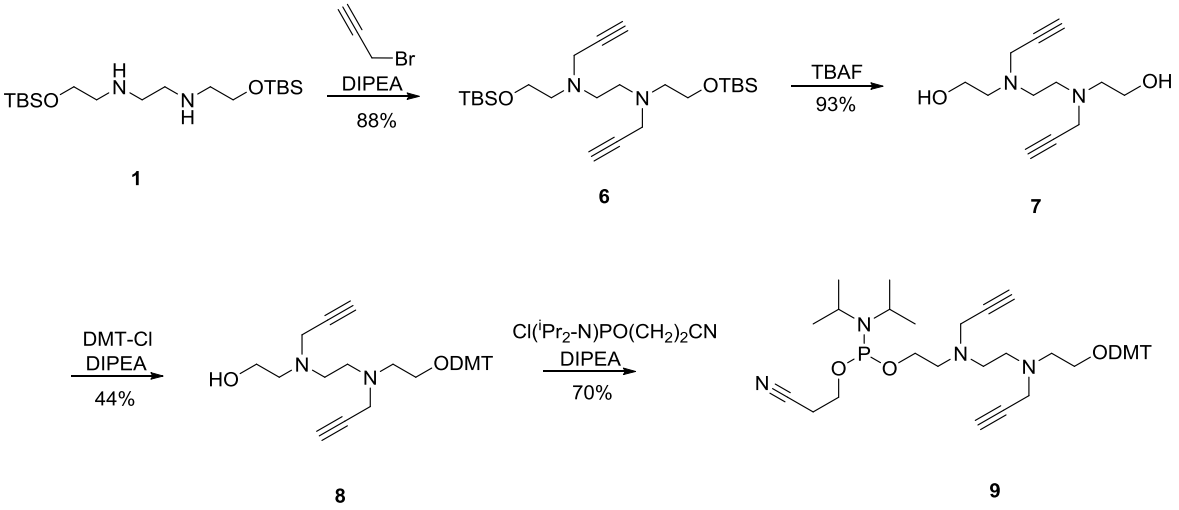

Scheme 3-2: Synthesis of propargyl modified phosphoramidite.

Synthesis of the acetyl linker (**Scheme 3-3**) was carried out the same as the allyl linker with the only difference coming at the alkylation of the nitrogen atoms. The acetylation was accomplished using DMAP as an activating agent and acetic anhydride is the alkylating agent. The combination of the nucleophilic character of nitrogen and the electron deficient character of the carbonyl group on acetic anhydride makes this a favourable transformation [89]. The attack of nitrogen forms a tetrahedral intermediate on acetic anhydride that collapses to liberate the stabilized acetate anion leaving the acetyl

group attached forming the amide functionality. Although this linker is being modified with an acetyl group it will be cleaved off during the nucleobase deprotection step leaving the linker with the original unmodified secondary nitrogen scaffold.

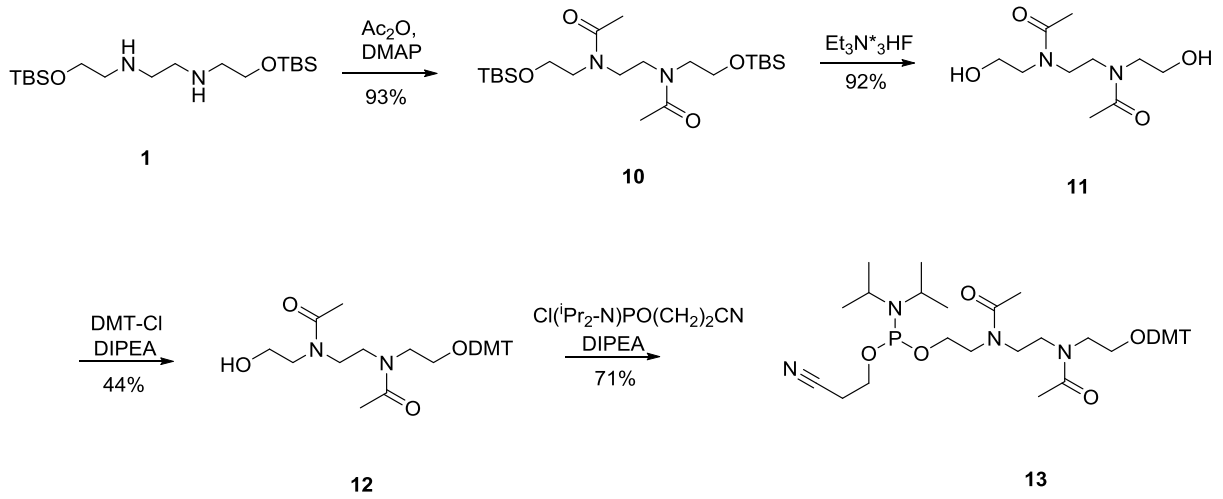

Scheme 3-3: Synthesis of acetyl modified linker phosphoramidite.

The synthesis of the small propargyl linker (**Scheme 3-4**) was accomplished using a slightly different approach than the three previous schemes due to difficulties with the TBS deprotection. The nitrogen was alkylated directly in the presence of five equivalents of weak base, K_2CO_3, with one equivalent of propargyl bromide to produce the product, **16**, in a low yield [90]. After this step the DMT protection and subsequent phosphitylation are the same as the previous three linkers described. More details regarding the synthesis of this small propargyl linker can be found in Roberts, 2014 [91]. One of the purposes of attaching propargyl groups on to these alkyl linkers is the ease and abundance of subsequent modifications that can follow such as the Pd^0 catalyzed Sonogashira coupling of alkynes with alkyl halides [92] or the Cu^I assisted Huisgen 1,3-dipolar cycloaddition of alkynes with azides [93].

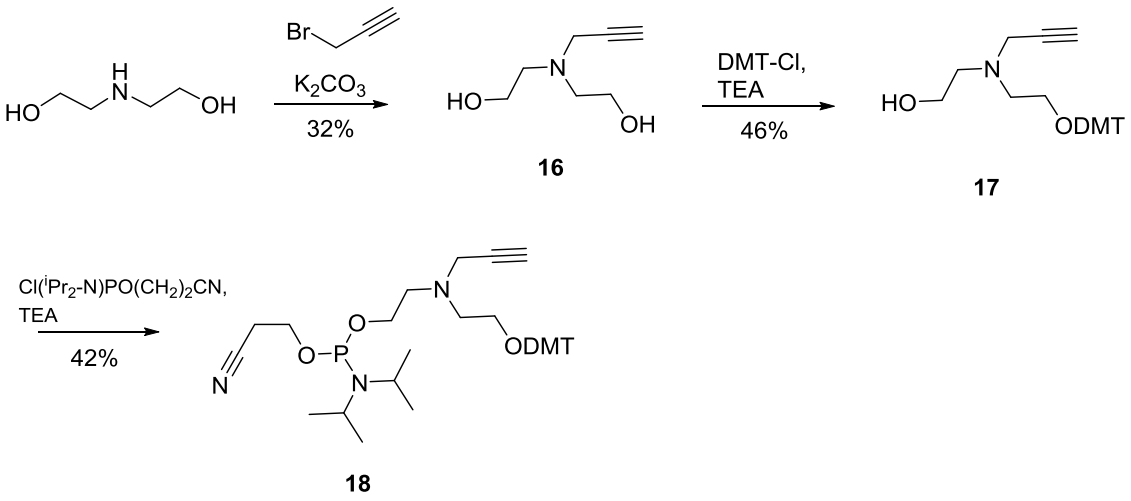

Scheme 3-4: Synthesis of small propargyl phosphoramidite.

Whereas the previous four synthetic schemes have focused on simple modifications on the alkylamino backbone, **Scheme 3-5** focuses on the further modification by performing chemistry on the propargyl group. There has been a lot of focus on attaching biomolecules, such as cholesterol, to enhance properties such as cellular uptake; however the majority of such modifications tend to be found as 3' modifications with comparatively few means on internal conjugation [94].A review paper published in 2012 by Efthymiou et al., describes how 1,2,3-triazole functionalities have been well tolerated as a nucleic acid modification [69] which was the route taken to attach the cholesterol group in this modification. A study in 2011 by Krishna and Verma described the simple synthesis of cholesterol with its alcohol replaced by an azide group, compound **15**, which was used to form the linker with the triazole-linked cholesterol. To form the triazole a copper (I) catalyst is needed; Cu_2SO_4-$5H_2O$ was used instead with an *in situ* reducing agent, sodium ascorbate, to accomplish the transformation which is a well-established method [95].

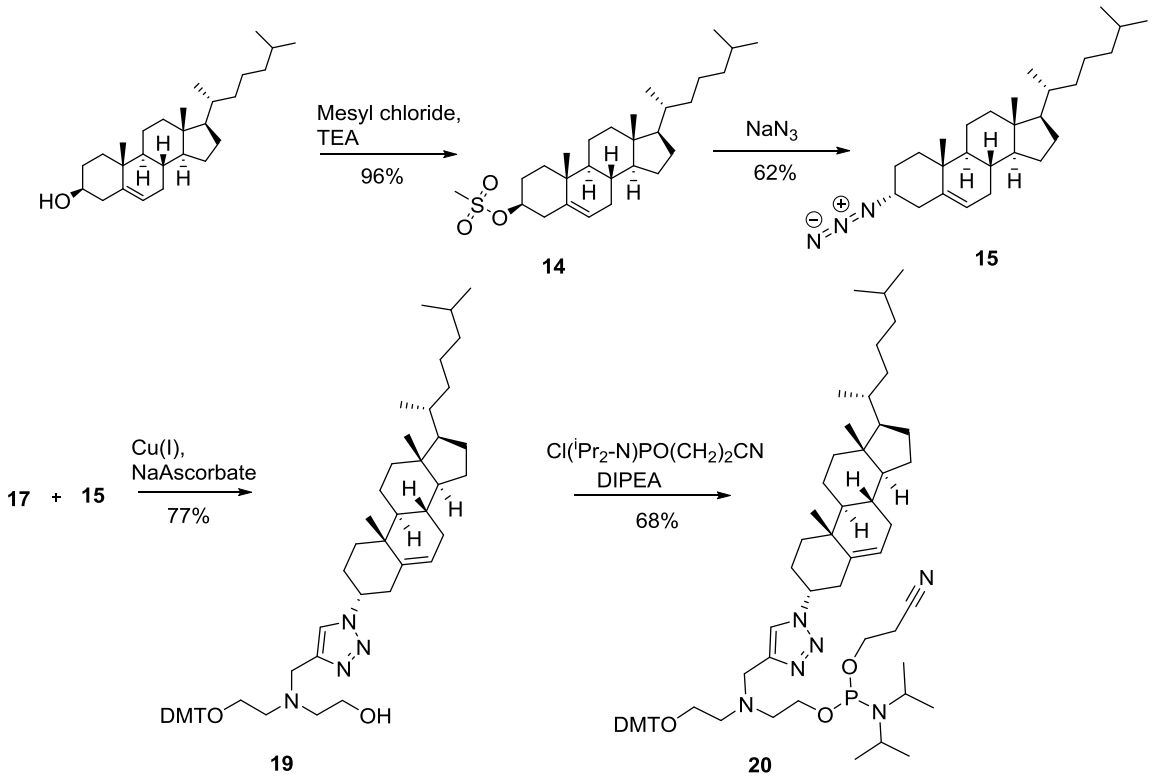

Scheme 3-5: Synthesis of click-cholesterol phosphoramidite.

The reaction begins with Cu(II) being reduced to Cu(I) by sodium ascorbate, an excess of sodium ascorbate is used to prevent the formation of oxidative homocoupling products [96]. The Cu(I) compound along with the linker's alkyne form a copper acetylide intermediate which is attacked by the azide at the copper center displacing a ligand. With the azide and alkyne within close proximity they form a six-membered copper (III) metallacycle which subsequently contracts in to a triazolyl-copper species that undergoes protonolysis to form the final product and completing the catalytic loop [97]. The synthetic loop can is depicted below in **Figure 3-1**. The method is selective in forming the 1,3 product; if the 1,2 product was ever sought there are well established methods using a ruthenium catalyst [98].

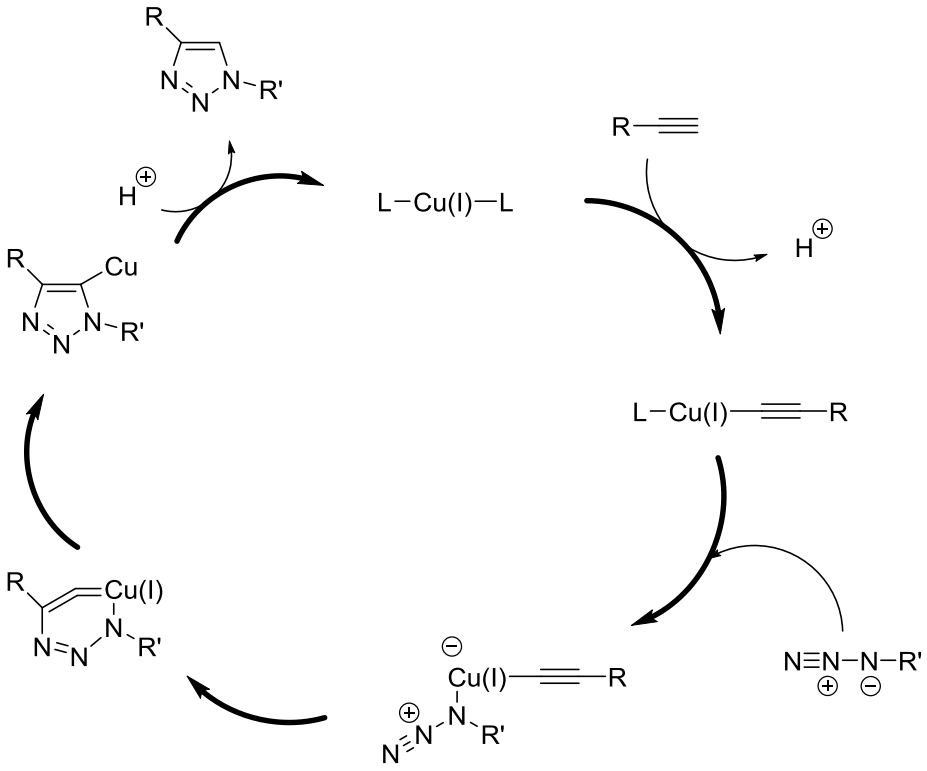

Figure 3-1: Cu(I) catalyzed azide-alkyne cycloaddition catalytic cycle forming the 1,3 triazole.

To ensure that these phosphoramidites have been successfully into the RNA oligonucleotides mass spectrometry was performed on the sense strand. The results of which are seen in the table below.

Table 3-1: Negative ESI of sense strand oligonucleotides.

Strand	Modification Type and Position	m/z Calculated	m/z Found
P1	Propargyl (9+10)	6186	6221 $[M+Cl]^-$
L1	Allyl (9+10)	6188	6223 $[M+Cl]^-$
A1	Acetyl (9+10)	6070	3077 $[M/2 + Cl]^-$

3.2 – Thermal Stability of siRNAs

The siRNA helix is stabilized through two main types of interactions; 1) hydrogen bonding and 2) base stacking [99]. Measuring the melting temperature (T_m), the temperature at which point the two strands dissociate, gives insight to the duplex's stability. Since nucleobases have high absorption at 260nm, measuring absorption as a function of temperature will allow T_m to be calculated due to the fact that the exposed nucleobases have higher absorption than equivalent bases in ds nucleic acid form [100]. Comparing the thermal stability to wild type can help shed insight on why the newly modified siRNAs display their activity, **Table 3-1** displays the synthesized strands sequences, modification position and T_m's of the linker replacing two nucleobases.

Table 3-2: Sequences of anti-luciferase siRNAs and T_m's of siRNAs containing the double base spacer.

siRNA	***siRNA Duplex***	***[a]T_m (°C)***	***ΔT_m (°C)***
wt	5'- C UUA CGC UGA GUA CUU CGAtt -3' (S) 3'- ttG AAU GCG ACU CAU GAA GCU – 5'(AS)	72.7	--
A1	5'- C UUA CGC UQQ GUA CUU CGAtt -3' 3'- ttG AAU GCG ACU CAU GAA GCU – 5'	55.1	-17.6
A2	5'- C UUA CGC UGQ-QUA CUU CGAtt -3' 3'- ttG AAU GCG ACU CAU GAA GCU – 5'	53.3	-19.4
A3	5'- C UUA CGC QQA GUA CUU CGAtt -3' 3'- ttG AAU GCG ACU CAU GAA GCU – 5'	54.6	-18.1
A4	5'- C UUA CGC UGA GUQ-QUU CGAtt -3' 3'- ttG AAU GCG ACU CAU GAA GCU – 5'	51.1	-21.6
L1	5'- C UUA CGC ULLGUA CUU CGAtt -3' 3'- ttG AAU GCG ACU CAU GAA GCU – 5'	65.9	-6.8
L2	5'- C UUA CGC LLA GUA CUU CGAtt -3' 3'- ttG AAU GCG ACU CAU GAA GCU – 5'	63.2	-9.5
L3	5'- C UUA CGC UGL-LUA CUU CGAtt -3' 3'- ttG AAU GCG ACU CAU GAA GCU – 5'	62.8	-9.9
L4	5'- C UUA CGC UGA GUL-LUU CGAtt -3' 3'- ttG AAU GCG ACU CAU GAA GCU – 5'	59.7	-13.0
P1	5'- C UUA CGC UPP GUA CUU CGAtt -3' 3'- ttG AAU GCG ACU CAU GAA GCU – 5'	64.6	-8.1
P2	5'- C UUA CGC UGP-PUA CUU CGAtt -3' 3'- ttG AAU GCG ACU CAU GAA GCU – 5'	60.9	-12.6
P3	5'- C UUA CGC PPA GUA CUU CGAtt -3' 3'- ttG AAU GCG ACU CAU GAA GCU – 5'	61.5	-11.2
P4	5'- C UUA CGC UGA GUP-PUU CGAtt -3' 3'- ttG AAU GCG ACU CAU GAA GCU – 5'	56.5	-16.7

[a]T_ms were measures in a sodium phosphate buffer (90 mM NaCl, 10 mM Na_2HPO_4, 1 mM EDTA, pH 7) at 260 nm, from 10 to 95 °C. **QQ**, **LL** and **PP** correspond to the acetyl, allyl and propargyl modified spacer respectively. '_' Shows the position of the Ago2 cleavage site.

What does not come as a surprise when viewing the T_m's in **Table 3-2** is the introduction of this linker introduces a significant degree of destabilization. This is due to the removal of the hydrogen bonding from the two missing bases as well as the base stacking interactions they would also participate in [101]. For each position the linker replaces one A-U bond and one G-C bond which means the destabilization effects seen will not be affected by replacing different numbers of H-bonds. When comparing the destabilization effect to the study done by Efthymiou et al., in 2012, which uses the same anti-luciferase sequence and two nucleobase spacers, on average this new linker is displaying a higher degree of thermal stabilization compared to the nine-carbon linker (C9) and eight-atom polyethylene glycol (E8) within the central region of the sense strand [74]. A possible explanation for this could be that the propargyl and allyl pi electrons are somehow interacting with the base stacking interactions which may be imparting a small degree of stabilization; when examining the T_m's of the acetyl modified strand it is apparent that this interaction is not possible and destabilization is comparable to what was observed by Efthymiou et al., in 2012. When examining the data there is a trend emerging, the linker imparts the least amount of destabilization when occupying the Argonaute2 cleavage site or the immediately adjacent sites while the modification at position 13 and 14 destabilized by a few more degrees which has been observed in several other modifications [101].

In **Table 3-3** shown below, the thermal destabilization of the smaller linker that replaces a single nucleobase is assessed. Again with no surprise the table shows that introduction of this linker results in destabilization of the duplex due to the same reasons as the longer spacer. The propargyl spacer when compared to its longer version is roughly

Table 3-3: Sequences of anti-luciferase siRNAs and T_m's of siRNAs containing the single base spacer.

siRNA	***siRNA Duplex***	***[a]T_m (°C)***	***ΔT_m (°C)***
wt	5'- C UUA CGC UGA GUA CUU CGAtt -3' (S) 3'- ttG AAU GCG ACU CAU GAA GCU – 5'(AS)	72.7	--
BR1	5'- C UUA CGC UPA GUA CUU CGAtt -3' 3'- ttG AAU GCG ACU CAU GAA GCU – 5'	69.1	-2.8
BR2	5'- C UUA CGC UGP GUA CUU CGAtt -3' 3'- ttG AAU GCG ACU CAU GAA GCU – 5'	70.2	-2.5
BR3	5'- C UUA CGC PGA GUA CUU CGAtt -3' 3'- ttG AAU GCG ACU CAU GAA GCU – 5'	67.7	-5.0
BR4	5'- C UUA CGC UGA PUA CUU CGAtt -3' 3'- ttG AAU GCG ACU CAU GAA GCU – 5'	68.5	-4.2
X1	5'- C UUA CGC UXAGUA CUU CGAtt -3' 3'- ttG AAU GCG ACU CAU GAA GCU – 5'	61.6	-11.1
X2	5'- C UUA CGC UGX GUA CUU CGAtt -3' 3'- ttG AAU GCG ACU CAU GAA GCU – 5'	62.5	-10.2
X3	5'- C UUA CGC XGA CUA CUU CGAtt -3' 3'- ttG AAU GCG ACU CAU GAA GCU – 5'	62.7	-10.0
X4	5'- C UUA CGC UGA XUA CUU CGAtt -3' 3'- ttG AAU GCG ACU CAU GAA GCU – 5'	61.8	-10.9
X5	5'- C UUA CGC UGA GUA CUU CGAXt -3' 3'- ttG AAU GCG ACU CAU GAA GCU – 5'	69.8	-2.9

[a]T_ms were measures in a sodium phosphate buffer (90 mM NaCl, 10 mM Na_2HPO_4, 1 mM EDTA, pH 7) at 260 nm, from 10 to 95 °C. **P** and **X** correspond to the propargyl and click-cholesterol modified spacer respectively. ' _ ' Shows the position of the Ago2 cleavage site.

half as destabilizing, which makes sense as there is only one abasic site as opposed to there being two. The click cholesterol linker displays destabilization similar to the allyl modified double spacer; although the linker replaces a single base the introduction of the large cholesterol group is surely imparting some steric effects on the duplex which is most likely

the main reason for destabilization. This agrees with the literature where internal cholesterol modifications tend to be quite destabilizing [102]. The click cholesterol modification on the 3' overhang however displays minimal destabilization as the linker is lying just outside of the duplex therefore destabilizing it to a lesser extent compared to all the other positions which agrees with what is seen in the literature [103].

3.3 - Circular Dichroism Conformation of siRNA Helical Structure

In order for siRNAs to retain activity they must be in the A-form helical conformation to be able to be a tolerable substrate for RISC [104]. By interacting asymmetrical molecules with polarized light distinct absorption patterns arise which can be used to identify secondary structures in nucleic acids [105]. One such example is the absorption profiles for A-form helices which are depicted in **Figure 3-2** to **Figure 3-4**.

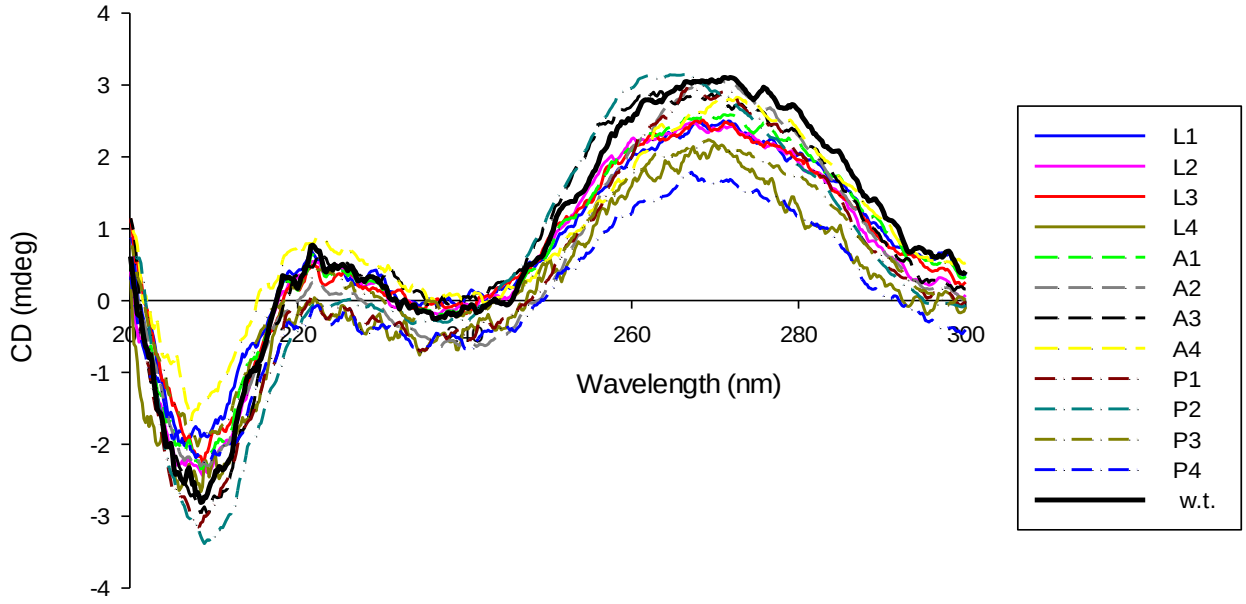

Figure 3-2: CD spectra of modified linkers replacing two nucleobases targeting firefly luciferase mRNA.

Each helical conformation (A, B and Z form) has a distinct absorption profile. A-form has a distinct shallow trough at ~210nm and a large absorption at ~260nm with the B-form helices exhibiting a similar profile except the aforementioned are values shifted to 220nm and 280nm respectively [106]. CD is a very useful technique for assessing the interactions of chemically modified nucleotides are their complementary sequences as any change in molar ellipticity is attributed primarily to the change in the conformation of the complex [107]. Examination of the three figures shows some deviation of the spectral plots from w.t., this is seen with several chemically modified due to the fact that the introduced chemical groups slightly distort the helical conformation which can be seen in the shift of λ_{max} around 260nm [107]. The shifts seen in **Figures 3-2** to **3-4** however are not significant enough to distort the overall shape from the A-form helix [106].

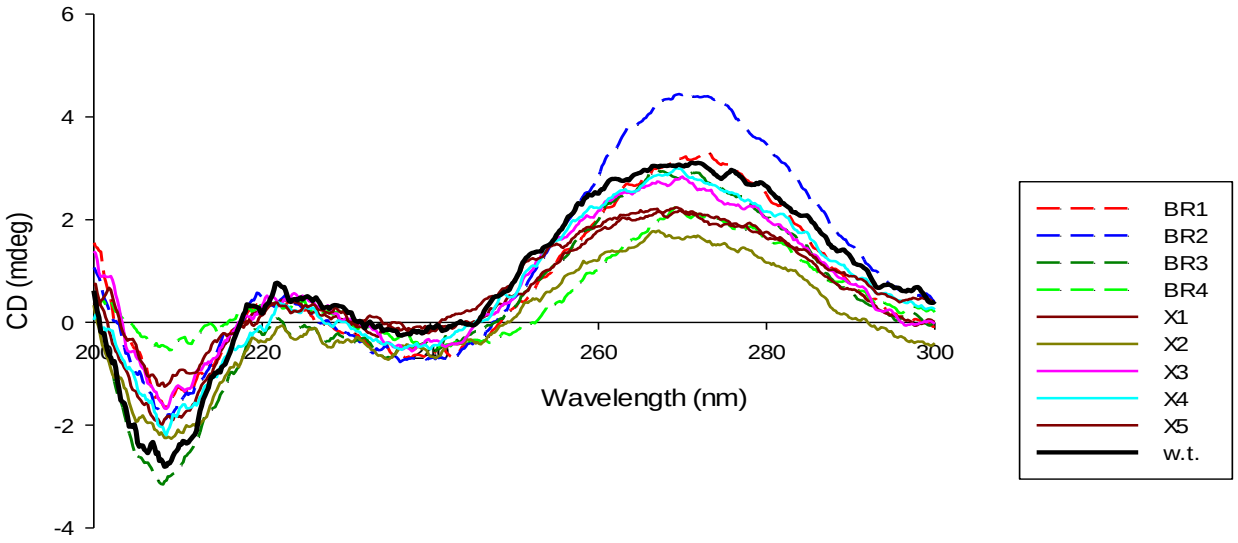

Figure 3-3: CD Spectra of propargyl and click-cholesterol spacers replacing a single nucleobase targeting firefly luciferase.

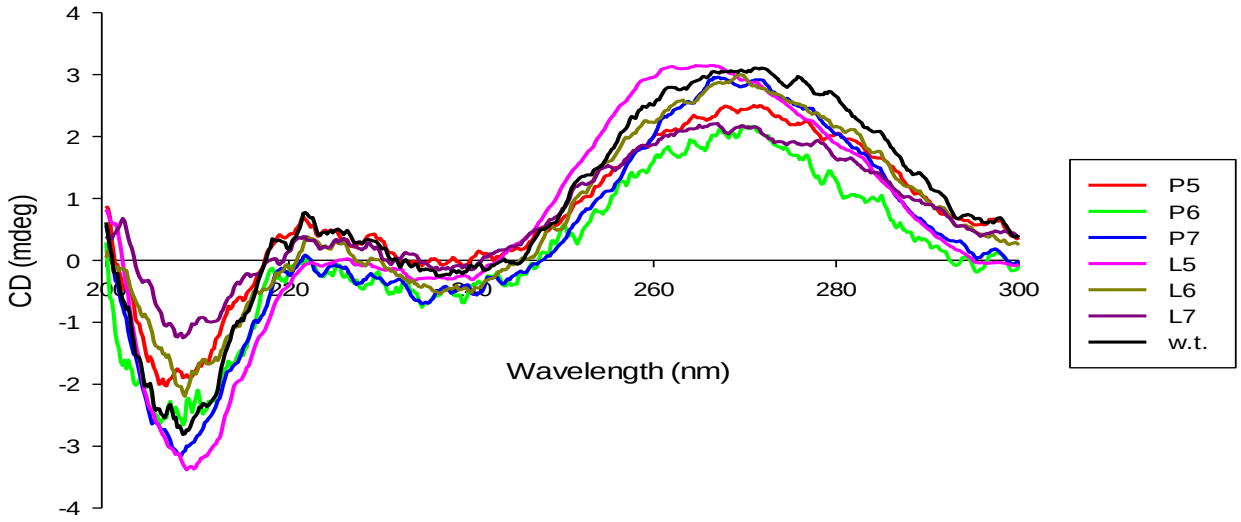

Figure 3-4: CD spectra of propargyl and allyl modified spacers replacing two nucleobases for the anti-BCL2 sequences.

Inspection of the CD spectra reveals that this linker retains the over A-form helical conformation as the characteristic trough is present at 210nm and large absorption at 267nm meaning that the modification does not disrupt the native conformation meaning this modification should be suitable for RNAi.

3.4 – Silencing Capability of the Endogenous Firefly Luciferase Gene

The biophysical characterization of the modified siRNAs has revealed traits that suggest they should be compatible with RNAi. The dual luciferase assay is a widely used assay that is used in this case to screen the new modifications for position and concentration dependant gene silencing activity. The siRNAs will target firefly luciferase mRNA while *Renilla* luciferase (expressed via the pGL10 and SV40 plasmids) expression will be used to normalize the signal. Both luciferase enzymes catalyse a reaction that produces light as one of the products [108] which will be used to assess expression levels

via luminescence intensity [109]. The controls for the HeLa cell studies were cell transfected with the plasmids with no siRNA to which luminescence is expressed as a percent. The results are seen in the **Figures 3-5** to **3-7** with the siRNAs being tested at three different concentrations.

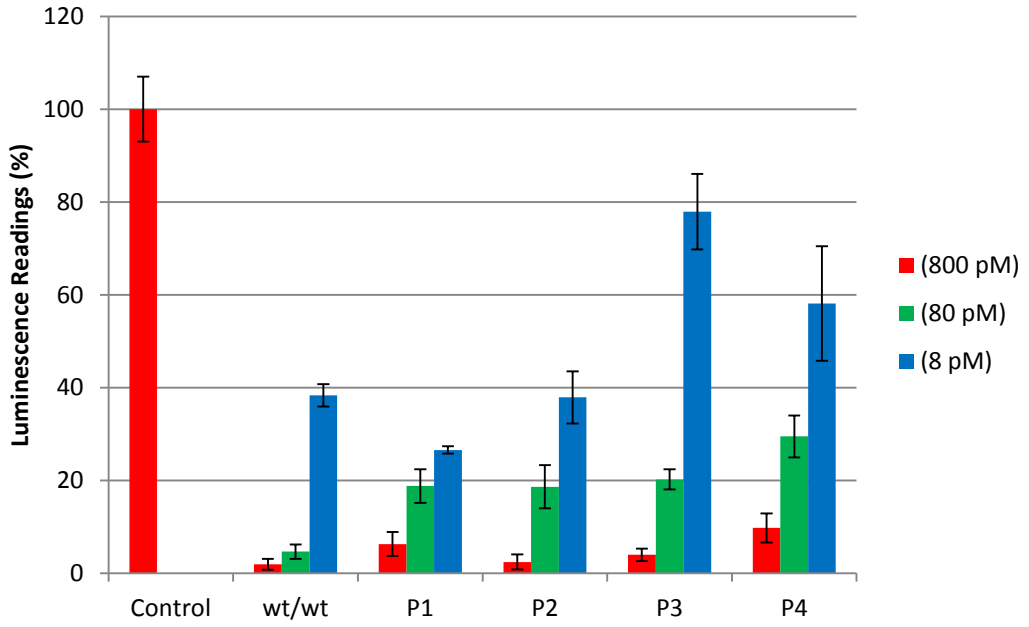

Figure 3-5: Gene silencing capability of HeLa cells treated with propargyl modified linker siRNA targeting firefly luciferase mRNA and normalized to *Renilla* luciferase.

The first four strands tested (siRNAs P1 – P4) contain the propargyl modified spacer (**Figure 3-5**) that spans two nucleobases. Comparing the modified strands to wt it becomes clear that the linker is well tolerated within the central even though it imparts destabilization (P1 – P3), which agrees with the work put forth by Maier et al., in 2010. Activity is very close to wt at the 800 pM concentration however activity decreases fast compared to wt as the concentration drops for strands P3 and P4. A possible explanation for the drop in activity compared to wt is the T_m of the modified strands which shows destabilization; meaning the modified strands form thermodynamically less favourable

duplex compared to wt [110]. Even when the linker is placed toward the 3' end of the sequence (P4) activity is still retained. Although this position isn't in the center it contributes to destabilizing the 5' of the desired antisense strand which has been shown to increase strand selection accuracy [111].

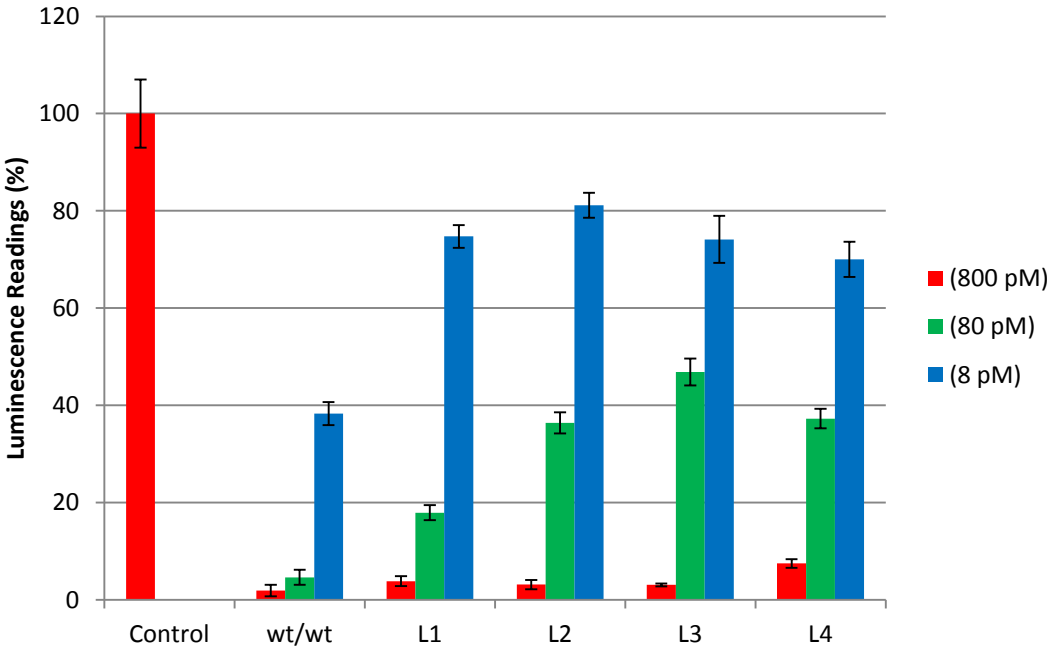

Figure 3-6: Gene silencing capability of HeLa cells treated with allyl modified linker siRNA targeting firefly luciferase mRNA and normalized to *Renilla* luciferase.

The allyl modified linker (siRNAs L1 – L4) activity (**Figure 3-6**) displayed very similar activity to that of the propargyl modified linker which is not surprising as the modifications are very similar. Again the centrally located linkers (siRNAs L1 – L3) display excellent silencing capability at 800 pM and decreased activity compared to wt at decreasing concentrations.

The final modification for the linker spanning two nucleobases is the bare linker (siRNAs A1 – A4), which used acetyl protecting groups during all the syntheses. Overall this linker performed modestly which does correlate to modification having the greatest

destabilization effect on the siRNA duplexes. One major difference compared to the previous two modifications is that the linker spanning the Argonaute2 site (A1) displays the least effective gene silencing capability at 800 pM which is the highest concentration that was tested.

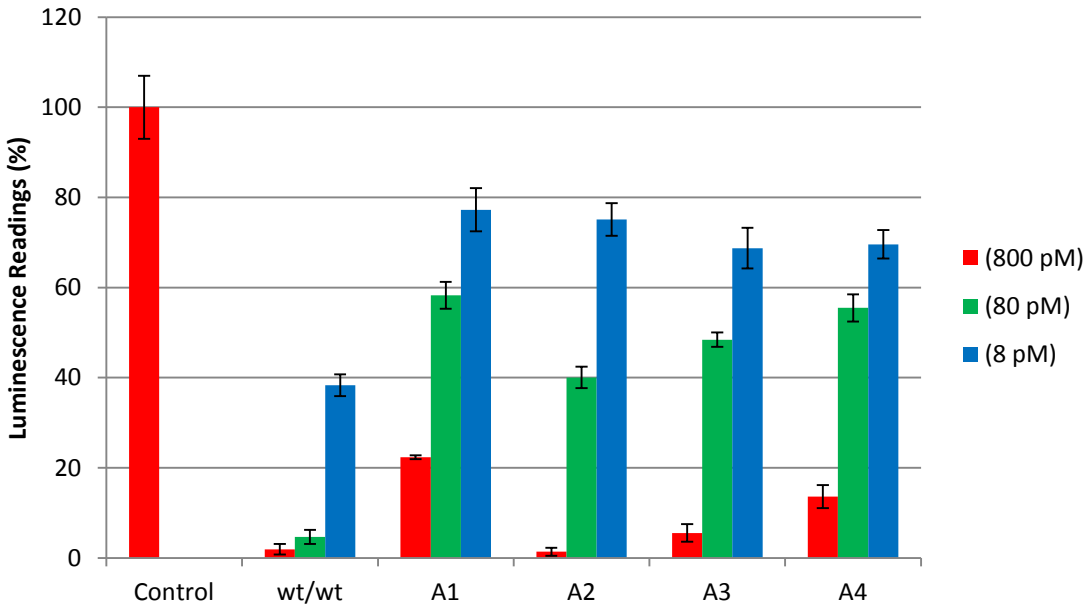

Figure 3-7: Gene silencing capability of HeLa cells treated with acetyl modified linker siRNA targeting firefly luciferase mRNA and normalized to *Renilla* luciferase.

One possibility for these strands having comparable potency to wt could be that it is believed this type of destabilization aides in the unwinding of dsRNA [111]. When taking each of the three modifications it is shown that the linkers that span the Argonaute2 cleavage sites (A1, L1 and P1) are silencing gene expression even though the linker is most likely not being cleaved. This agrees with the findings of Efthymiou et al., in 2012 and Maier et al., 2010. An explanation for these results could be that Argonaute2 site destabilization inhibits cleavage-mediated sense strand dissociation and promotes the bypass mechanism

of sense strand dissociation [112] as opposed to the cleavage mechanism. It has been shown that other than terminal asymmetry of the RNA duplex, lowered central duplex stability is directly correlated with increased siRNA potency [113]. In their study targeting two different anti-luciferase mRNA Maier et al., determined position 10 on the sense strand showed the best potency in terms of introducing site specific destabilization [50]. Examination of the luciferase knock-down figures the linkers that spanned positions 10+11 (siRNAs A2, L3, and P2) were the most potent or very close to at 800 pM, however activity worsens at the two lower concentrations with the propargyl modification retaining activity comparable to wt over each concentration. The linkers spanning the Argonaute2 site (siRNAs A1, L1, and P1) displayed mixed results with the propargyl modification being well tolerated at each concentration whereas the acetyl linker being one of the poorest gene silencers when taking each modification position into consideration. When Maier et al., replaced the Argonaute2 cleavage site with a destabilizing factor potency was increased ~2.5 fold; this was not the case with this two nucleobase linker and is most likely due to the fact that this modification imparts much greater destabilization which is most likely hindering its ability to some extent. The final linkers to be assessed are the single nucleobase (siRNAs BR 1-4 and X 1-5) replacing linker featuring a propargyl or click-cholesterol modification (**Figure 3-8**).

With the excellent activity of the larger spacer it does not come as a surprise that the siRNAs that contain the smaller spacers (siRNAs BR 1-4 and X 1-5) also display potent gene-silencing activity even when compared to w.t. Even the internally conjugated cholesterol modified siRNAs can display potent gene silencing capabilities whereas most internal cholesterol modified siRNAs generally display significantly decreased activity

which is thought to occur as the large cholesterol group may be interfering in key interactions within RISC [114]. Being attached on an alkyl backbone however gives the cholesterol group quite a bit a freedom to move around and potentially adopt a position that allows for these key interactions to proceed relatively unhindered.

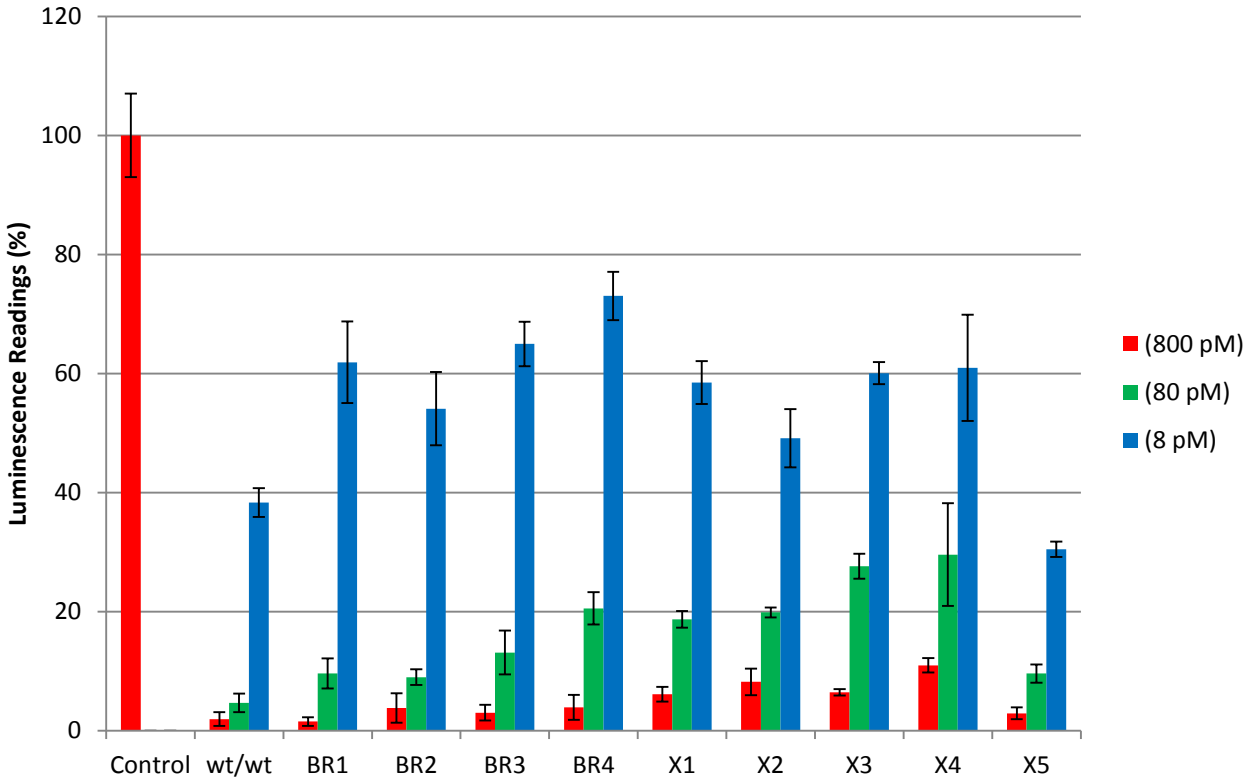

Figure 3-8: Gene silencing capability of HeLa cells treated with small propargyl and click-cholesterol modified siRNA targeting firefly luciferase mRNA and normalized to *Renilla* luciferase.

The siRNA modified with the cholesterol at the 3' end (X5) retained the best activity over all three concentrations. Not only can 3' destabilizing modifications increase antisense strand selection by destabilizing the antisense 5' end the linker also enhances cell membrane permeability due to the cholesterol group [115]. Since this group is also attached on the overhang there isn't much duplex destabilization which also contributes to the excellent potency [116].

Thinking back to the study by Maier et al., in 2010 the site specific abasic modifications do not appear to increase potency as previously reported within the central region [50], even at position 10 of the sense strand. Comparing the propargyl modified small linker siRNAs (siRNAs Br 1- 4) they display activity comparable if to w.t. at 800 pM while retaining better activity over the two smaller concentrations compared to the linker replacing two nucleobases which is most likely attributed to the lesser extent of thermal destabilization.

3.5 – Silencing Capability of the Clinically Relevant BCL2 Oncogene

Although the dual luciferase assay is a decent screening method for new modifications it does not accurately represent the potency because an abundant exogenous mRNA sequence is being targeted as opposed to many problematic genes, such as oncogenes, which exist at expression levels folds less than the luciferase mRNA [117]. The BCL2 oncogene has been directly implicated in several major cancers because damage to this gene can result in anti-apoptosis [118]. With the propargyl and allyl modified two nucleobase spacers having excellent activity in the central region of the sense strand those positions and modifications were chosen to target BCL2, the sequences of which are shown in **Table 3-3** below.

In order to assess the gene silencing capability of the anti-BCL2 siRNAs the expression levels of need to assessed against control genes. For this study the GAPDH and 18S genes will be used at the controls as each are very well characterized and have been used extensively in literature for PCR work [119]. To ensure that the primers were not

forming any products a no-template control was run along with a no-reverse transcriptase control to ensure no genomic contamination [120].

Table 3-4: Sequences of anti-BCL2 siRNAs containing the double base spacer and their melting temperatures.

siRNA	***siRNA Duplex***	***[a]T_m (°C)***	***ΔT_m (°C)***
wt	5' – GUG AAG UCA ACA UGC CUG Ctt – 3' (S) 3' – ttCAC UUC AGU UGU ACG GAC G – 5' (AS)	81.7	0
P5	5' – GUG AAG UCX-XCA UGC CUG Ctt – 3' 3' – ttCAC UUC AGU UGU ACG GAC G – 5'	73.2	-8.5
P6	5' – GUG AAG UXX ACA UGC CUG Ctt – 3' 3' – ttCAC UUC AGU UGU ACG GAC G – 5'	70.8	-10.9
P7	5' – GUG AAG UCA XXA UGC CUG Ctt – 3' 3' – ttCAC UUC AGU UGU ACG GAC G – 5'	72.1	-9.6
L5	5' – GUG AAG UCL-LCA UGC CUG Ctt – 3' 3' – ttCAC UUC AGU UGU ACG GAC G – 5'	73.4	-8.3
L6	5' – GUG AAG ULL ACA UGC CUG Ctt – 3' 3' – ttCAC UUC AGU UGU ACG GAC G – 5'	69.9	-11.8
L7	5' – GUG AAG UCA LLA UGC CUG Ctt – 3' 3' – ttCAC UUC AGU UGU ACG GAC G – 5'	72.6	-9.1

[a]T_ms were measures in a sodium phosphate buffer (90 mM NaCl, 10 mM Na_2HPO_4, 1 mM EDTA, pH 7) at 260 nm, from 10 to 95 °C. **XX** and **LL** correspond to the propargyl and allyl modified spacer respectively. ' _ ' Shows the position of the Ago2 cleavage site.

Examining the gene silencing data in **Figure 3-9** shows that this linker is extremely well tolerated within the central region when targeting an endogenous gene. What immediately stands out is that the modified siRNAs (P5 – P7 and L5 – L7) have greater activity than wild type at the 1 pM concentration which was not seen in the anti-luciferase trials but agrees more with the finding put out by Maier et al., in 2010. Another noticeable difference from the anti-luciferase trials is that the siRNAs exhibiting the best potency across all

concentrations appear to be the linkers spanning the Argonaute2 site (P5 and L5). Examining the sequences in **Table 3-3** shows that when the linker is spanning the Argonaute2 site for this sequence two A-U bonding interactions are disrupted, which totals only 4 H-bonds, whereas the other two modification sites (siRNAs P6, P7, L6 and L7) replace on A-U and one G-C bonding interaction, totalling 5 H-bonds. This most likely means that the Argonaute2 site modified siRNAs (P5 and L5) are introducing less destabilization than the other two positions which is seen in the gene silencing ability of the siRNAs [121].

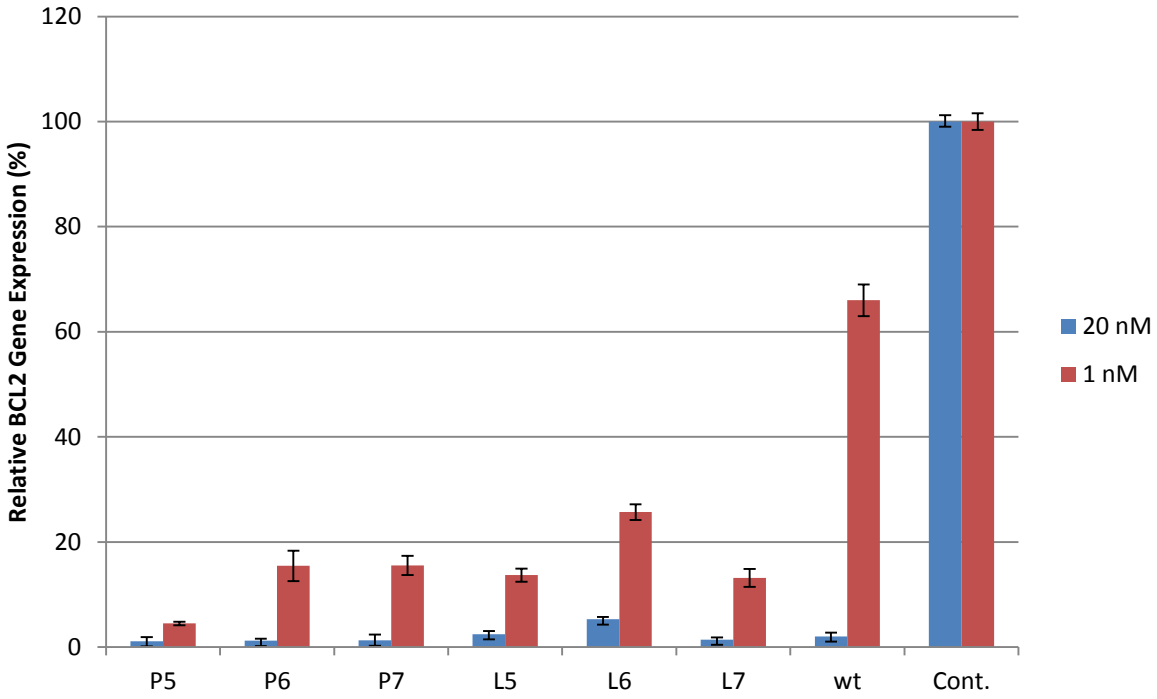

Figure 3-9: BCL2 oncogene knock-down using allyl and propargyl modified siRNAs assessed using qRT-PCR using 18s and GAPDH as controls.

Although the introduction of these linkers imparts a significant degree of destabilization on siRNA duplexes the aforementioned results show that this destabilization can be utilized in a positive way when incorporated near the central region

of the sense strand. With extremely promising results targeting exogenous and endogenous genes these findings have been submitted for application of intellectual property

4.0 - Future Directions

With the success of the silencing capability of the modified alkyl linkers there is no doubt that this project should be pursued farther in terms of expanding the scope of this type of modification. To do this however there should be some synthetic optimization, particularly at the TBS protection step. The yield obtained is modest, which occurs when straightforward alcohol TBS protection is attempted in basic conditions; however by utilizing 2.5 equivalents (eq) of imidazole and 1.2 eq of TBS-Cl per alcohol group in DMF yields can be greatly increased [122]. This could potentially raise the overall synthesis yield by upwards of 7%.

With the successful introduction of simple modifications on this linker the logical next step would be utilizing those modifications to affix other modifications. An example of this would be performing a Sonogashira coupling reaction with the alkyne linkers and iodouracil which would help in trying to fine tune the destabilization by introducing controlled addition of H-bonding in to the duplex. Conjugating more biomolecules would also be another interesting avenue to explore such as trying to turn the larger propargyl linker in to a x2 click cholesterol linker which would make an interesting 3' overhang modification on the sense strand as cholesterol modifications are well tolerated in this region [115].

Although these linkers presented herein displayed excellent knockdown 24 hours after transfection it is entirely possible that the maximum knockdown is occurring at some other time [123]. A time-dependency analysis should be performed to determine when the

optimal knockdown is occurring which should then be implemented in to the procedure for testing the siRNAs to determine optimal knockdown.

Another useful test that could be done would be a simple incubation experiment without a transfection agent to see if the introduction of the two protonated nitrogen atoms can facilitate crossing of the cellular membrane. This is a common simple study done with modified siRNAs that are designed to increase cell membrane permeability, such as cholesterol modifications [124]. This study would be of particular interest with the single click cholesterol which not only possesses the positively charged nitrogen but also the lipophilic cholesterol moiety. The cell permeability could be increased even further if multiple click cholesterol modifications were incorporated; examining the thermal stability of the single click cholesterols the incorporation of the 3' overhang modification as well as a centrally located modification could possibly retain enough thermal stability to function effectively.

5.0 - Conclusion

This study presents a simple and novel means of central region destabilization through sense strand modification in siRNAs through the use of modifiable alkylamino linkers. Even when the non-cleavable linkers span the catalytic region of the Argonaute2 catalytic site activity is retained that is comparable to wild type. In the case of silencing the clinically relevant BCL2 oncogene, siRNAs with the modified linkers demonstrated that they are capable of greater gene silencing at lowered concentrations wild type indicating that the modification is imparting favourable characteristics upon siRNAs. The single and double nucleobase modified linkers show their applicability by introducing site-specific destabilization which can be strategically used to retain or enhance potency compared to wild type. With these promising preliminary results there is no doubt that further modification and introduction of newer simple modifications should be explored in an effort to elucidate a nucleic acid modification that has wide-spread applicability.

References

[1] B. Alberts (**2008***). Molecular biology of the cell*. New York: Garland Science. ISBN 0-8153-4105-9

[2] J. Jankowski and J. Polak (**1996**). *Clinical gene analysis and manipulation: Tools, techniques and troubleshooting*. Cambridge University Press. ISBN 0-521-47896-0.

[3] J. Berg, L. Tymoczko and L. Stryer (**2002**). *Biochemistry (5th ed.)*. New York: W.H. Freeman and Company. ISBN 0-7167-4684-0.

[4] M. Egli, G. Minasov, V. Tereshko, P. Pallan, M. Teplova, G. Inamati, E. Lesnik, S. Owens, B. Ross, T. Prakash, M. Manoharan. *Biochem.* **2005.** *44:* p. 9045 – 9057.

[5] I. Tinoco and C. Bustamante. *J. Mol. Biol.***1999.** *293(2)*: p. 271 - 281.

[6] P. Higgs. *Quarterly Rev. of Biophys*. **2000.** *33(3)*: p. 199 - 253.

[7] N. Campbell, B. Williamson and R. Heyden. (**2006**). *Biology: Exploring Life*. Boston: Pearson Prentice Hall. ISBN 0-13-250882-6.

[8] J. Wang. *PNAS*. **1979.** *76(1)*: p. 200 - 203.

[9] L. Allison (**2007**). *Fundamental Molecular Biology.* London: Blackwell Publishing. ISBN 978-1-4051-0379-4.

[10] A. Griffiths (**2008***). Introduction to Genetic Analysis (9th ed.).* New York: W.H. Freeman and Company. ISBN 978-0-7167-6887-6.

[11] D. Baltimore. *Nature*. **1970.** *226*: p. 1209 – 1211.

[12] O. Bagasra and K.R. Prilliman. *J. Mol. Histol*. **2004.** *35(6)*: p. 545 - 553.

[13] H. Cerutti and J. Casas-Mollano. *Curr. Genet*. **2006.** *50(2)*: p. 81 - 99.

[14] J. Opalinska and A. Gerwitz. *Nat. Rev. Drug Discov.* **2002**. *1:* p. 503 – 514.

[15] B. Zhang, X. Pan, G. Cobb, T. Anderson. *Dev. Biol.* **2006.** *289(1)*: p. 3 – 16.

[16] S. Shalbalina and E. Koonin. *Trends in Ecological Evolution.* **2008.** *23*: p. 578 – 587.

[17] A. Fire, S. Xu, M. Montgomery, S. Kostas, S. Driver and C. Mello. *Nature.* **1998.** *39*: p. 806 – 811.

[18] K. Gavrilov and M.W. Saltzman. *Yale J. Biol. Med.* **2012**. *85(2)*: p. 187 – 200.

[19] E. Bernstein, A. Caudy, S. Hammond and G. Hannon. *Nature*. **2001**. *409*: p. 363 – 366.

[20] Y-L. Chiu and T. Rana. *Mol. Cell.* **2002**. *10*: p. 549 – 561.

[21] G. Sen and H. Blau. *FASEB Journal.* **2006**. *20*: p. 1293 – 1299.

[22] J. Gredell, M. Dittmer, M. Wu, C. Chan and P. Walton. *Biochem***. 2010**. *49*: p. 3148 – 3155.

[23] S. M. Elbashir, J. Harborth, W. Lendeckel, A. Yalcin, K. Weber and T. Tuschl. *Nature*. **2001.** *411*: p. 494 – 498.

[24] R. Wilson and J. Doudna. *Annual Rev. of Biophys*. **2013**. *42*: p. 217 – 239.

[25] B. Haley and P.D. Zamore. *Nat. Struct. Mol. Biol.* **2004**. *11*: p. 599 – 606.

[26] O. Bagasra and K. Prilliman. *J. Mol. Histol.* **2004**. *35(6)*: p. 545 – 553.

[27] B. L. Bass. *Cell*. **2000.** *101*: p. 235 – 238.

[28] G. Hutvagner. *Science.* **2001.** *293*: p. 834 – 838.

[29] G. Meister, M. Landthaler, A. Patkaniowska, Y. Dorsett, G. Teng and T. Tuschl. *Cell*. **2004.** *15*: p. 185 – 197.

[30] A. van den Berg, J. Mols and J. Han. *Biochim. Biophys. Acta.* **2008**. *1779*: 668 – 677.

[31] S. Daniels and A. Gatignol. *Microbiol. Mol. Biol. Rev.* **2012**. *76*: p. 652 – 666.

[32] N. Schirle and I. MacRae. *Science*. **2012**. *336*: p. 1037 – 1040.

[33] T. Rand, S. Petersen, F. Du and X. Wang. *Cell*. **2005**. *123(4)*: p. 621 – 629.

[34] J. Liu, M.A. Carmell, F. Rivas, C.G. Marsden, J. M. Thomson, J. Song, S. Hamond, L. Joshua-Tor and G. Hannon. *Science*. **2004.** *305*: p. 1437 – 1441.

[35] W. Lima, H. Wu, J. Nichols, H. Sun, H. Murray and S. Crooke. *J. Biol. Chem.* **2009**. *284*: p. 26017 – 26028.

[36] C. Allerson, N. Sioufi, R. Jarres, T.P. Prakash, N. Naik, A. Berdeja, L. Wanders, R. Griffey, E. Swayze and B. Bhat. *J. Med. Chem.* **2005.** *48*: p. 901 – 904.

[37] L. Stephenson and P. Zamecnik. *Proc. Natl. Acad. Sci. USA.* **1978.** *75*: p. 2761 – 2769.

[38] D. Loakes and D.M. Brown. *Nucleic Acid. Res.* **1994.** *22*: p. 4039 – 4043.

[39] A. Pollack. *"F.D.A. Approves Genetic Drug to Treat Rare Diseases."* The New York Times. Retreived January 31, 2013.

[40] D.R. Corey. *J. Clin. Invest.* **2007.** *117*: p. 3615 – 3622.

[41] F. Li, P. Pallan, M. Maier, K. Rajeev, S. Mathieu, S. Kreutz, Y. Fan, J. Sanghvi, R. Micura and E. Rozners. *Nucleic Acid. Res.* **2007**. *35*: p. 6424 – 6438.

[42] M. Collingwood, S. Rose, L. Huang, C. Hillier, M. Amarzguioui, M. Wiiger, H. Soifer, J. Rossi and M. Behlke. *Oligonucleotides.* **2008.** *18*: p. 187 – 199.

[43] J. Turner, S. Jones, S. Moschos, M. Lindsay and M. Gait. *Mol. Biosyst.* **2007.** *3*: p. 43 – 50.

[44] S. Kennedy, D. Wang and G. Ruvkun. *Nature.* **2004.** *427*: p. 645 – 649.

[45] B. Weiss. *Adv. Cycl. Nucl. Res.* **1975.** *5*: p. 195 – 211.

[46] A. Bibillo, K. Ziomek, M. Figlerowicz, and R. Kierzek. *Acta Biochim. Pol.* **1999.** *46(1)*: p. 145 – 153.

[47] J. Jeong, H. Mok, Y-K. Oh and T. Park. *Bioconjugate Chem.* **2009.** *20*: p. 5 – 14.

[48] J. Watts, G. Deleavey and M. Damha. *Drug Discovery Today.* **2008.** *13*: p. 842 – 855.

[49] G. Deleavey and M. Damha. *Chem. and Biol. Rev.* **2012**. *19*: p. 937 – 956.

[50] A. Jackson, J. Burchard, J. Schelter, B. Chau, M. Cleary, L. Lim and P. Linsley. *RNA.* **2006.** *12*: p. 1179 – 1187.

[51] E. Ohtsuka, M. Ikehara and D. Soll. *Nucleic Acid Res.* **1982.** *10*: p. 6553 – 6570.

[52] B. Dahl, J. Nielsen and O. Dahl. *Nucleic Acid Res.* **1987.** *15*: 1729 – 1743.

[53] S. Beaucage. *Curr. Opin. Drug. Discov. Devel.* **2008.** *11*: p. 203 – 216.

[54] S. Muller, J. Wolf and S.A. Ivanov. *Curr. Org. Syn.* **2004**. *1*: p. 293 – 307.

[55] S. Shukla, C.S. Sumaria and P. Pradeepkumar. *ChemMedChem.* **2009.** *5(3)*: p. 328 – 349.

[56] O. Merkel, I. Rubenstein and T. Kissel. *Adv. Drug Delev. Rev.* **2014**. In press. DOI: 10.1016/j.addr.2014.05.018

[57] F. Eckstein. *Nucleic Acid Drug Dev.* **2000.** *10*: p. 117 – 121.

[58] Y. Sanghvi. (**2011**). *A status update of modified oligonucleotides for chemotherapeutics applications.* Hoboken, NJ: John Wiley & Sons.

[59] F. Eckstein. *Biochimie.* **2002.** *84*: p. 841 – 848.

[60] P. Guga and W. Stec. *Curr. Protoc. Nucleic Acid Chem.* **2003.** *4*: 4.17.1 – 4.17.27.

[61] C. Bennett and E. Swayze. *Annu. Rev. Pharmacol. Toxicol.* **2010.** *50*: p. 259 – 293.

[62] P. Leuschner, S. Ameres, S. Kueng and J. Martinez. *EMBO Rep. 7*: p. 314 – 320.

[63] G. Blackburn, M. Gait and D. Loakes. (**2006**). *DNA and RNA structure.* Cambridge, UK: RSC Publishing.

[64] M. Olejniczak, K. Polak, P. Galka-Marciniak and W. Krzyosiak. *Curr. Gene. Ther.* **2011.** *11(6)*: p. 532 – 543.

[65] H. Ikeda, R. Fernandez, A. Wilk, J. Barchi, X. Huang and V. Marquez. *Nucleic Acid Res.* **1998.** *26*: p. 2237 – 2244.

[66] P. Herdewijn. *Antisense Nucleic Acid Drug Dev.* **2000.** *10*: p. 297 – 310.

[67] P. Gioanni. *Proc. Natl. Acad. Sci.* **2011**. *108(26)*: p. 10443 – 10447.

[68] T. Kim and E. Kool. *J. Org. Chem.* **2005.** *70*: p. 2048 – 2053.

[69] T. Efthymiou, W. Gong and J-P. Desaulniers. *Molecules*. **2012.** *17*: p. 12665 – 12703.

[70] J. Xia, A. Noronha, I. Toudjarska, F. Li, A. Akinc, R. Braich, M. Frank-Kamenetsky, K. Rajeev, M. Egli and M. Manoharan. *ACS Chem. Biol.* **2006.** *1*: p. 176 – 183.

[71] P. Nielsen. *Pure Appl. Chem.* **1998.** *70*: p. 105 – 110.

[72] W. Filipowicz. *Cell.* **2005.** *122(1)*: p. 17 – 20.

[73] M. Tijsterman and R. Plasterk. *Cell.* **2004.** *117(1)*: p. 1 – 3.

[74] T. Efthymiou, B. Peel, V. Huynh and J-P. Desaulniers. *Bioorg. & Med. Chem. Lett.* **2012.** *22*: p. 5590 – 5594.

[75] A. Kannan, E. Fostvedt, P. Beal and C. Burrows. *J. Am. Chem. Soc.* **2011.** *133*: p. 6343

[76] A. Hernandez, L. Peterson and E. Cool. *ACS CHEM. Biol.* **2012.** *7(8)*: p. 1454 – 1461.

[77] A. Somoza, R. Miller, J. Chelliserrykattil and E. Cool. *Chemistry*. **2008.** *14*: p. 7978.

[78] Y. Ueno, K. Yoshikawa, Y. Kitamura and Y. Kitade. *Bioorg. & Med. Chem. Lett.* **2009.** *19*: p. 875 – 877.

[79] M. Sobczak, K. Kubiak, M. Janicka, M. Sierant, B. Mikolajczyk and B. Nawrot. *Collect. Czech. Chem. Commun.* **2011.** *76(12)*: p. 1471 – 1486.

[80] K. Whitehead, R. Langer and D. Anderson. *Nat. Rev. Drug. Discov.* **2009.** *8*: p. 129 – 138.

[81] S. Singer and G. Nicolson GL. *Science.* **1972.** *175 (4023)*: p. 720 – 731.

[82] H. Addepalli, Meena, C. Peng, G. Wang, Y. Fan, K. Charisse, N. Jayaprakash, K. Rajeev, R. Pandey, G. Lavine, L. Zhang, K. Jahn-Hofmann, P. Hadwiger, M. Manoharan and M. Maier. *Nucleic Acid Res.* **2010.** *38(20)*: p. 7320 – 7331.

[83] H. Uchiro, R. Kato, Y. Arai, M. Hasegawa and Y. Kobayakawa. *Org. Lett.* **2011.** *13(23)*: p. 6268 – 6271.

[84] D. Nelson, D. Crouch. *Synthesis*. **1996**. 1031 – 1069. doi: 10.1055/s-1996-4350

[85] M. Bessodes, D. Komiotis and K. Antonakis. *Tet. Lett.* **1986.** *27(5)*: p. 579 – 580.

[86] Z. Kupihar, G. Varadi, E. Monostori and G. Toth. *Tetrahedron.* **2000.** *41*: p. 4457 – 4461.

[87] T. Muller and M. Beller. *Chem. Rev.* **1998.** *98*: p. 675 – 703.

[88]G. Jakab, C. Tancon, Z. Zhang, K. Lippert and P. Schreiner. *Org. Lett.* **2012.** *14(7)*: p. 1724 – 1727.

[89] D. Berry, C. Digiovanna, S. Metrick and R. Murugan. *Arkivoc*. **2001.** p. 201 – 226.

[90] J. Kotek, P. Hermann, P. Vojtisek, J. Rohovec and I. Lukes. *Collect. Czech. Chem. Commun.* **2000.** *65(2)*: p. 243 – 266.

[91] B. Roberts. **2014**. UOIT Honour's Thesis Project: UOIT, Canada.

[92] R. Chinchilla and N. Carmen. *Chem. Rev.* **2007.** *107(3)*: p. 875.

[93] J. Willibald, J. Harder, K. Sparrer, K. Conzelmann and T. Carell. *J. Am. Chem. Soc.* **2012.** *134(30)*: p. 12330 – 12333.

[94] A. de Fougerolles, H-P. Vornlocher, J. Maraganore and J. Lieberman. *Nat. Rev. Drug. Discov.* **2007.** *6*: p. 443 – 453.

[95] H. Kolb amd B. Sharpless. *Drug Discov. Today.* **2003.** *8(24)*: p. 1128 – 1137.

[96] F. Himo, T. Lovell, R. Hilgraf, V. Rostovtsev, L. Noddleman, B. Sharpless. and V. Fokin. *J. Am. Chem. Soc.* **2005.** *127*: p. 210 – 216.

[97] V. Rostovtsev, L. Green, V. Fokin and B. Sharpless. *Angew. Chem. Int. Ed.* **2002.** *41*: p. 2596 – 2599.

[98] B. Boren, S. Narayan, L. Rasmussen, L. Zhang, H. Zhao, G. Lia and V. Fokin. *J. Am. Chem. Soc.* **2008.** *130*: p. 8923 – 8930.

[99] K.M. Guckian, B. Schweitzer, R.X. Ren, C. Shiels, P. Paris and E. Cool. *J. Am. Chem. Soc.* **1996.** *118*: p. 8182 – 8183.

[100] A. Nygaard and B.D. Hall. *Biochem. & Biophys. Res. Comm.* **1963.** *12(2)*: p. 98 – 104.

[101] B. Schweitzer and E. Kool. *J. Am. Chem. Soc.* **1995**. *117*: p. 1863 – 1872.

[101] J. Bramsen, M. Pakula, T. Hansen, C. Bus, N. Langkjaer, D. Odadzic, R. Smicius, S. Wengel, J. Chattopadhyaya, J. Engels, P. Herdewijn, J. Wengel and J. Kjems. *Nucleic Acid Research.* **2010.** *38(17)*: p. 5761 – 5773.

[102] S. Li and L. Huang. *Gene Therapy.* **2006.** *13*: p. 1313 – 1319.

[103] S. Akhtar and I. Benter. *J. Clin. Invest.* **2007.** *117(12)*: p. 3623 – 3632.

[104] R. Gregory, T. Chendrimada, N. Cooch and R. Shiekhattar. *Cell*. **2005.** *123(4)*: p. 631 – 640.

[105] F. Wold. (**1971**). Macomolecules: Structure and Function. New York: Garland Science.

[106] W. Saenger. (**1984**). Principles of Nucleic Acid Structure: New York: Springer Verlag.

[107] J.C. Maurizot. (**2000**). Circular dichroism of nucleic acids: nonclassical conformations and modified oligonucleotides. Circular Dichroism: Principals and Applications. New York: Wiley-VCH.

[108] J. de Wet, K. Wood, M. DeLuca, D. Helinski and S. Subramani. *Mol. & Cell Biol.* **1987.** p. 725 – 737.

[109] Promega Technical Manual: Dual Luciferase Reporter Assay. Revised June 2011. www.promega.com

[110] N. Vaish, F. Chen, S. Seth, K. Fosnaugh, Y. Liu, R. Adami, T. Brown, Y. Chen, R. Johns, G. Severson, B. Grange, P. Charmley, M. Templin and B. Polisky. *Nucleic Acid Res.* **2010.** *39(5)*: p. 1823 – 1832.

[111] D. Bumcrot, M. Manoharan, V. Koteliansky and D. Sah. *Nat. Chem. Biol*. **2006**. *2*: p. 711.

[112] C. Matranga, Y. Tomari, C. Shin, D.P. Bartel and P.D. Zamore. *Cell.* **2005.** *123*: p. 621 – 629.

[113] A. Khvorova, A. Reynolds and S.D. Jayasena. *Cell*. **2003**. *115*: p. 209 – 216.

[114] M. Amarzguioui, T. Holen, E. Babaie and H. Prydz. *Nucleic Acid Res.* **2003.** *31(2)*: p. 589 – 595. [d26] Y. Otake, T.K. Sengupta, E. Kio, J. Smith and D. Fernandes. *Blood.* **2007.** *109(7)*: p. 3069 – 3075.

[115] C. Wolfrum, S. Shi, N. Jayaprakash, M. Jayaraman, G. Wang, R. Pandley, K. Rajeev, T. Nakayama, K. Charisse, E. Ndungo, T. Zimmerman, V. Koteliansky, M. Manoharan and M. Stoffel. *Nat. Biotech.* **2007.** *25(10)*: p. 1149 – 1157.

[116] M. Masud, T. Masuda, Y. Inoue, M. Kuwahara, H. Sawai and H. Ozaki. *Bioorg. & Med. Chem. Lett.* **2011.** *21(2)*: p. 715 – 717.

[117] M. Chawla-Sarkar, S. Bae, F. Reu, B. Jacobs, D. Lindner and E. Borden. *Cell Death and Differentiation.* **2004.** *11*: p. 915 – 923.

[118] M. Ocker, D. Neureiter, M. Leuders, S. Zopf, M. Ganslmayer, E. Hahn, C. Harold and D. Schuppan. *Pancreatic Cancer.* **2005.** *54*: p. 1298 – 1308.

[119] R.D. Barber, D. Harmer, R. Coleman and B. Clarke. *Physiol. Genomics.* **2005**. *21(3)*: p. 389 – 395.

[120] W. Strapps, V. Pickering, G. Muiru, J. Rice, S. Orsborn, B. Polisky, A. Sachs and S. Bartz. *Nucleic Acid Res.* **2010**. *38(14)*: p. 4788 – 4798.

[121] J. Xia, A. Noronha, I. Toudjarska, F. Li, A. Akinc, R. Braich, M. Frank-Kamenetsky, K. Rajeev, M. Egli and M. Manoharan. *ACS Chem. Biol.* **2006**. *1*: p. 176 – 183.

[122] E. J. Corey, A. Venkateswarlu. *J. Am. Chem. Soc.* **1972.** *94:* p. 6190 – 6191.

[123] N. Kobayashi, Y. Matsui, A. Kawase and K. Hirata. *J. of Pharm. & Exp. Ther.* **2004.** *308(2)*: p. 688 – 693.

[124] A. Akinc, A. Zumbuehl, M. Goldberg, E. Leshchiner, V. Busini, N. Hossain, S. Bacallado, D. Nguyen, J. Fuller, R. Alvarez, A. Borodovsky, T. Borland, R. Constien, A. de Fougerolles, R. Dorkin, M. John, V. Koteliansky, M. Manoharan, L. Nechev, J. Qin, D. Sah, J. Soutscjek, I. Toudjarska, H-P. Vornlocher, T. Zimmerman, R. Langer and D. Anderson. *Nat. Biotech.* **2008.** *26*: p. 561 – 569.

Appendix

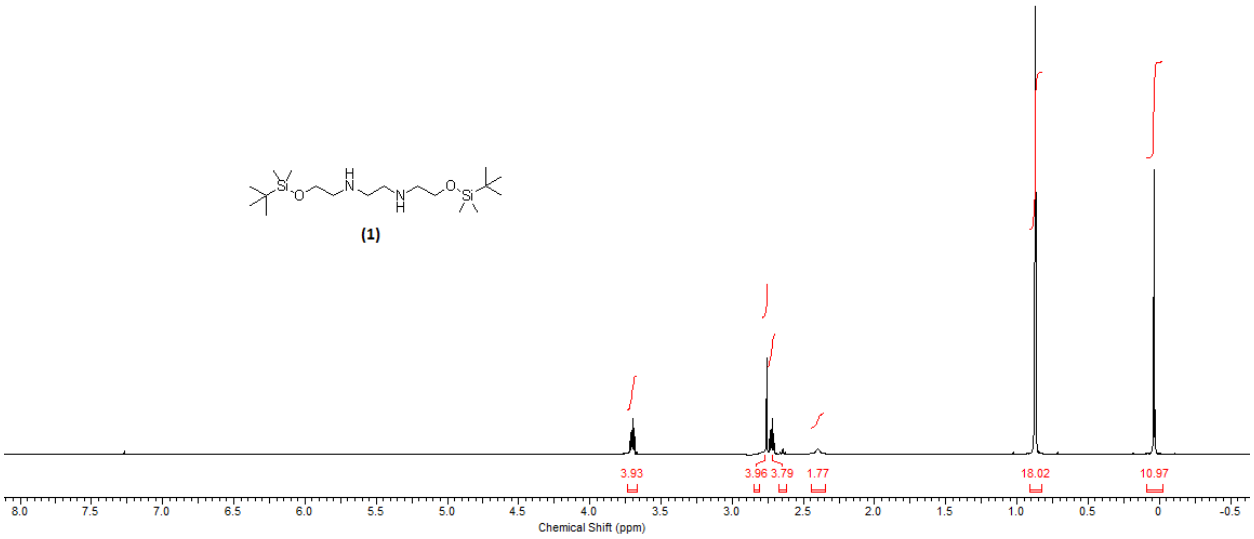

A1-1: ^{1}H NMR Spectrum of *N,N'*-bis(2-((tert-butyldimethylsilyl)oxy)ethyl)ethane-1,2-diamine – Compound (1)

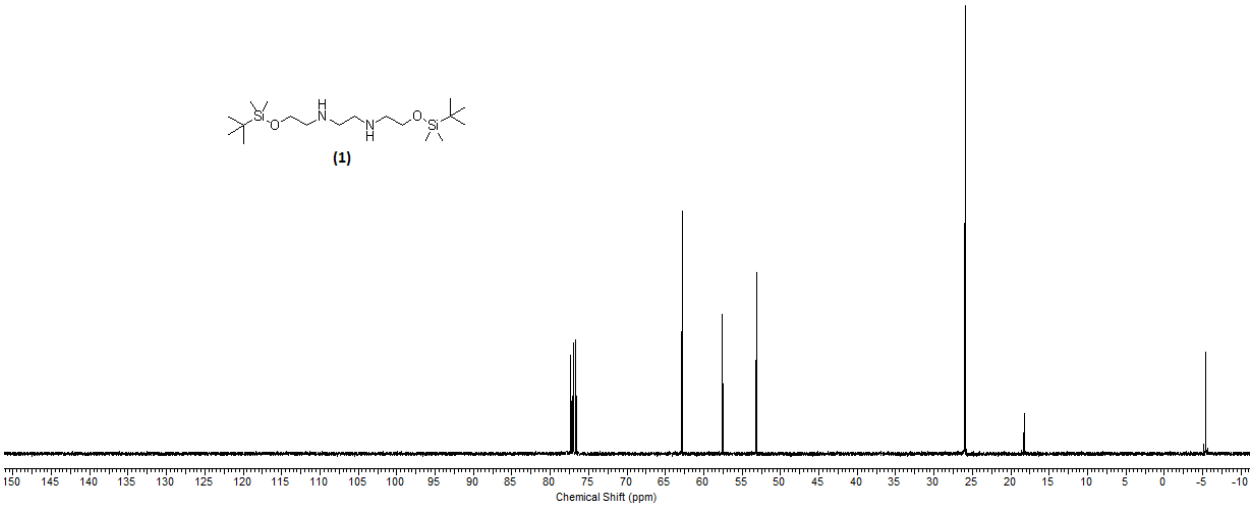

A1-2: ^{13}C NMR Spectrum of *N,N'*-bis(2-((tert-butyldimethylsilyl)oxy)ethyl)ethane-1,2-diamine – Compound (1)

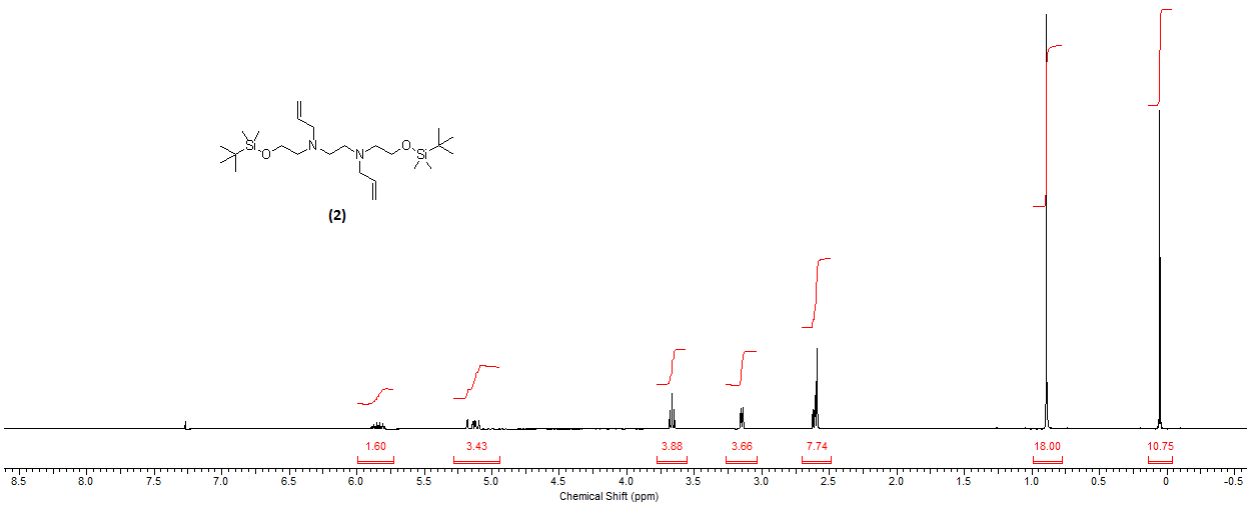

A2-1: ^{1}H NMR spectrum of *N,N'*-diallyl-*N,N'*-bis(2-((tert-butyldimethylsilyl)oxy)ethyl)ethane-1,2-diamine – Compound (2)

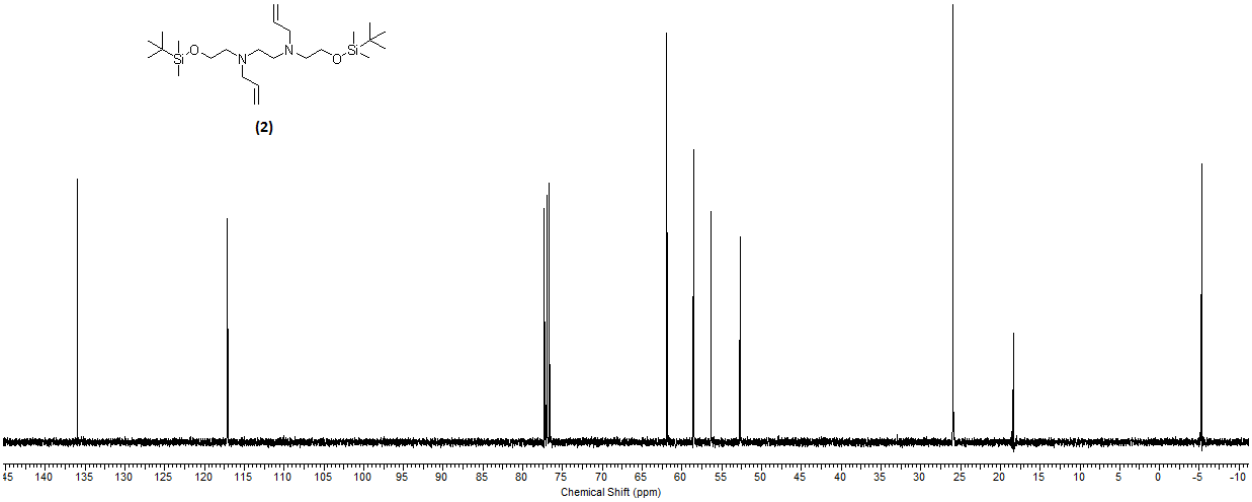

A2-2: ^{13}C NMR spectrum of *N,N'*-diallyl-*N,N'*-bis(2-((tert-butyldimethylsilyl)oxy)ethyl)ethane-1,2-diamine – Compound (2)

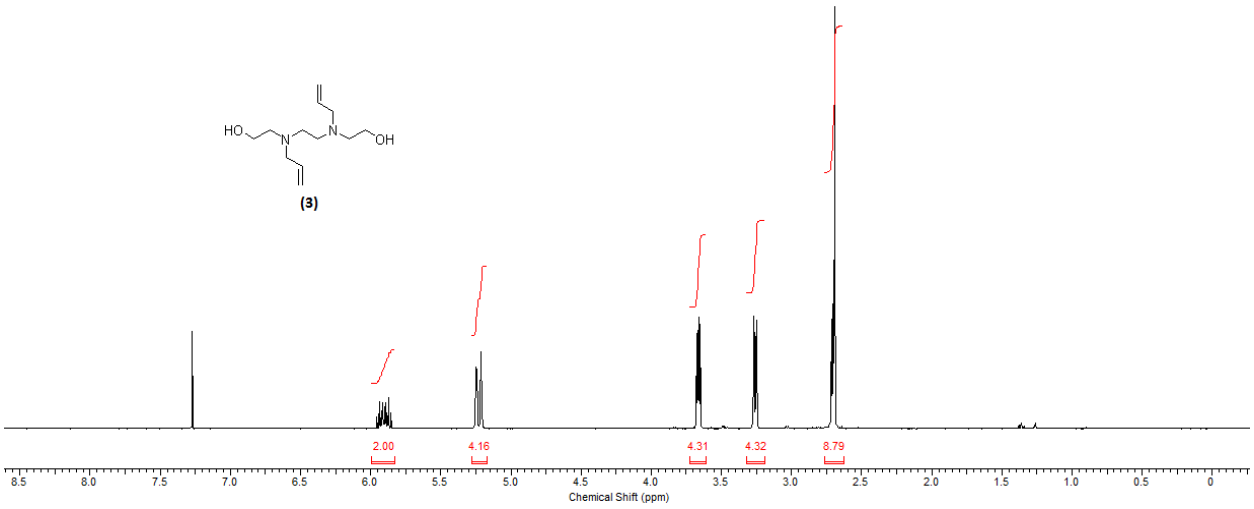

A3-1: ^{1}H NMR spectrum of 2,2'-(ethane-1,2-diylbis(allylazanediyl))bis(ethan-1-ol) – Compound (3)

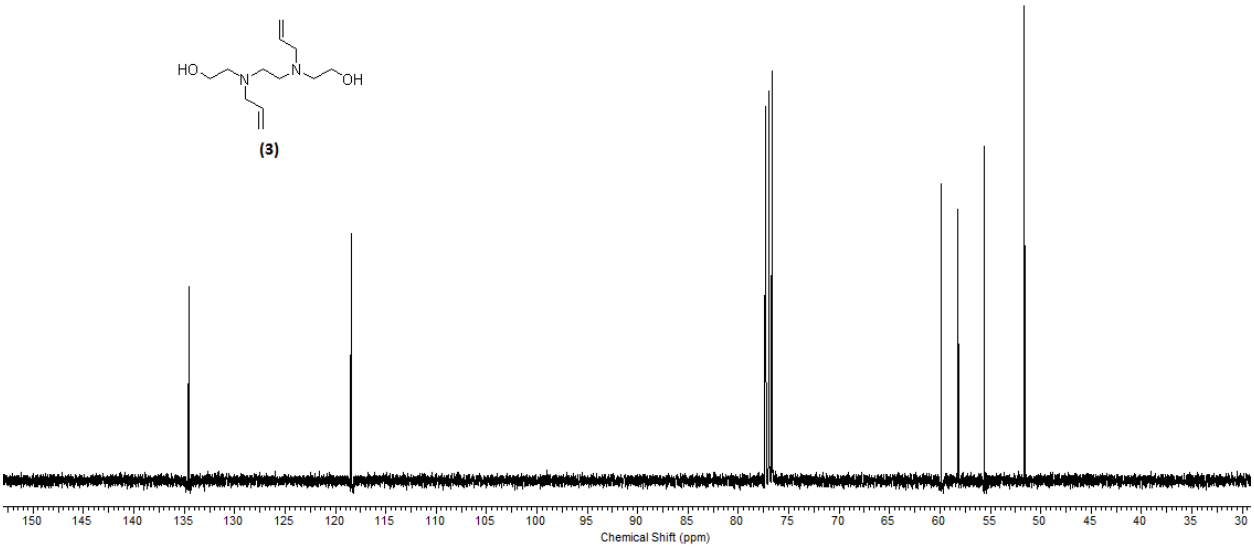

A3-2: ^{13}C NMR spectrum of 2,2'-(ethane-1,2-diylbis(allylazanediyl))bis(ethan-1-ol) – Compound (3)

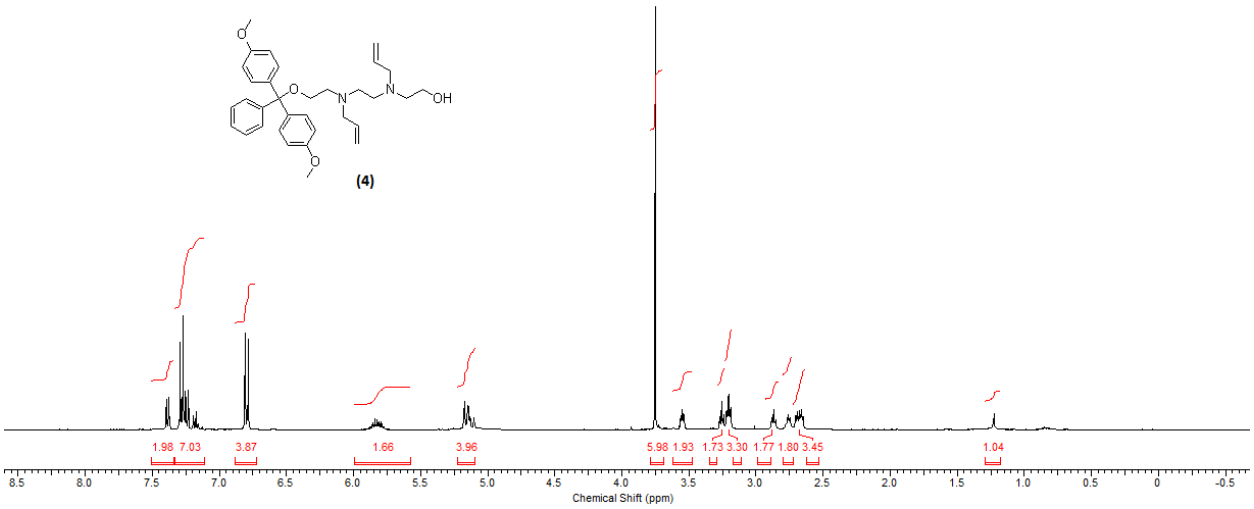

A4-1: ^{1}H NMR spectrum of 2-(allyl(2-(allyl(2-(bis(4 -methoxyphenyl)(phenyl)methoxy)ethyl)amino)ethyl)amino)ethan-1-ol – Compound (4)

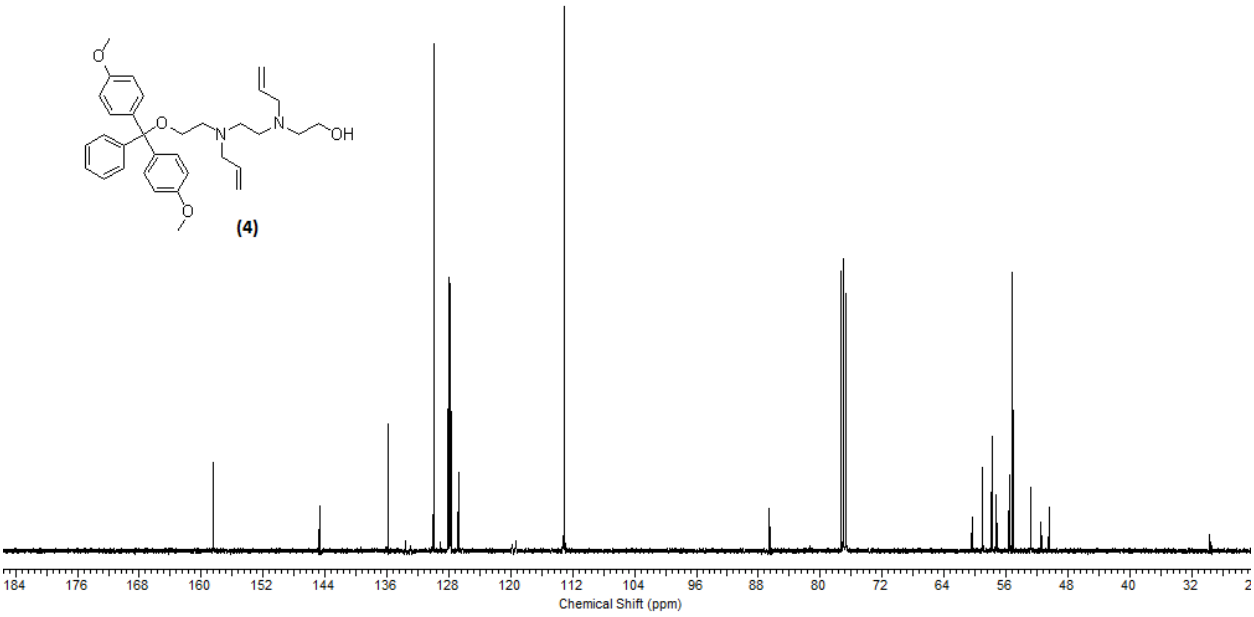

A4-2: ^{13}C NMR spectrum of 2-(allyl(2-(allyl(2-(bis(4 -methoxyphenyl)(phenyl)methoxy)ethyl)amino)ethyl)amino)ethan-1-ol – Compound (4)

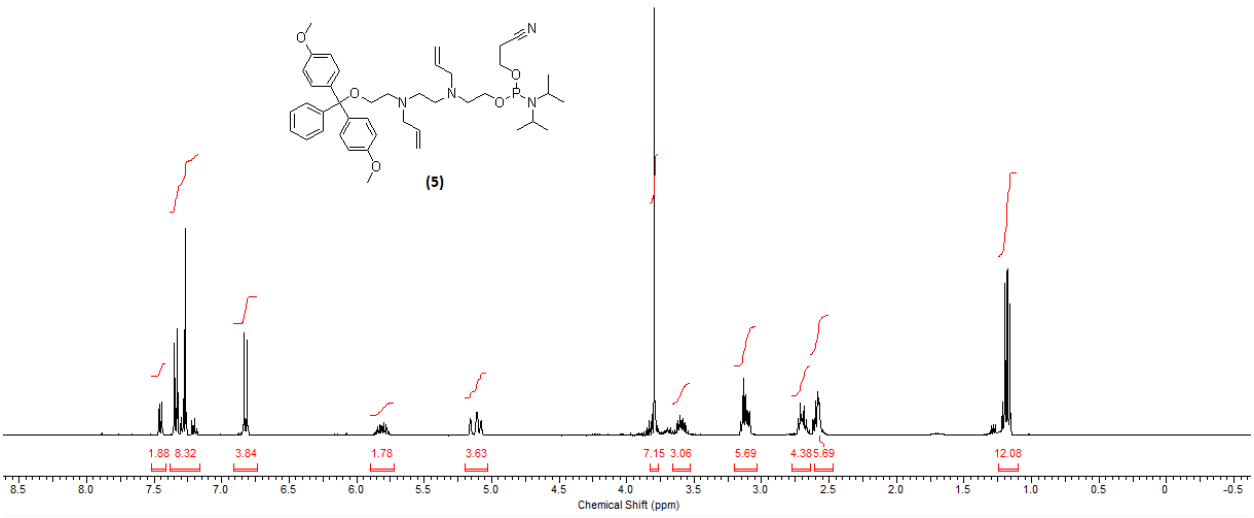

A5-1: ^{1}H NMR spectrum of 2-(allyl(2-(allyl(2-(bis(4-methoxyphenyl)(phenyl)methoxy)ethyl)amino)ethyl)amino)ethyl (2-cyanoethyl) diisopropylphosphoramidite – Compound (5)

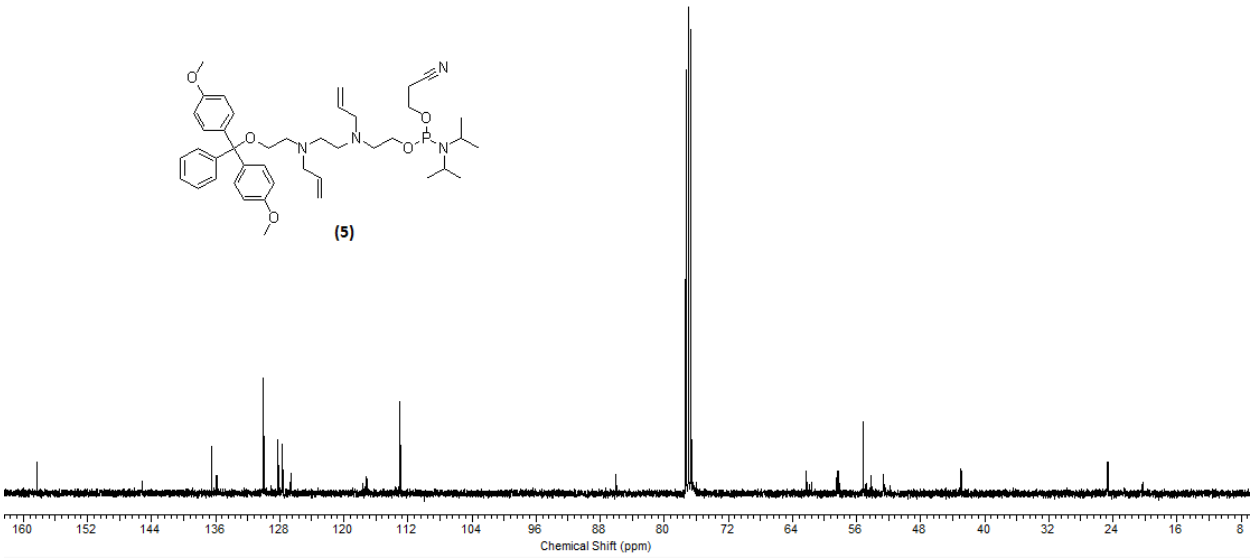

A5-2: ^{13}C NMR spectrum of 2-(allyl(2-(allyl(2-(bis(4-methoxyphenyl)(phenyl)methoxy)ethyl)amino)ethyl)amino)ethyl (2-cyanoethyl) diisopropylphosphoramidite – Compound (5)

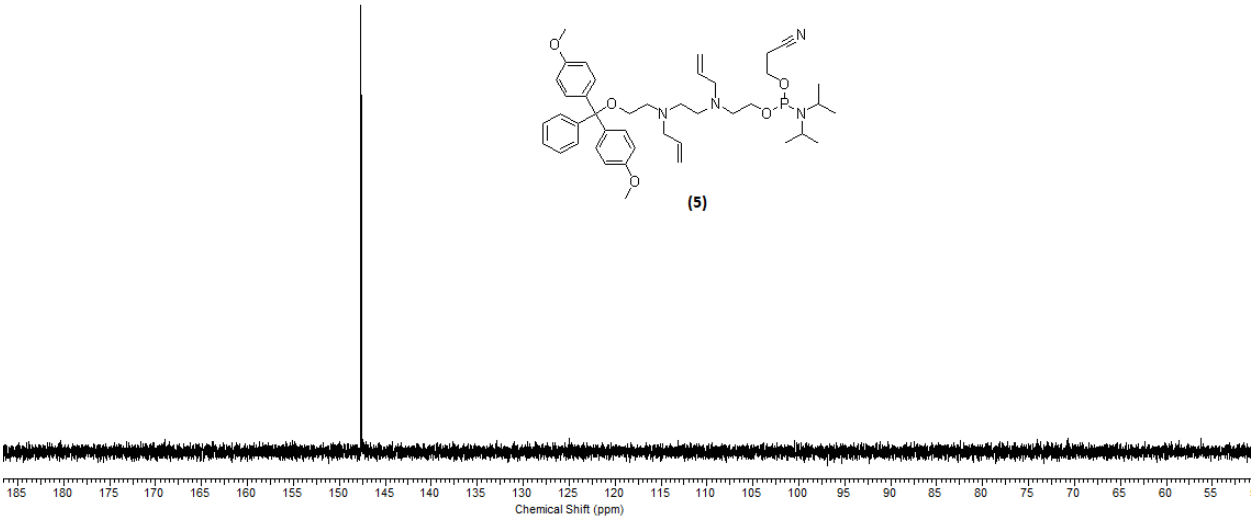

A5-3: ^{31}P NMR spectrum of 2-(allyl(2-(allyl(2-(bis(4-methoxyphenyl)(phenyl)methoxy)ethyl)amino)ethyl)amino)ethyl (2-cyanoethyl) diisopropylphosphoramidite – Compound (5)

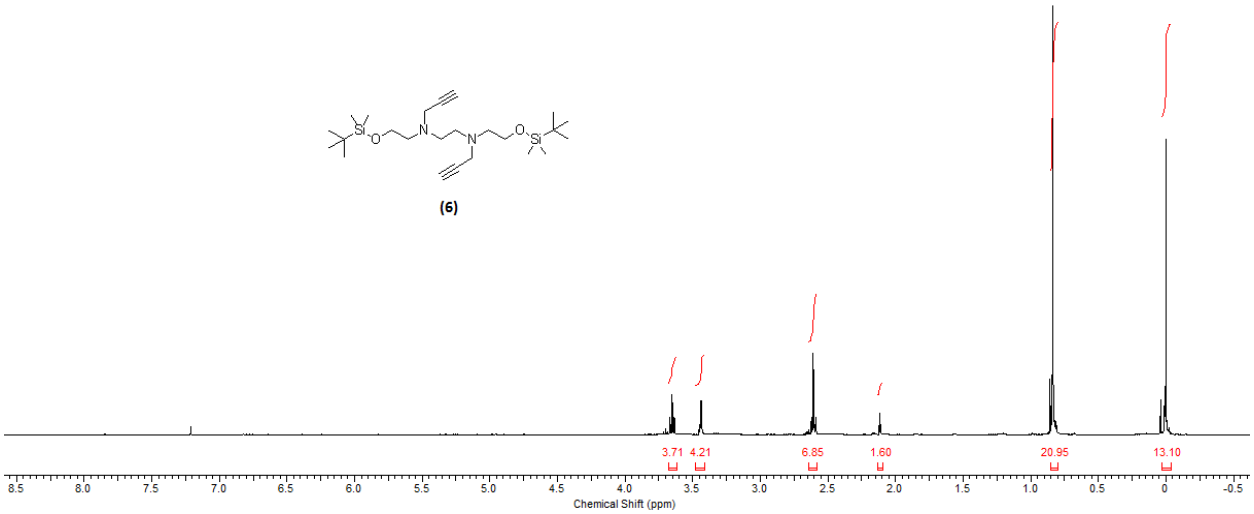

A6-1: ^{1}H NMR spectrum of *N,N'*-bis(2-((tert-butyldimethylsilyl)oxy)ethyl)-*N,N'*-di(prop-2-yn-1-yl)ethane-1,2-diamine – Compound (6)

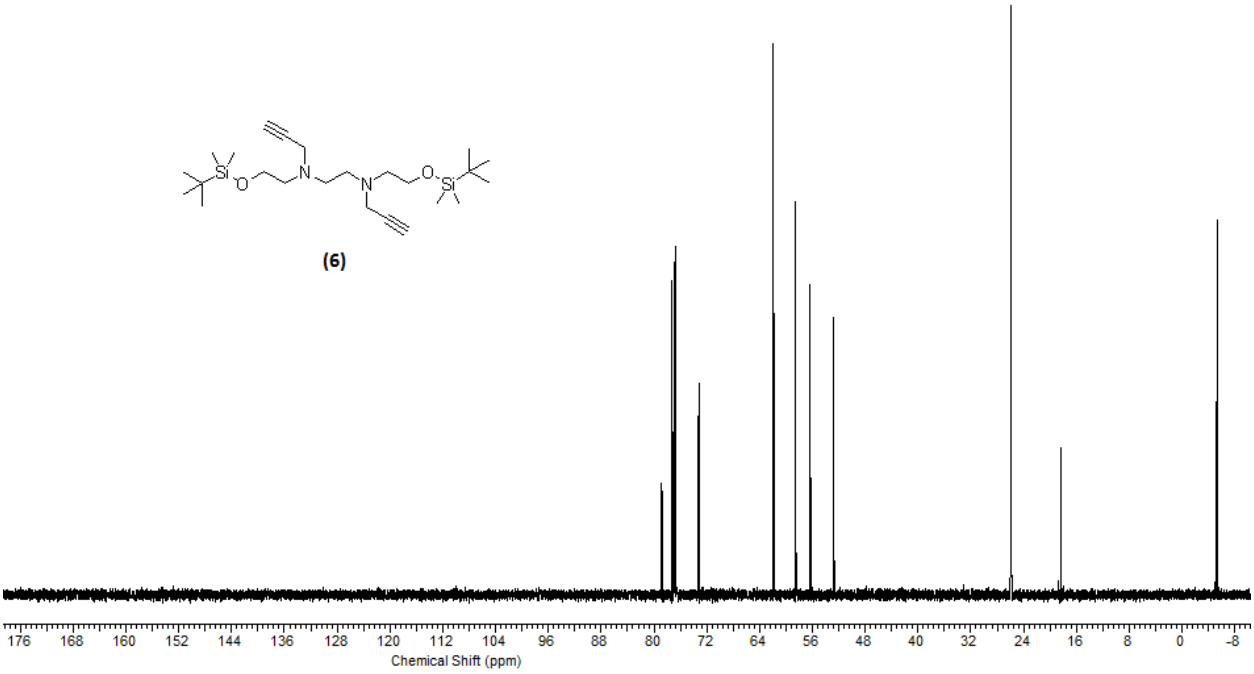

A6-2: ^{13}C NMR spectrum of N,N'-bis(2-((tert-butyldimethylsilyl)oxy)ethyl)-N,N'-di(prop-2-yn-1-yl)ethane-1,2-diamine – Compound (6)

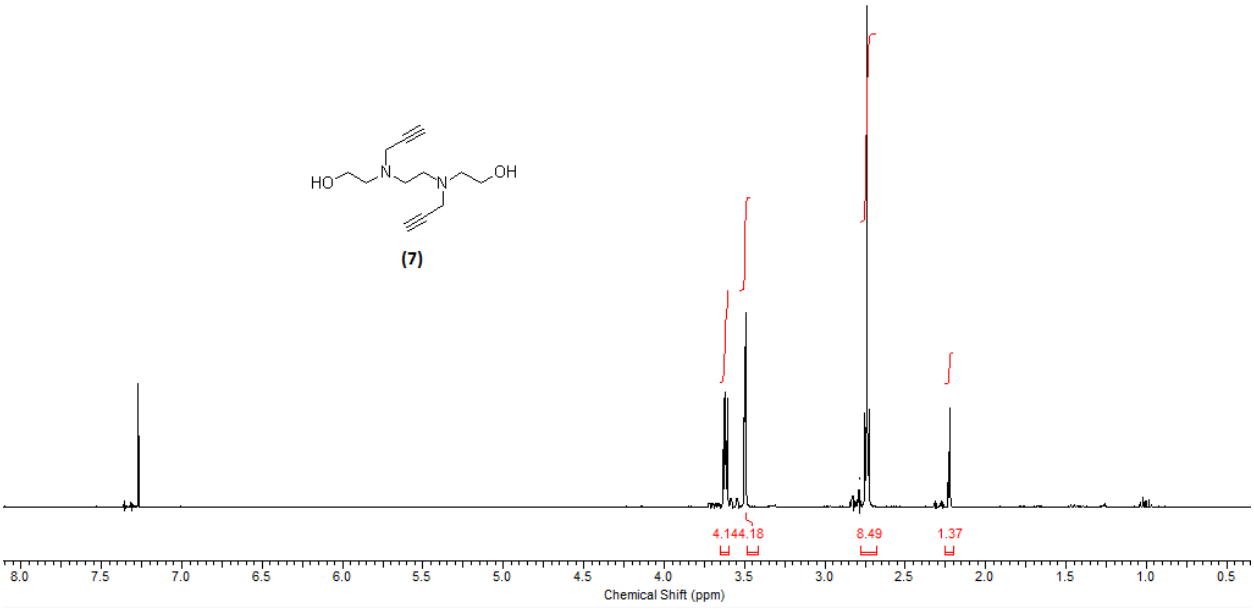

A7-1: ^{1}H NMR spectrum of 2,2'-(ethane-1,2-diylbis(prop-2-yn-1-ylazanediyl))bis(ethan-1-ol) – Compound (7)

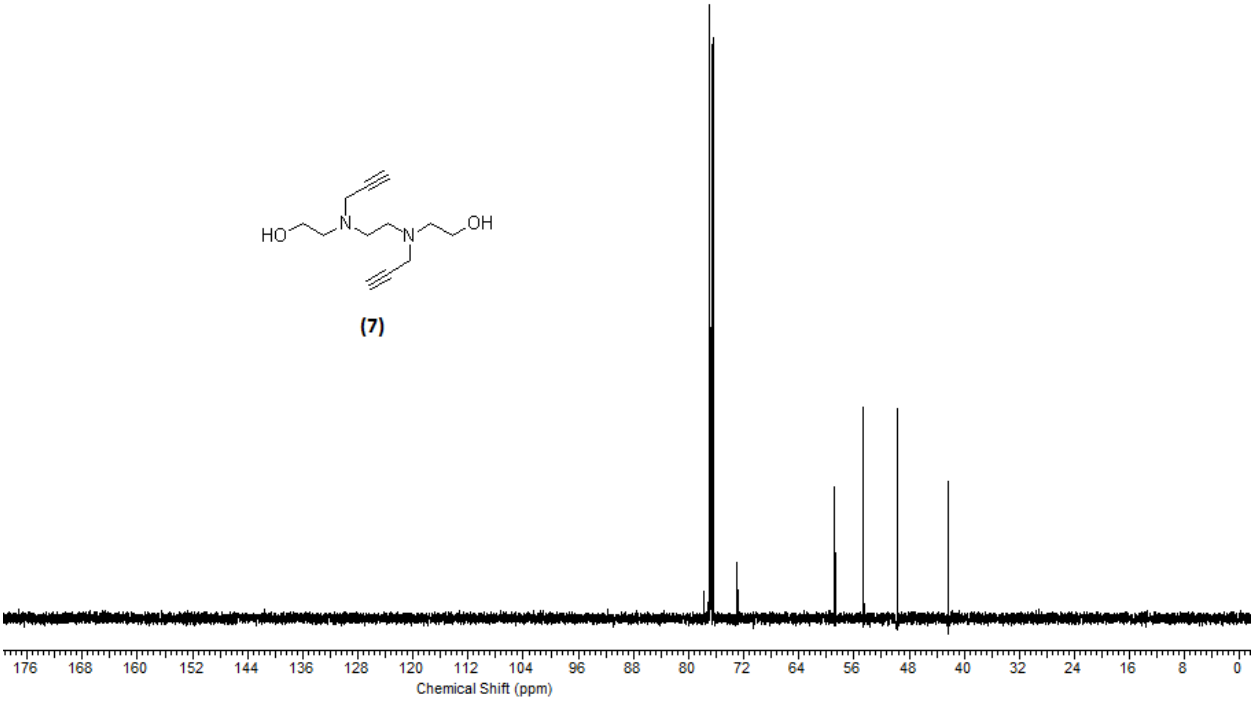

A7-2: ^{13}C NMR spectrum of 2,2'-(ethane-1,2-diylbis(prop-2-yn-1-ylazanediyl))bis(ethan-1-ol) – Compound (7)

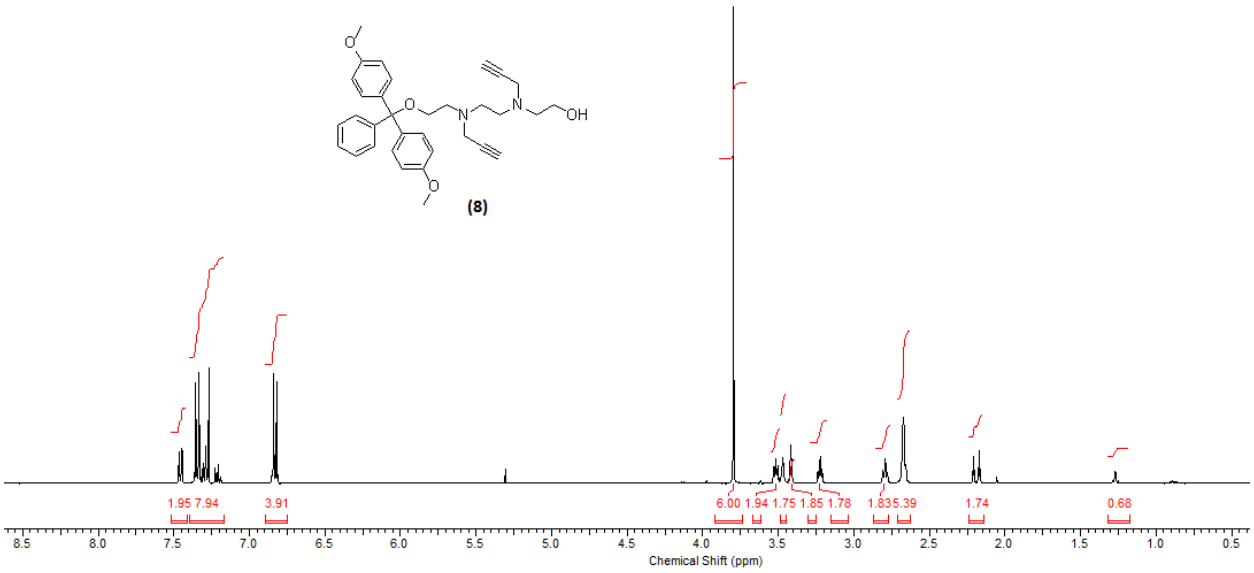

A8-1: ^{1}H NMR spectrum of 2-((2-((2-(bis(4-methoxyphenyl)(phenyl)methoxy)ethyl)(prop-2-yn-1-yl)amino)ethyl)(prop-2-yn-1-yl)amino)ethan-1-ol – Compound (8)

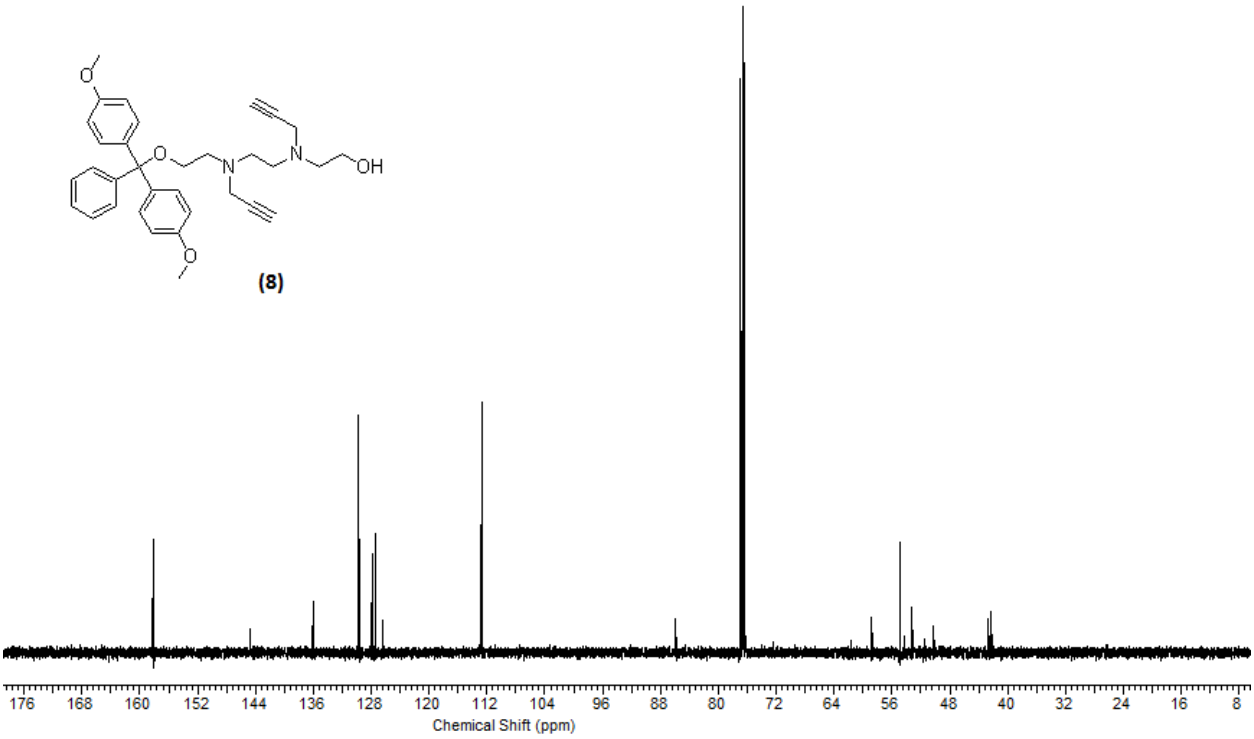

A8-2: ^{13}C NMR spectrum of 2-((2-((2-(bis(4-methoxyphenyl)(phenyl)methoxy)ethyl)(prop-2-yn-1-yl)amino)ethyl)(prop-2-yn-1-yl)amino)ethan-1-ol – Compound (8)

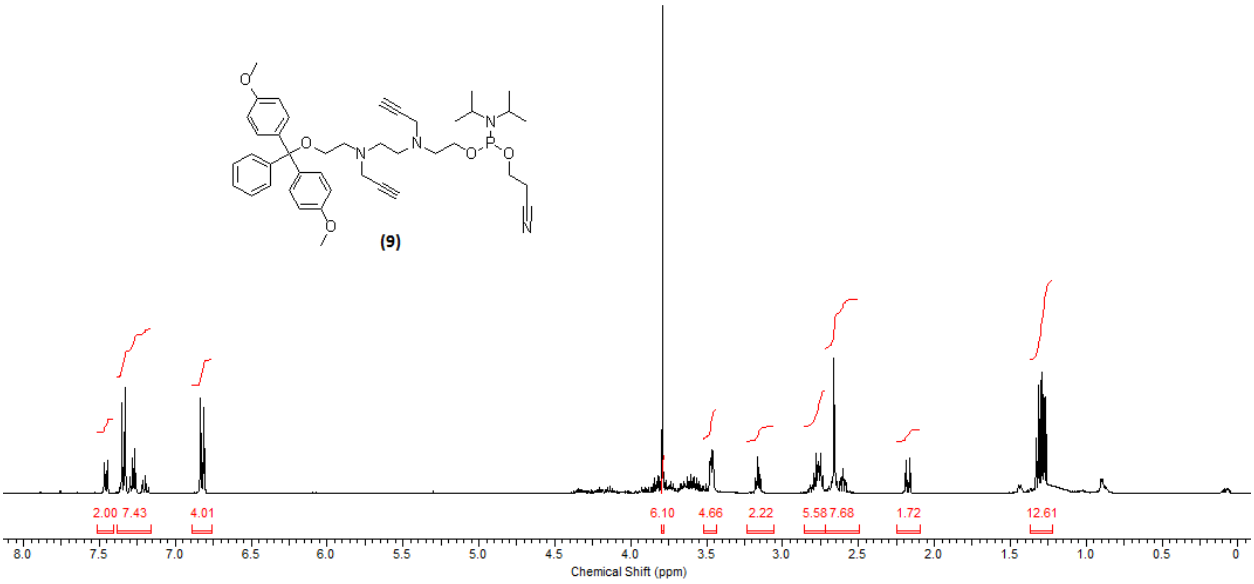

A9-1: ^{1}H NMR spectrum of 2-((2-((2-(bis(4-methoxyphenyl)(phenyl)methoxy)ethyl)(prop-2-yn-1-yl)amino)ethyl)(prop-2-yn-1-yl)amino)ethyl (2-cyanoethyl) diisopropylphosphoramidite – Compound (9)

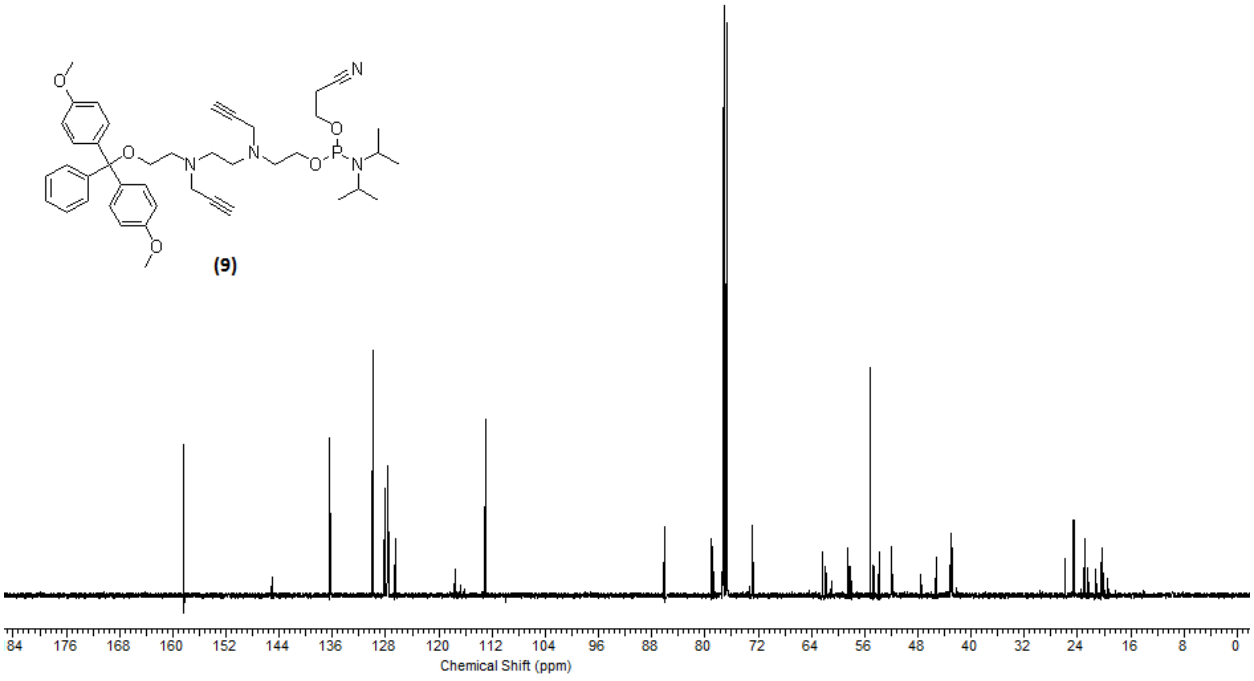

A9-2: ^{13}C NMR spectrum of 2-((2-((2-(bis(4-methoxyphenyl)(phenyl)methoxy)ethyl)(prop-2-yn-1-yl)amino)ethyl)(prop-2-yn-1-yl)amino)ethyl (2-cyanoethyl) diisopropylphosphoramidite – Compound (9)

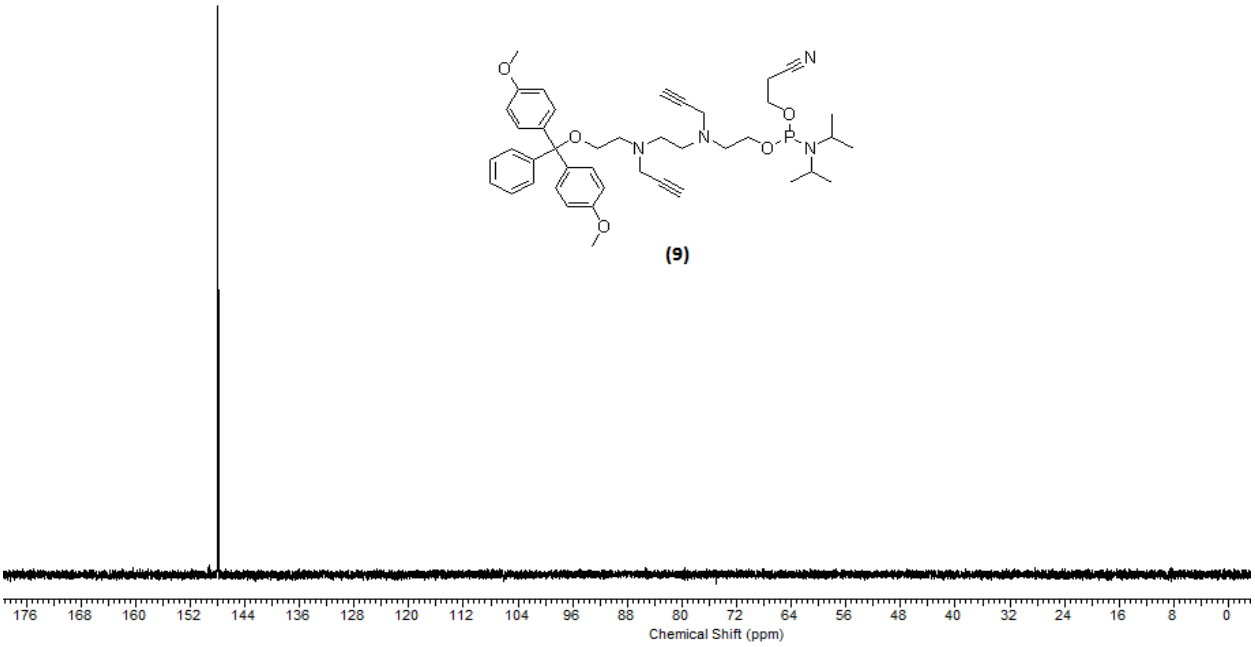

A9-3: 31P NMR spectrum of 2-((2-((2-(bis(4-methoxyphenyl)(phenyl)methoxy)ethyl)(prop-2-yn-1-yl)amino)ethyl)(prop-2-yn-1-yl)amino)ethyl (2-cyanoethyl) diisopropylphosphoramidite – Compound (9)

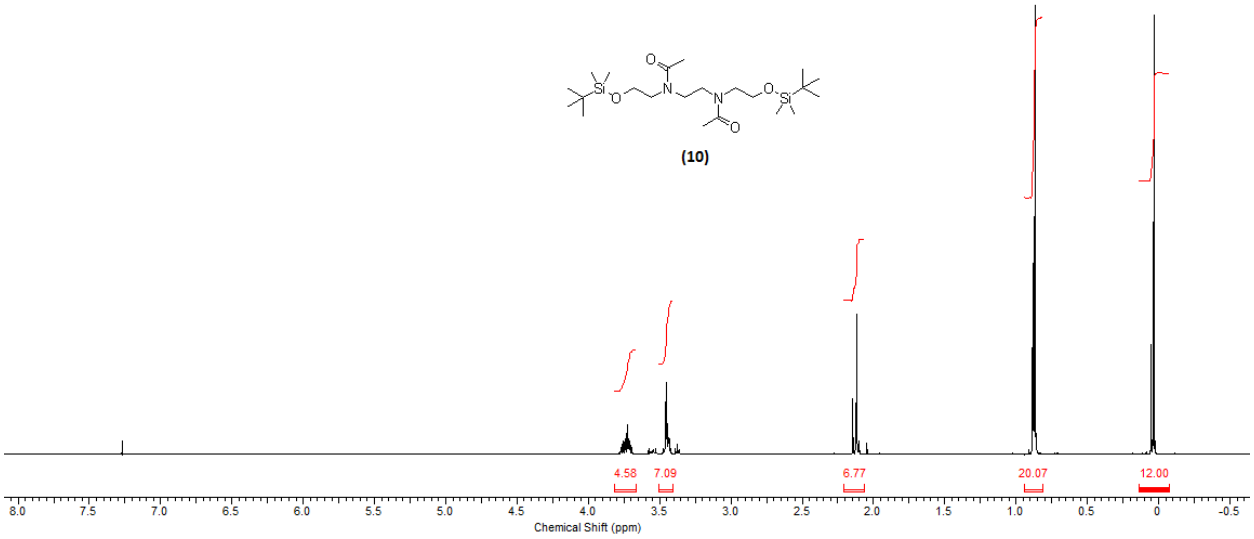

A10-1: ^{1}H NMR spectrum of N,N'-(ethane-1,2-diyl)bis(N-(2-((tert butyldimethylsilyl) oxy)ethyl)acetamide) – Compound (10)

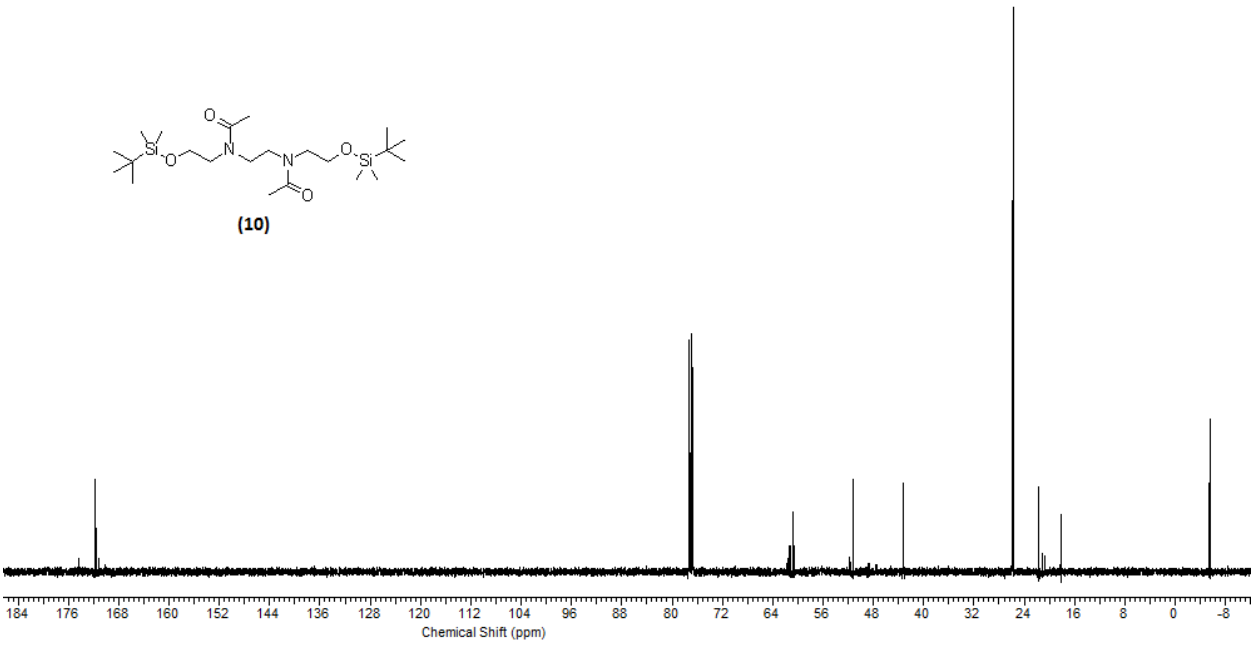

A10-2: ^{13}C NMR spectrum of *N,N'*-(ethane-1,2-diyl)bis(*N*-(2-((tert butyldimethylsilyl) oxy)ethyl)acetamide) – Compound (10)

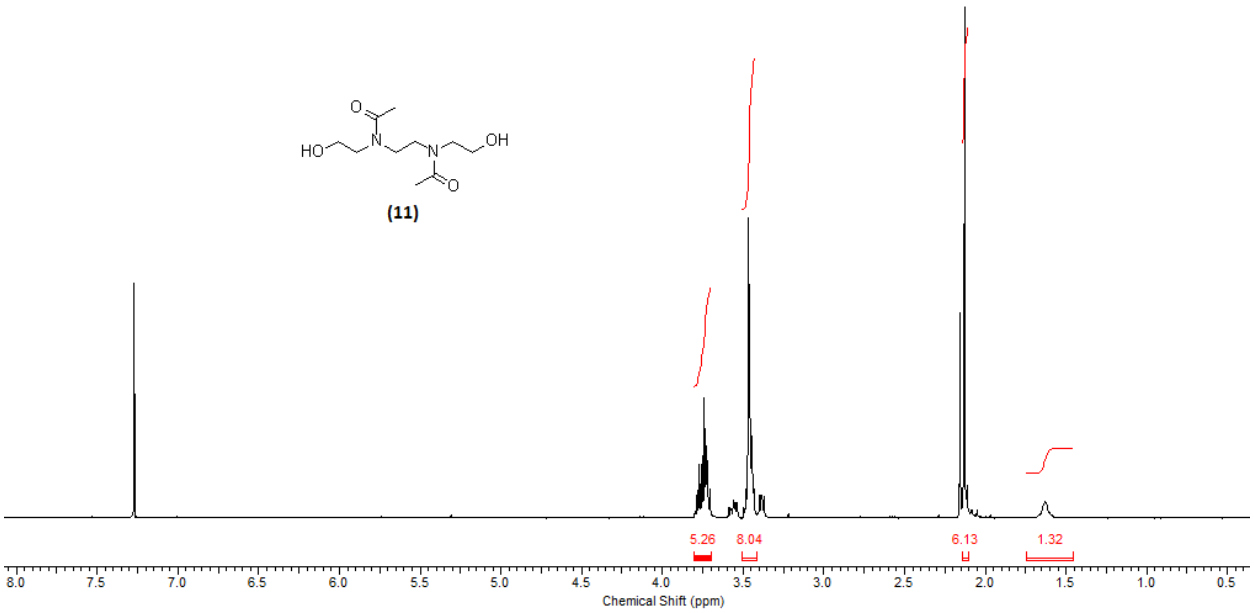

A11-1: ^{1}H NMR Spectrum of *N,N′*-(ethane-1,2-diyl)bis(N-(2-hydroxyethyl)acetamide) – Compound (11)

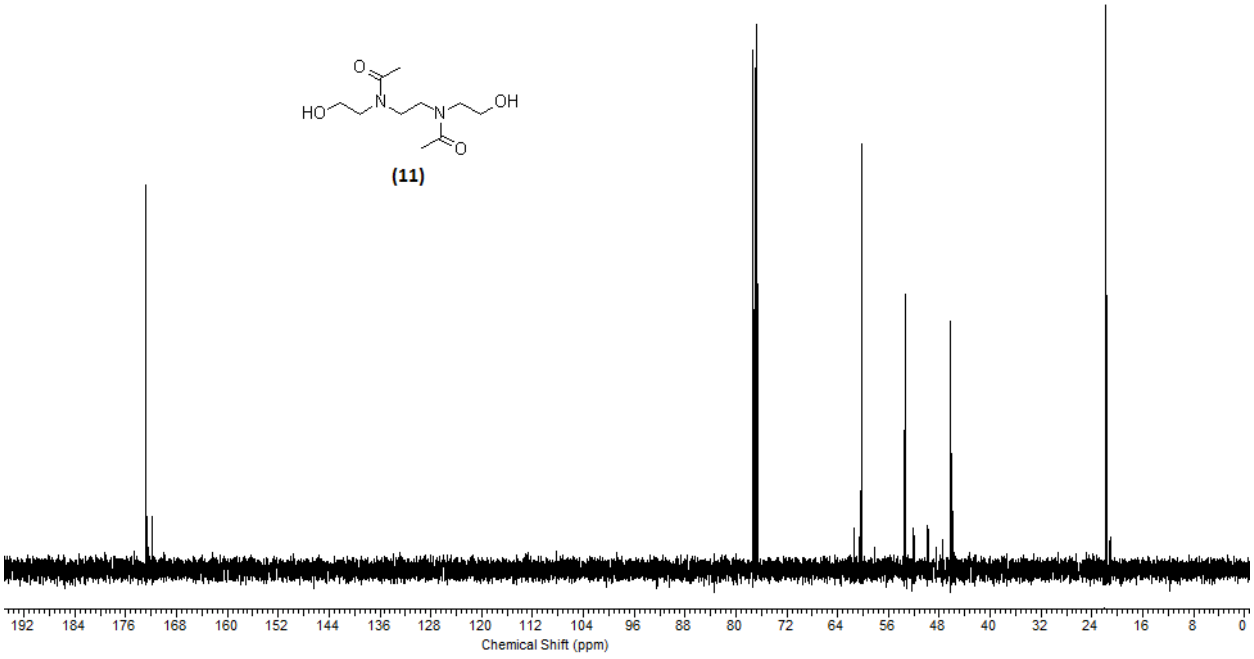

A11-2: ^{13}C NMR spectrum of *N,N′*-(ethane-1,2-diyl)bis(N-(2-hydroxyethyl)acetamide) – Compound (11)

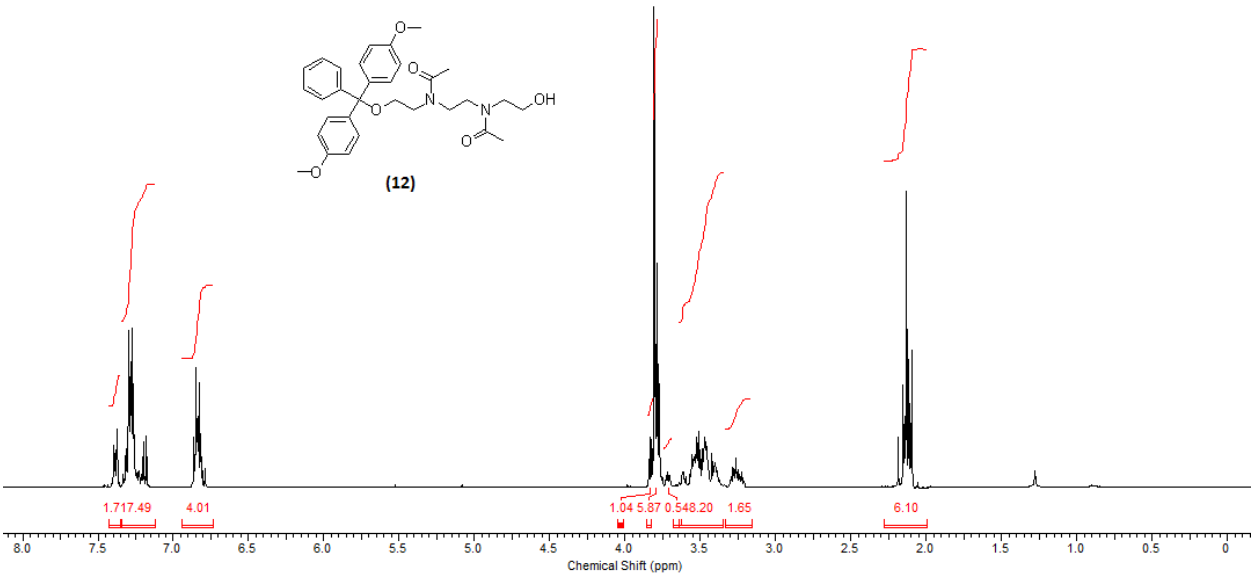

A12-1: ^{1}H NMR Spectrum of *N*-(2-(bis(4-methoxyphenyl)(phenyl)methoxy)ethyl)-*N*-(2-(N-(2-hydroxyethyl)acetamido)ethyl)acetamide – Compound (12)

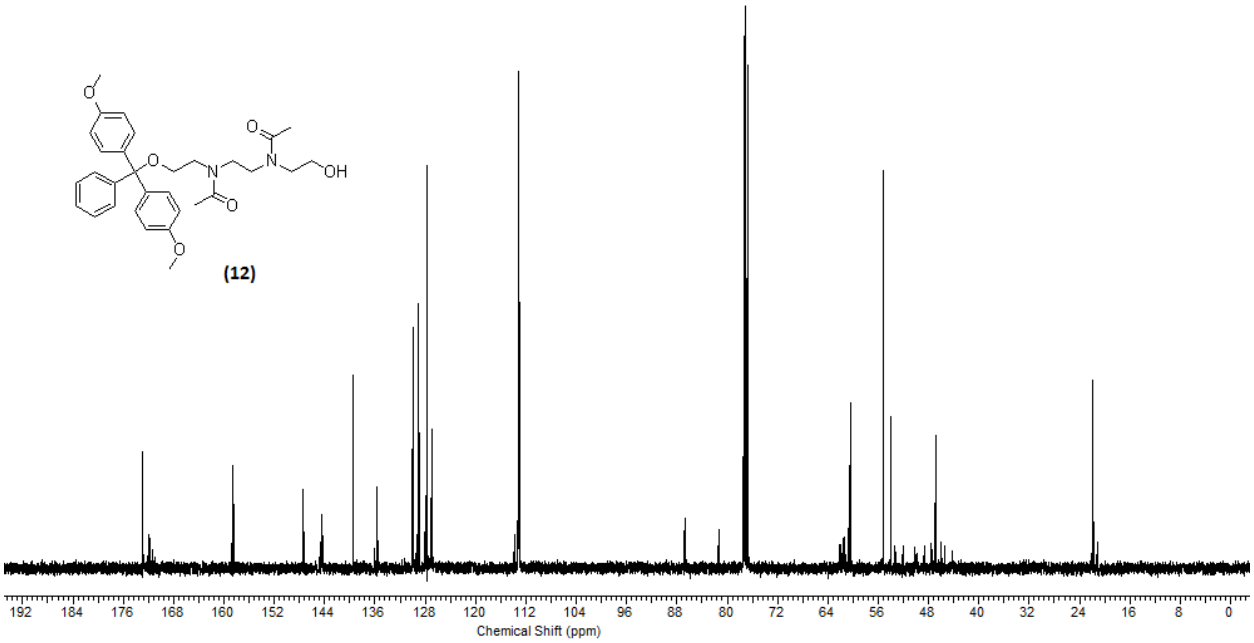

A12-2: ^{13}C NMR spectrum of *N*-(2-(bis(4-methoxyphenyl)(phenyl)methoxy)ethyl)-*N*-(2-(N-(2-hydroxyethyl)acetamido)ethyl)acetamide – Compound (12)

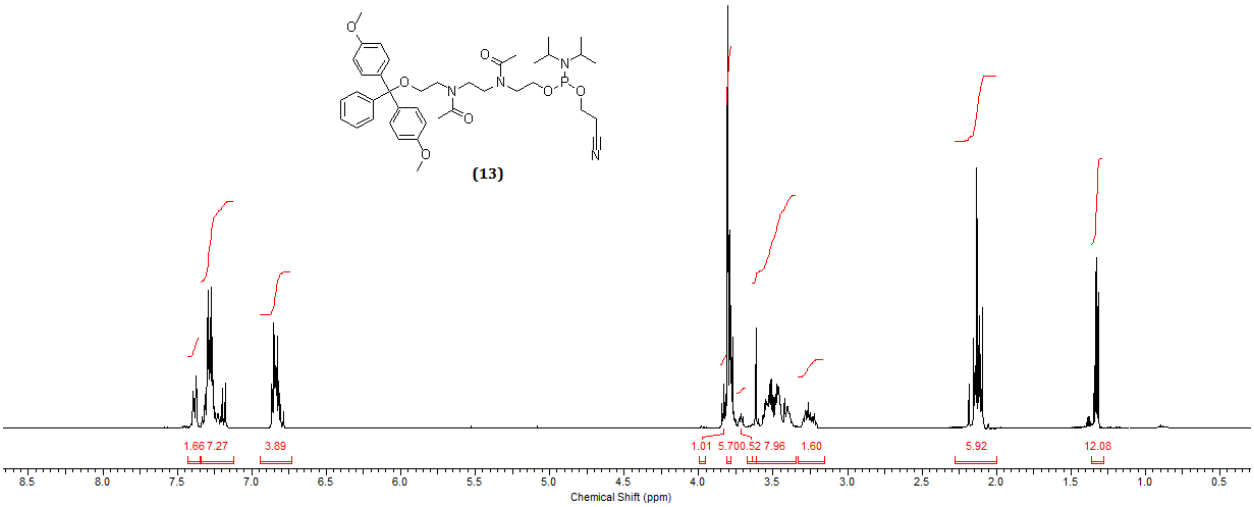

A13-1: ^{1}H NMR spectrum of Synthesis of 2-(N-(2-(N-(2-(bis(4-methoxyphenyl)(phenyl)methoxy)ethyl)acetamido)ethyl)acetamido)ethyl (2-cyanoethyl) diisopropylphosphoramidite – Compound (13)

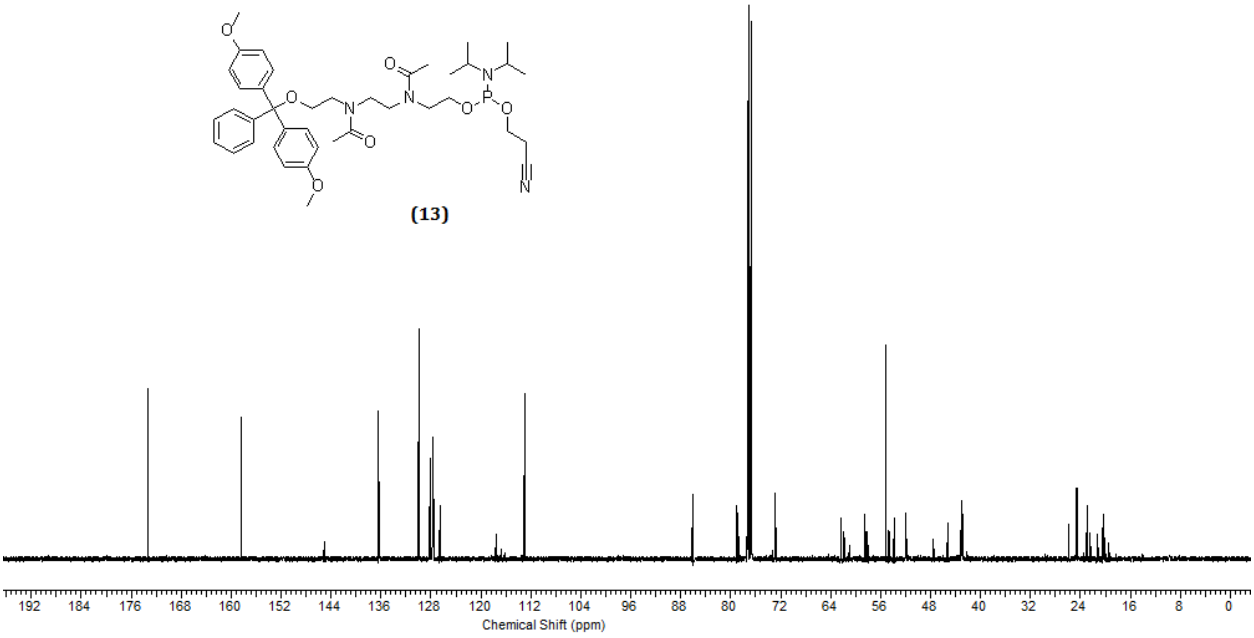

A13-2: ^{13}C NMR spectrum of Synthesis of 2-(N-(2-(N-(2-(bis(4-methoxyphenyl)(phenyl)methoxy)ethyl)acetamido)ethyl)acetamido)ethyl (2-cyanoethyl) diisopropylphosphoramidite – Compound (13)

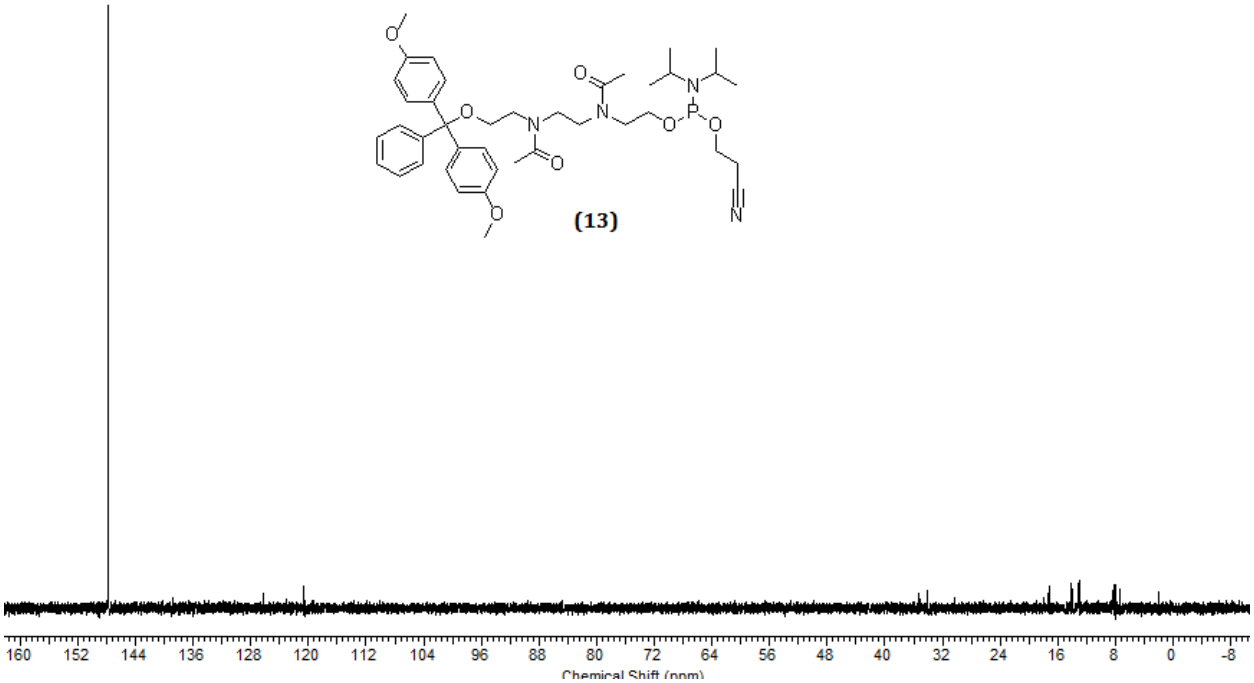

A13-3: ^{31}P NMR spectrum of Synthesis of 2-(N-(2-(N-(2-(bis(4-methoxyphenyl)(phenyl)methoxy)ethyl)acetamido)ethyl)acetamido)ethyl (2-cyanoethyl) diisopropylphosphoramidite – Compound (13)

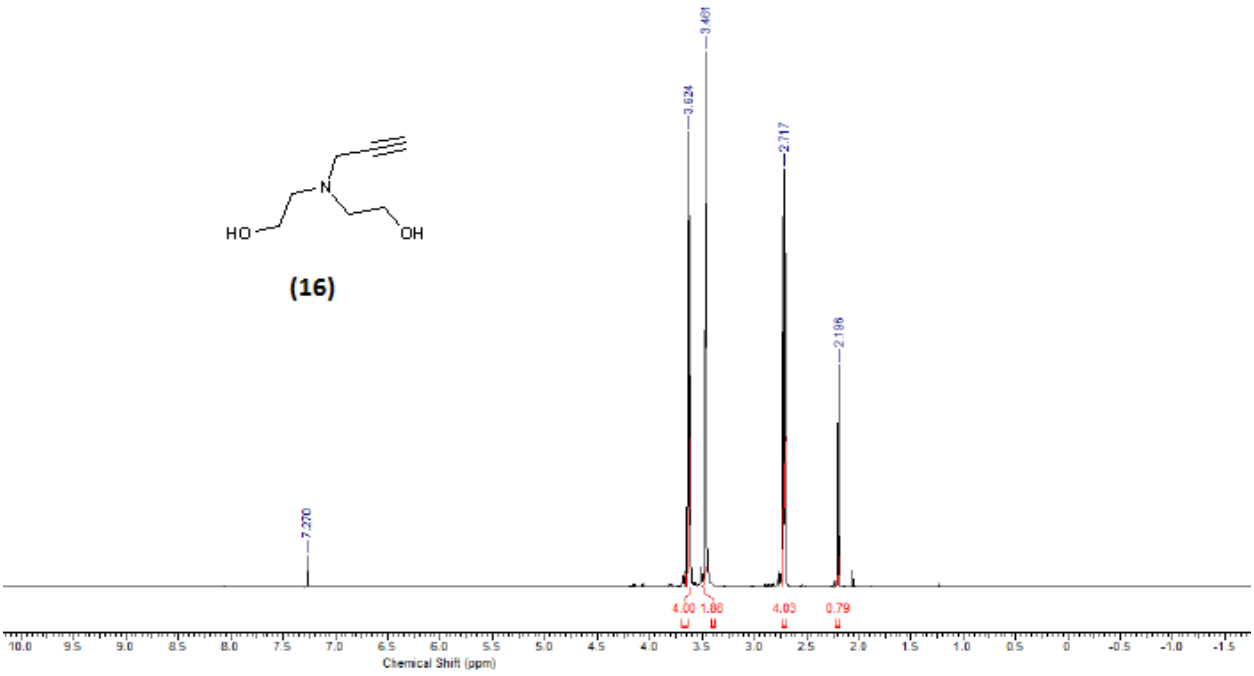

A16-1: ^{1}H NMR spectrum of 2,2'-(prop-2-yn-1-ylazanediyl)bis(ethan-1-ol) – Compound (16)

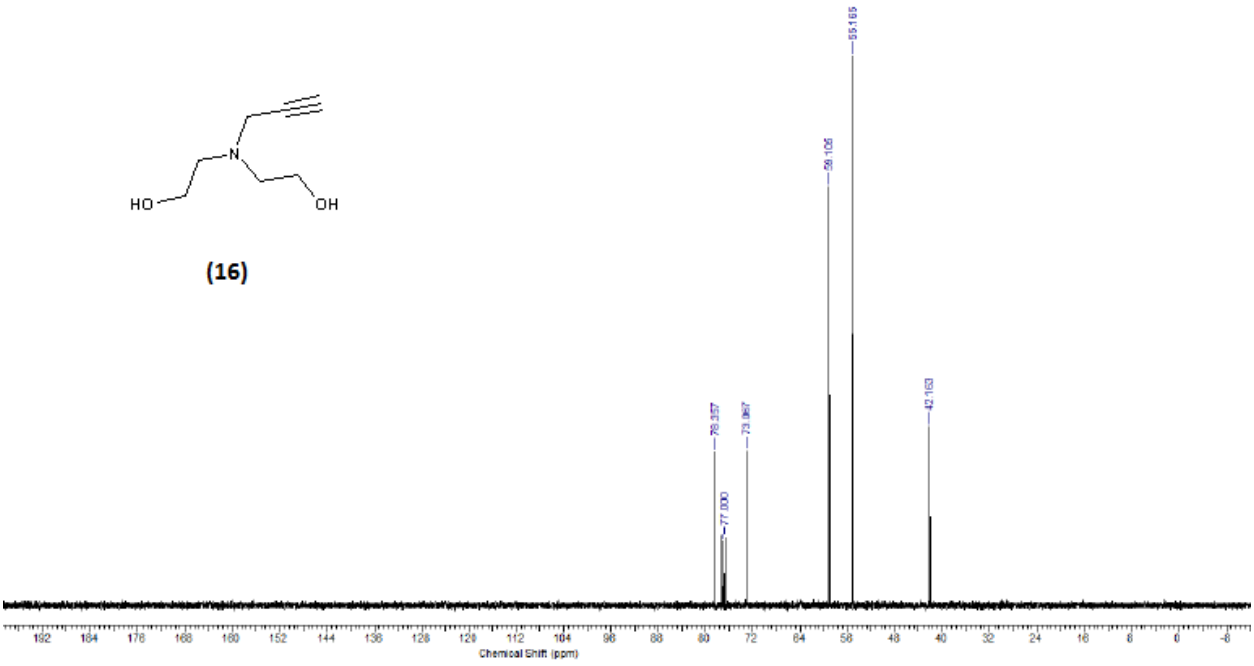

A16-2: ^{13}C NMR spectrum of 2,2'-(prop-2-yn-1-ylazanediyl)bis(ethan-1-ol) – Compound (16)

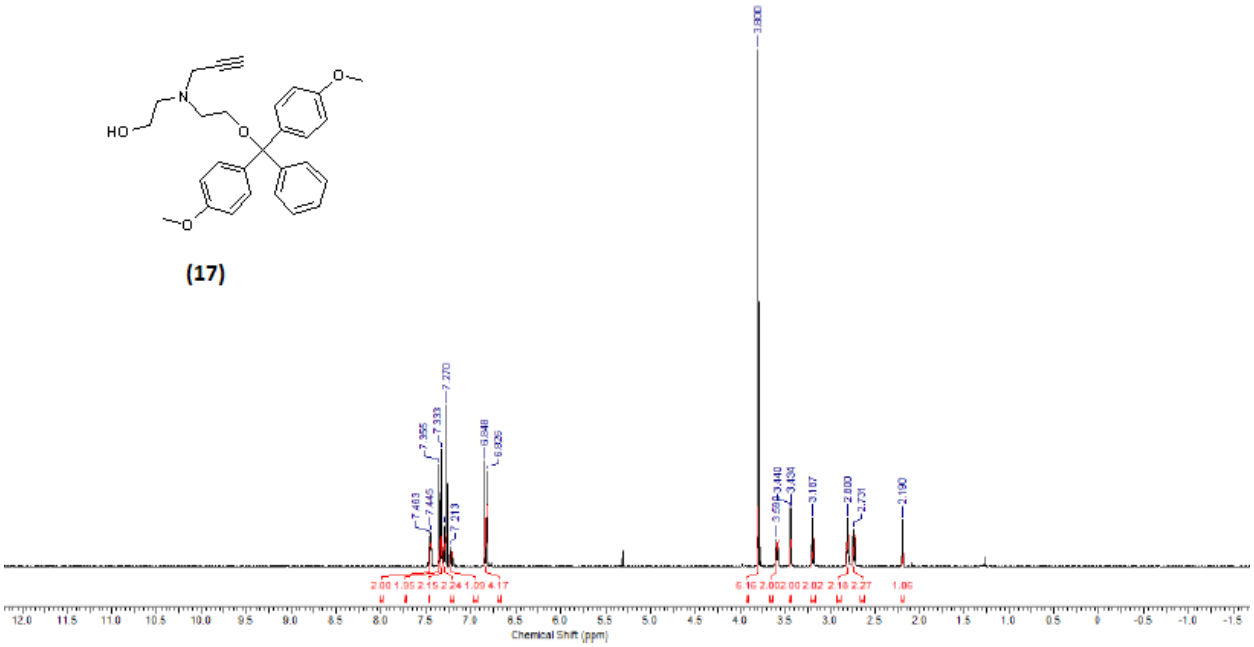

A17-1: ^{1}H NMR spectrum of 2-((2-(bis(4-methoxyphenyl)(phenyl)methoxy)ethyl)(prop-2-yn-1-yl)amino)ethan-1-ol – Compound (17)

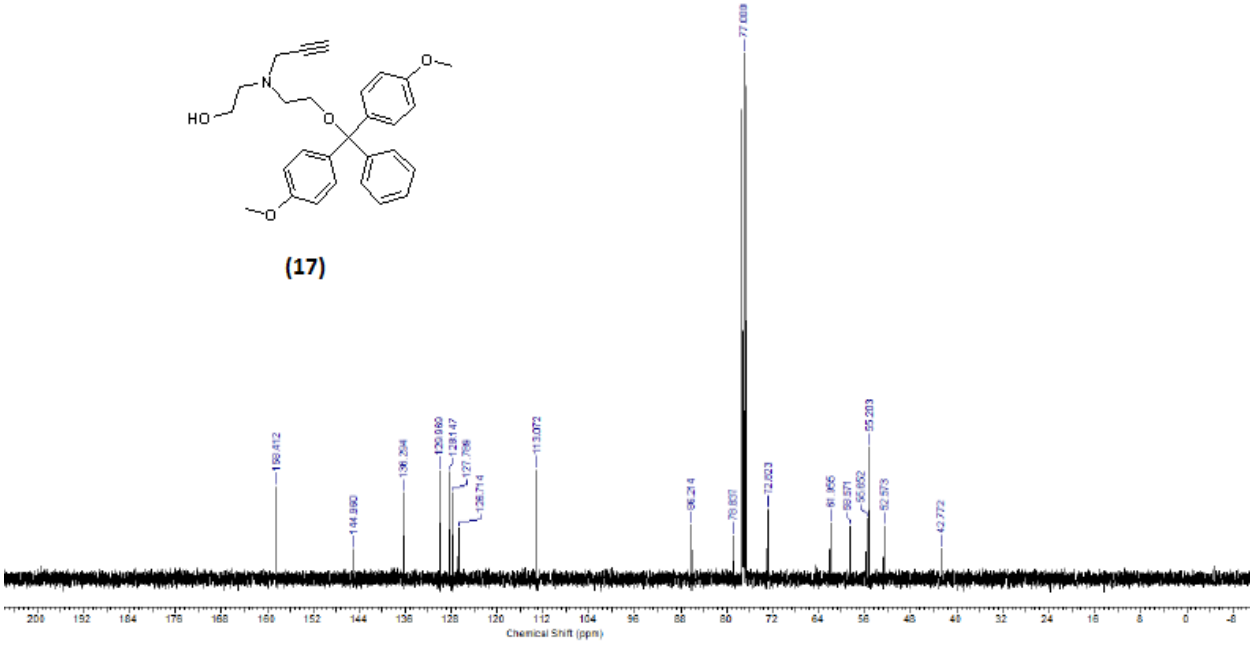

A17-2: ^{13}C NMR spectrum of 2-((2-(bis(4-methoxyphenyl)(phenyl)methoxy)ethyl)(prop-2-yn-1-yl)amino)ethan-1-ol – Compound (17)

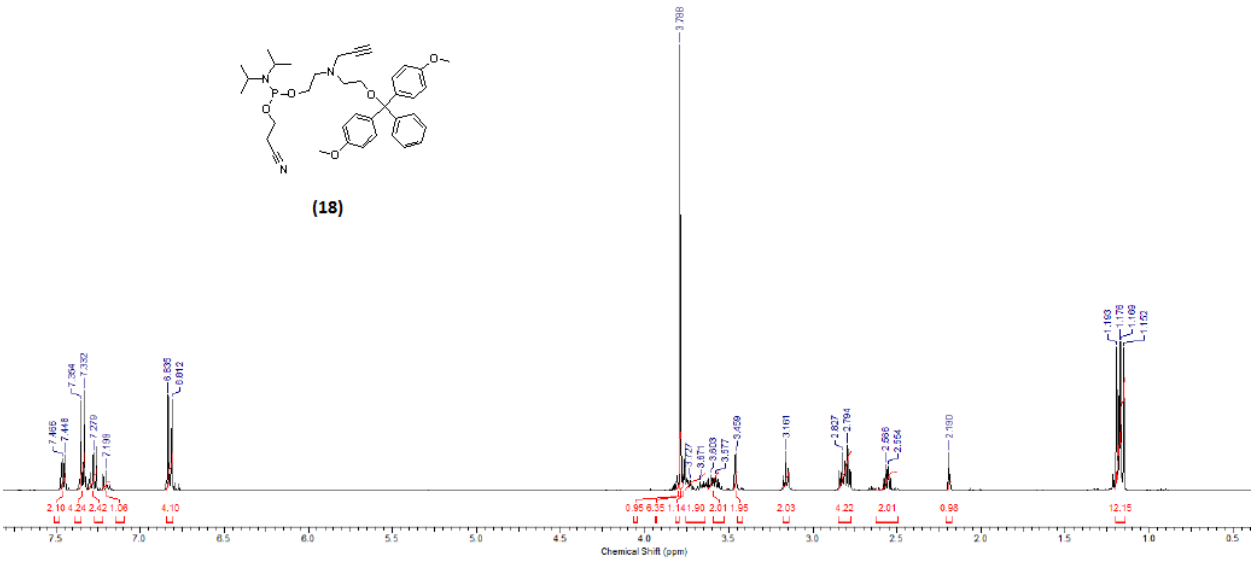

A18-1: ^{1}H NMR spectrum of 2-((2-(bis(4-methoxyphenyl)(phenyl)methoxy)ethyl)(prop-2-yn-1-yl)amino)ethyl (2-cyanoethyl) diisopropylphosphoramidite – Compound (18)

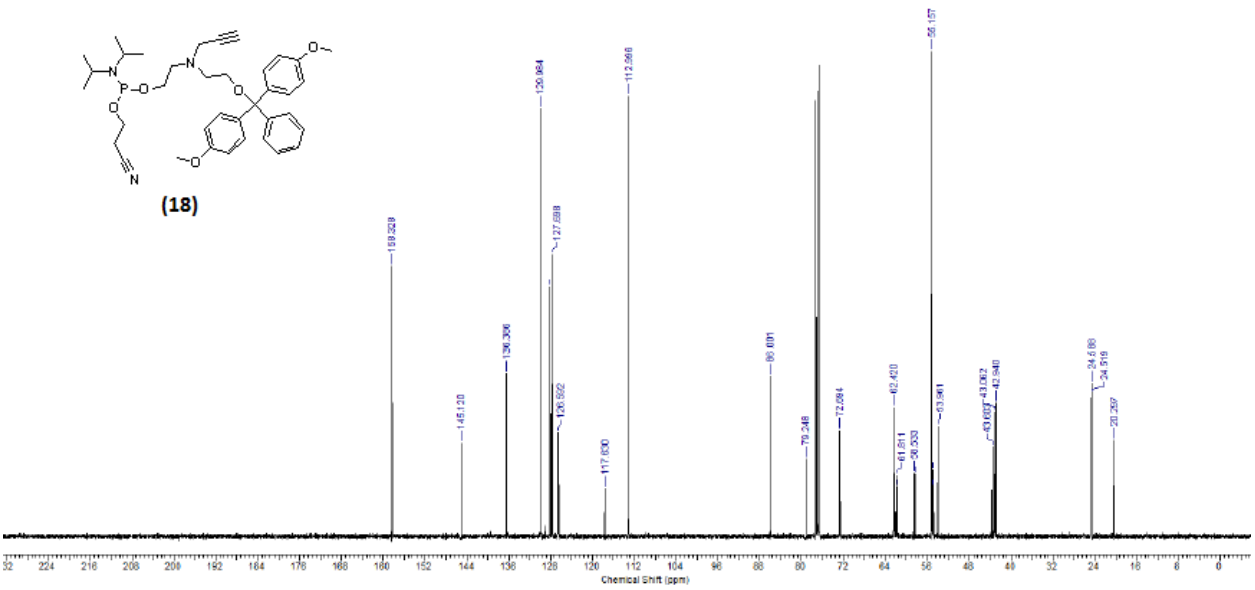

A18-2: ^{13}C NMR spectrum of 2-((2-(bis(4-methoxyphenyl)(phenyl)methoxy)ethyl)(prop-2-yn-1-yl)amino)ethyl (2-cyanoethyl) diisopropylphosphoramidite – Compound (18)

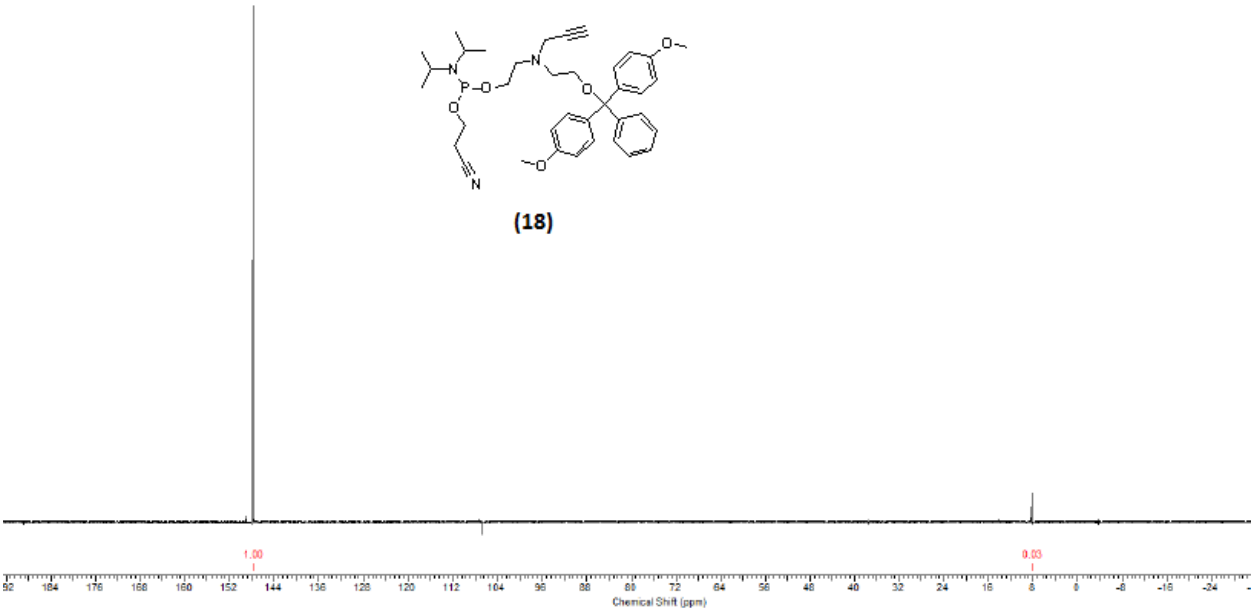

A18-3: ^{31}P NMR spectrum of 2-((2-(bis(4-methoxyphenyl)(phenyl)methoxy)ethyl)(prop-2-yn-1-yl)amino)ethyl (2-cyanoethyl) diisopropylphosphoramidite – Compound (18)

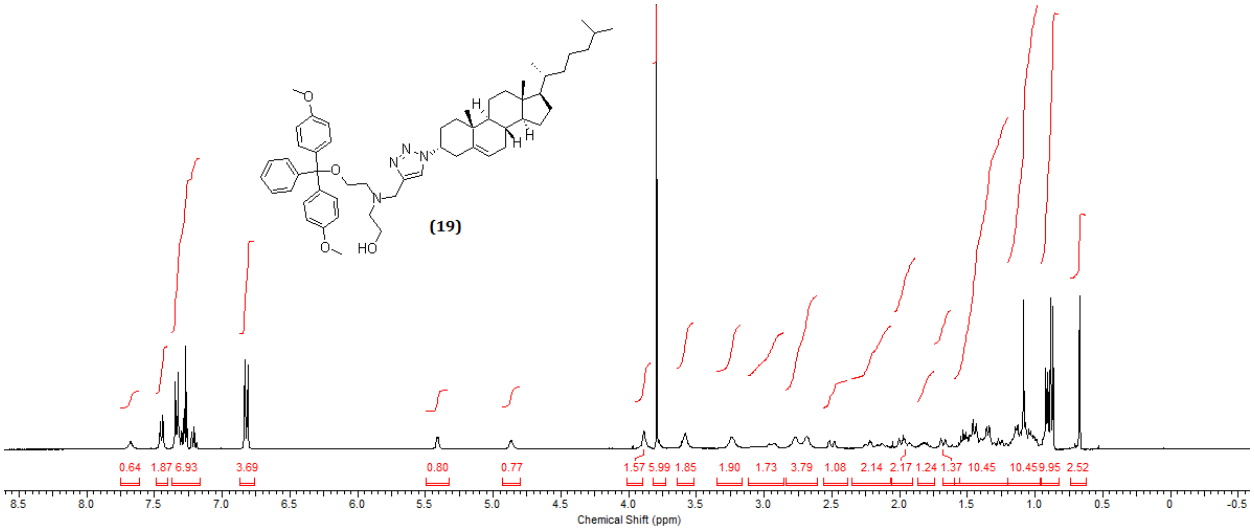

A19-1: ^{1}H NMR spectrum of 2-((2-(bis(4-methoxyphenyl)(phenyl)methoxy)ethyl)((1-(((3R,8S,9S,10R,13R,14S,17R)-10,13-dimethyl-17-((R)-6-methylheptan-2-yl)-2,3,4,7,8,9,10,11,12,13,14,15,16,17-tetradecahydro-1H-cyclopenta[a]phenanthren-3-yl)methyl)-1H-1,2,3-triazol-4-yl)methyl)amino)ethan-1-ol – Compound (19)

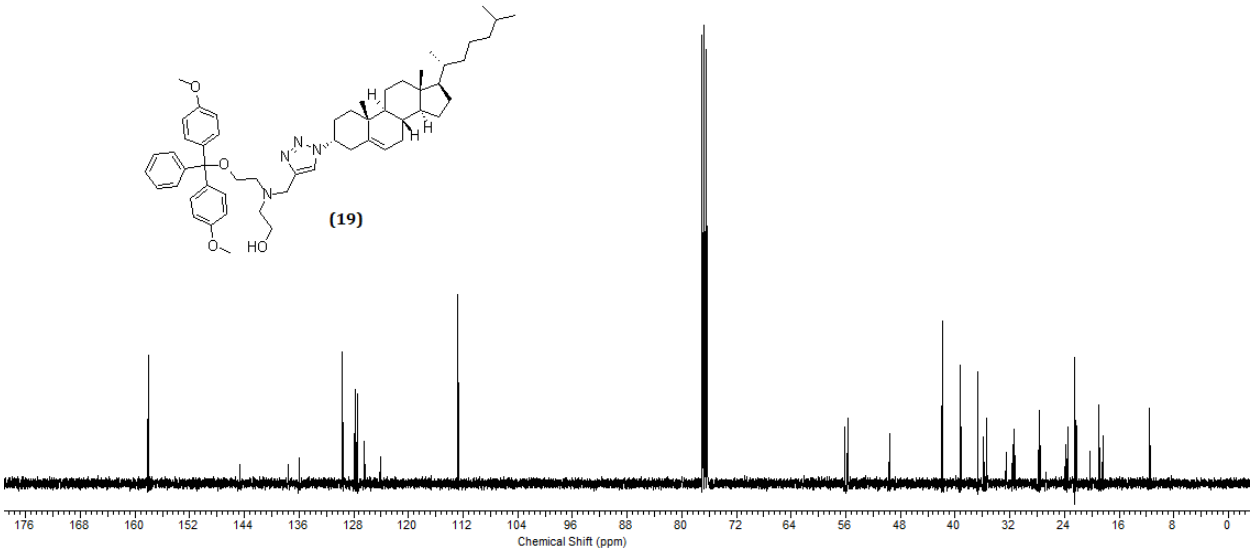

A19-2: ^{13}C NMR spectrum of 2-((2-(bis(4-methoxyphenyl)(phenyl)methoxy)ethyl)((1-(((3R,8S,9S,10R,13R,14S,17R)-10,13-dimethyl-17-((R)-6-methylheptan-2-yl)-2,3,4,7,8,9,10,11,12,13,14,15,16,17-tetradecahydro-1H-cyclopenta[a]phenanthren-3-yl)methyl)-1H-1,2,3-triazol-4-yl)methyl)amino)ethan-1-ol – Compound (19)

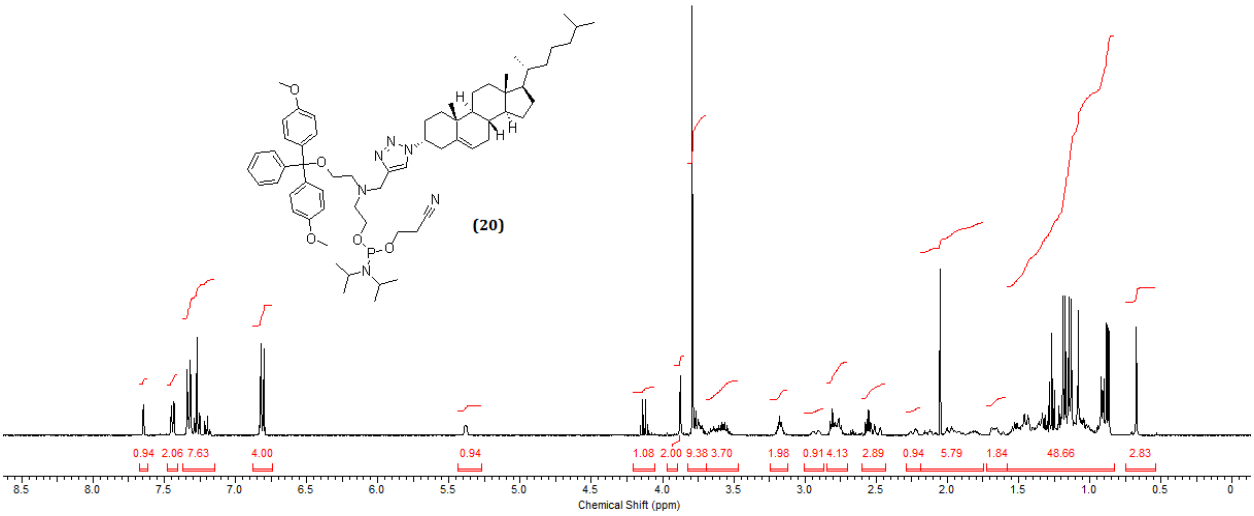

A20-1: ^{1}H NMR spectrum of 2-((2-(bis(4-methoxyphenyl)(phenyl)methoxy)ethyl)((1-(((3R,8S,9S,10R,13R,14S,17R)-10,13-dimethyl-17-((R)-6-methylheptan-2-yl)-2,3,4,7,8,9,10,11,12,13,14,15,16,17-tetradecahydro-1H-cyclopenta[a]phenanthren-3-yl)methyl)-1H-1,2,3-triazol-4-yl)methyl)amino)ethyl (2-cyanoethyl) diisopropylphosphoramidite – Compound (20)

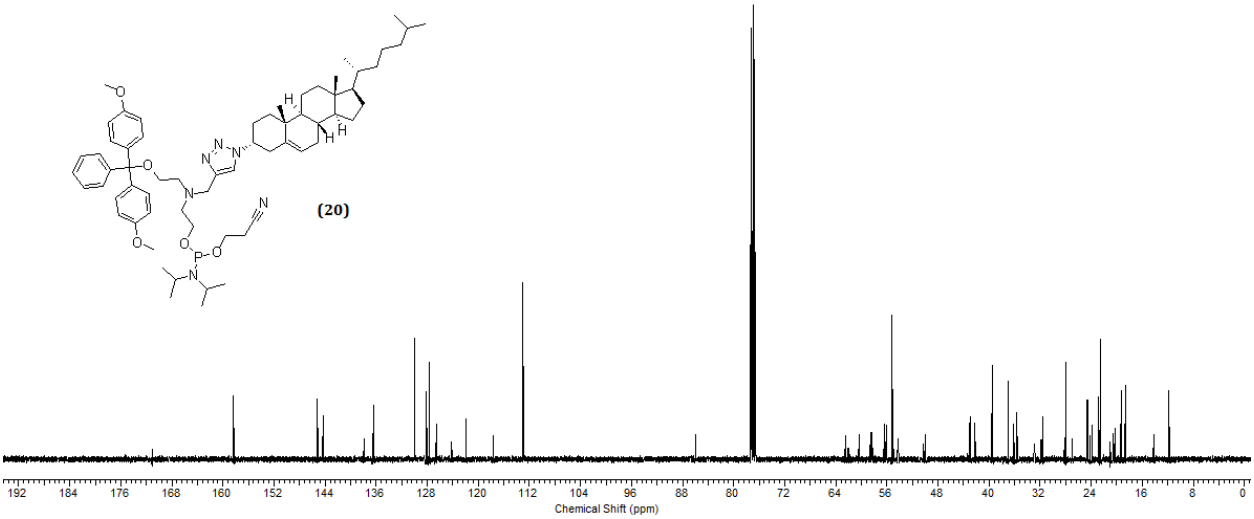

A20-2: ^{13}C NMR spectrum of 2-((2-(bis(4-methoxyphenyl)(phenyl)methoxy)ethyl)((1-(((3R,8S,9S,10R,13R,14S,17R)-10,13-dimethyl-17-((R)-6-methylheptan-2-yl)-2,3,4,7,8,9,10,11,12,13,14,15,16,17-tetradecahydro-1H-cyclopenta[a]phenanthren-3-yl)methyl)-1H-1,2,3-triazol-4-yl)methyl)amino)ethyl (2-cyanoethyl) diisopropylphosphoramidite – Compound (20)

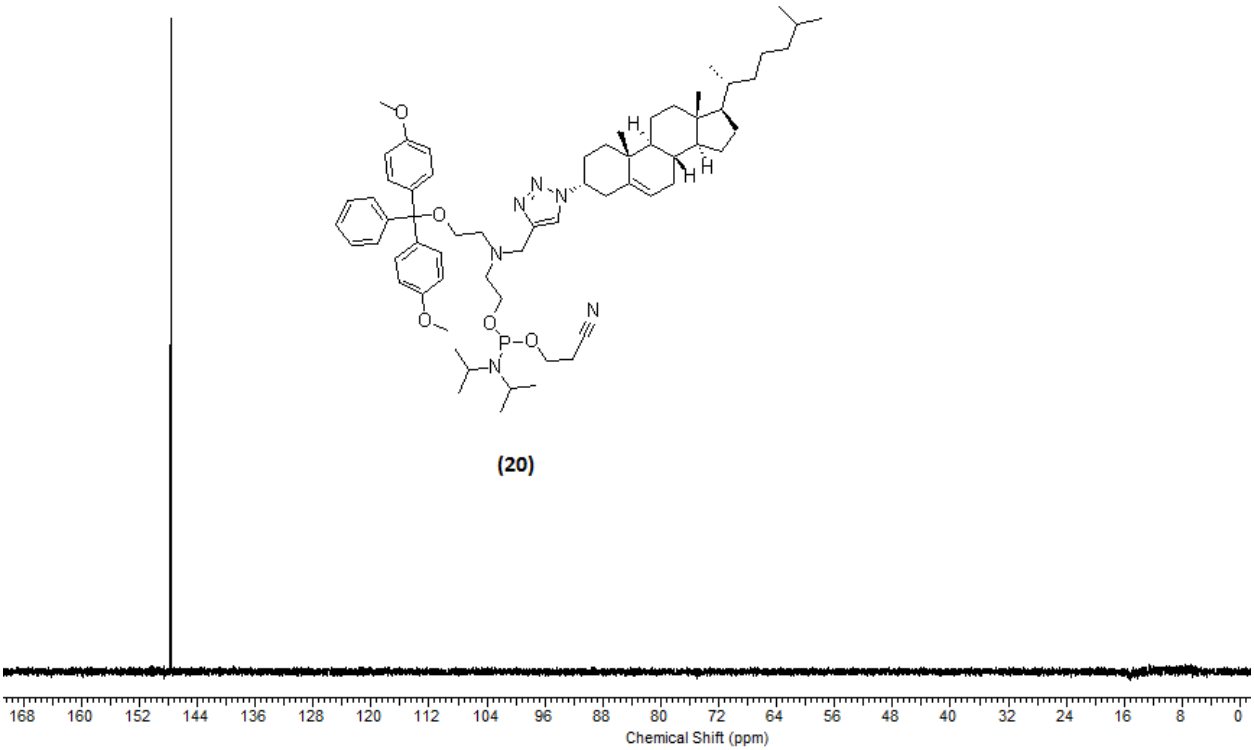

A20-3: ^{31}P NMR of 2-((2-(bis(4-methoxyphenyl)(phenyl)methoxy)ethyl)((1-(((3R,8S,9S,10R,13R,14S,17R)-10,13-dimethyl-17-((R)-6-methylheptan-2-yl)-2,3,4,7,8,9,10,11,12,13,14,15,16,17-tetradecahydro-1H-cyclopenta[a]phenanthren-3-yl)methyl)-1H-1,2,3-triazol-4-yl)methyl)amino)ethyl (2-cyanoethyl) diisopropylphosphoramidite – Compound (20)